The role of PPARβ/δ in diabetic retinopathy

By

Sara Renee Savage

Dissertation

Submitted to the Faculty of the

Graduate School of Vanderbilt University

in partial fulfillment of the requirements

for the degree of

DOCTOR OF PHILOSOPHY

in

Pharmacology

December, 2015

Nashville, Tennessee

Approved:

John S. Penn, Ph.D.

Joey V. Barnett, Ph.D.

Vsevolod V. Gurevich, Ph.D.

David Robertson, M.D.

To my parents, Jim and Linda Savage, for their unfailing love and support

ACKNOWLEDGEMENTS

The work presented in this dissertation would not have been possible without the funding provided by the grant for Training in Pharmacological Sciences (T32-GM07628), grants from the National Eye Institute (R01-EY07533 and P30-EY08126), a voucher from the Vanderbilt Institute for Clinical and Translational Research, an unrestricted grant from Research to Prevent Blindness, and the Phyllis G. and William B. Snyder Endowed Chair. Additionally I would like to acknowledge the Vanderbilt VANTAGE and VANGARD cores, particularly Lana Olson and Yan Guo, for all of their help with RNA-sequencing and analysis.

Of course, this project would also not have been possible without the support from my mentor, Dr. John Penn, who has been instrumental in my education. Dr. Penn has given me incredible learning experiences, guidance, and encouragement. Additionally, all of the members of the Penn Lab have been invaluable in my success as a graduate student. Their willingness to offer collaboration, support, and ask questions have been extremely helpful. In particular, I would like to thank Rong Yang for her support with experiments and dissections and Colin Bretz for his advice on project directions. I would also like to thank the members of my dissertation committee, Dr. Joey Barnett, Dr. Seva Gurevich, Dr. David Robertson, and Dr. Mary Zutter, for their suggestions and guidance.

I wouldn't be here today without those who helped foster my interest in science along the way. I would like to thank my grade school and high school science teachers, particularly Mrs. Lisella, Mrs. Heinrich, Mrs. Marot, and Mrs. Collins, for teaching engaging experiments. Additionally I would like to thank my undergraduate mentor, Dr. Paul Urayama, who never fails to spark my love of science.

Finally, I would like to thank my friends and family for making my life more exciting and complete. I would not be the person I am today without their love, support, and adventures.

TABLE OF CONTENTS

LIST OF TABLES

Table Page

LIST OF FIGURES

LIST OF ABBREVIATIONS

ACCORD	Action to Control Cardiovascular Risk in Diabetes
ACTB	β-actin
AGE	Advanced glycation end products
AMD	Age-related macular degeneration
ANGPTL4	Angiopoietin-like protein-4
BCL6	B-cell lymphoma 6
BrdU	Bromodeoxyuridine
ChIP-seq	Chromatin immunoprecipitation sequencing
DAVID	Database for Annotation, Visualization, and Integrated Discovery
DME	Diabetic macular edema
DMEM	Dulbecco's Modified Eagle Medium
DMSO	Dimethyl sulfoxide
DR	Diabetic retinopathy
EBM	Endothelial basal medium
EPC	Endothelial progenitor cell
ERK	Extracellular signal-related kinase (1 and 2)
ETDRS	Early Treatment Diabetic Retinopathy Study
FBS	Fetal bovine serum
FDA	Food and Drug Administration
GO	Gene ontology
HBSS	Hank's buffered salt solution
HCEC	Human choroidal endothelial cell
HRMEC	Human retinal microvascular endothelial cell
HUVEC	Human umbilical vein endothelial cell
ICAM-1	Intercellular adhesion molecule 1
IL-1β	Interleukin-1 beta
JNK	c-Jun N-terminal kinase
KEGG	Kyoto Encyclopedia of Genes and Genomes
LPS	Lipopolysaccharide
MAPK	Mitogen-activated protein kinases
MEM	Minimal essential medium
NCBI	National Center for Biotechnology information
NDRI	National Disease Research Interchange
NF-κB	Nuclear factor kappa B
NPDR	Nonproliferative diabetic retinopathy
NSAID	Nonsteroidal anti-inflammatory drug
OIR	Oxygen-induced retinopathy
PBMC	Peripheral blood mononuclear cells
PBS	Phosphate-buffered saline
PDR	Proliferative diabetic retinopathy
PE	Phycoerythrin

PMN	Polymorphonuclear cells
PPAR	Peroxisome proliferator-activated receptor (α, β/δ, γ)
PPFC	Parallel plate flow chamber
PPRE	Peroxisome proliferator-activated response element
RNA-seq	RNA-sequencing
RPE	Retinal pigmented epithelium
RRMEC	Rat retinal microvascular endothelial cell
RXR	Retinoid X receptor
STZ	Streptozotocin
TBST	Tris-buffered saline with Tween 20
TNFα	Tumor necrosis factor alpha
TNFR	TNFα receptor (1, 2)
UCSC	University of California, Santa Cruz
VCAM-1	Vascular cell adhesion molecule 1
VEGF	Vascular endothelial growth factor
VEGFR	VEGF receptor

Chapter 1

Introduction

Diabetes and diabetic retinopathy: background and prevalence

Diabetes mellitus is a common metabolic disease and has become a growing problem worldwide. The International Diabetes Federation reports nearly 26 million people in the United States and over 380 million people worldwide have been diagnosed with diabetes.[1] These numbers are projected to increase to a total of 592 million patients by 2035. A large majority of these patients, nearly 95%, have type 2 diabetes.[2] Type 2 diabetes is caused by insulin resistance or reduced insulin secretion. The remaining patients have type 1 diabetes, which is typically diagnosed in children ages 10-14 and is caused by destruction of insulin-producing pancreatic beta cells. Both types are characterized by hyperglycemia which can cause numerous systemic complications.[3, 4]

One of the complications associated with diabetes is diabetic retinopathy (DR), which is one of the leading causes of irreversible blindness in the US.[5] About 35% of diabetics have DR and nearly 12% have DR that is considered to be vision-threatening.[6] This equates to about 20 million people worldwide in 2010 with vision-threatening DR. The main risk factors for DR include high HbA_{1C}, high blood pressure, and duration of diabetes.[6] HbA_{1C} is glycated hemoglobin and serves as a general measure of blood glucose levels. Several large clinical trials found that tight control of blood glucose levels reduced the risk of developing DR.[3, 4] In the Diabetes Control and Complications Trial (DCCT), specifically, a 10% lower HbA_{1C} (7.2% HbA_{1C} compared to 8%) resulted in a 43% lower risk of retinopathy progression.[7] While evidence for a relationship between

hypertension and DR varies, high blood pressure is believed to result in capillary damage in the eyes of diabetic patients. The United Kingdom Prospective Diabetes Study (UKPDS) showed that patients with a systolic blood pressure ≥ 140 mmHg were 2.8 times more likely to develop DR than patients with a systolic blood pressure < 125 mmHg.[8] Finally, duration of diabetes is the strongest predictor for development and progression of DR. The Wisconsin Epidemiologic Study of Diabetic Retinopathy (WESDR) trial found the prevalence of retinopathy was 8% at 3 years after diabetes diagnosis and 80% at 15 years.[5]

Diabetic retinopathy pathology

DR is primarily a set of retinal vascular complications and presents in two clinically distinct stages: nonproliferative (NPDR) and proliferative (PDR). NPDR, the early stage, is characterized by several abnormalities including hemorrhages, microaneurysms, hard exudates, and cotton wool spots. Microaneurysms and hemorrhages occur due to weakened capillary walls. Hard exudates are lipid and protein deposits from leaking capillaries and cotton wool spots are accumulations of axoplasmic debris from damaged nerve fibers.[9, 10] While these features are usually not symptomatic or clinically significant, their number and severity can predict further progression.[11] Finally, basement membrane thickening, retinal capillary nonperfusion, endothelial and pericyte cell death, and capillary atrophy are more severe signs of NPDR.[12, 13]

Capillary atrophy is one factor that contributes to progression to PDR, through focal areas of ischemia resulting in upregulation of growth factors and subsequent neovascularization.[14, 15] The angiogenesis that occurs in PDR results in leaky vessels which may lead to vision loss through blood leakage into the vitreous. Additionally, these

vessels may attach to the vitreous leading to sudden and severe vision loss through tractional retinal detachment.[16]

Diabetic macular edema (DME) is another complication of DR that may occur during either NPDR or PDR and is actually the leading cause of vision loss in patients with DR.[17] Normally, nutrient flow into the retina from its two separate vascular beds (the choroid and the retinal vasculature) is tightly regulated by the blood-retina barrier, which contains two components. The outer blood-retina barrier is formed by the retinal pigmented epithelium (RPE) which controls fluid flow into the retina from the fenestrated choroidal vasculature. The inner blood-retina barrier is formed by tight junctions between retinal endothelial cells. Breakdown of either component of the blood-retina barrier leads to leakage of fluid into the retina, resulting in vision loss due to disruption of the macular structure. Of note, DME can spontaneously resolve, while PDR is typically irreversible without surgery.

Treatments for diabetic retinopathy

There have been several treatments developed for DR aimed at either DME or PDR. For PDR, treatments focus on the predominant hypothesis that tissue ischemia leads to upregulation of growth factors which drive neovascularization. The primary form of treatment for PDR is panretinal photocoagulation. For this treatment, 1000-2000 laser burns are delivered to the peripheral retina, resulting in destruction of hypoxic tissue.[18] The Diabetic Retinopathy Study (DRS) and the Early Treatment Diabetic Retinopathy Study (ETDRS) demonstrated the efficacy afforded by panretinal photocoagulation treatment. Only 5% of eyes receiving laser therapy progressed to severe vision loss after 5 years compared to 50% of untreated eyes.[19] Besides laser therapy, vitrectomy may

be performed on PDR patients to clear vitreous hemorrhage or to ease vitreoretinal traction.

DME may also be treated with laser therapy using focal and/or grid laser photocoagulation. Focal laser therapy directly targets and cauterizes leaking microaneurysms while grid laser photocoagulation is used in areas of diffuse leakage near the macula. These treatments are believed to reduce DME by improving blood-retina barrier function, stopping fluid leakage from leaky vessels, and decreasing blood flow to the macula.[20] In the ETDRS trial, a 50% reduction in risk of moderate vision loss was seen in patients given laser therapy.[20]

While laser therapy has been shown to be effective in preventing progression to severe vision loss in patients with DME or PDR, there is room for development of an improved therapy. In the ETDRS trial, only 3% of patients with DME had significant visual acuity gains.[20] Additionally, laser therapy may have side effects and/or lead to further damage. These effects include decreased central or peripheral vision, reduced night vision, and a risk of accidental laser burn to the fovea.[21-23] Panretinal photocoagulation for PDR may also result in worsening of macular edema.[24] Some of these complications, including pain, may be reduced by using subthreshold micropulse diode laser therapy, which utilizes short pulses to minimize tissue damage.[20]

For most patients, the best outcome from laser therapy is stabilization of vision. Therefore, other therapeutic options focusing on the molecular mechanisms of DR have been explored to improve vision. The most promising of these agents is anti-VEGF therapy. Vascular endothelial growth factor (VEGF) is a protein known to stimulate both vessel permeability and angiogenesis, the main features in DME and PDR. Anti-VEGF

therapy was originally developed for the wet form of age-related macular degeneration (AMD) in which upregulation of VEGF causes choroidal neovascularization.[25] Levels of VEGF have also been reported to be increased in both DME and PDR.[26, 27] Therefore, several clinical trials have been developed to determine efficacy of anti-VEGF for DR. Ranibizumab (Lucentis®), a humanized monoclonal antibody fragment for VEGF, was developed by Genentech and has been approved by the FDA for treatment of AMD. The RIDE and RISE trials to determine efficacy of ranibizumab for treatment of DME found that 36.8% to 51.2% of patients gained ≥ 15 letters of visual acuity with ranibizumab treatment, and this effect remained over 36 months.[28] With the success of these trials, the FDA approved ranibizumab for treatment of DME. Additional trials have been performed with aflibercept (Eylea®, Regeneron), a human recombinant fusion protein of VEGFR and IgG1, pegaptanib (Macugen®, Eyetech Inc.), a VEGF aptamer, and bevacizumab (Avastin®, Genentech), a humanized full-length monoclonal antibody against VEGF, but these agents have not yet been approved for use in DME or PDR.

Anti-VEGF therapy, while efficacious, is not without complications. For PDR, bevacizumab causes initial regression of neovascularization, but the effect is lost with rapid recurrence and by 16 weeks performs no better than a sham injection.[29] For DME, only about 50% of patients had ≥ 15 letters of improvement, signifying many patients are non-responders.[28] Additionally, anti-VEGF therapy carries a number of risks of adverse events, although the incidence rate appears to be low. First, monthly intravitreal injections are not ideal for patients and each injection carries a small risk of endophthalmitis.[28] Additionally, systemic anti-VEGF therapy is associated with a number of adverse effects including hypertension, hemorrhage, congestive heart failure, thromboembolic events,

and wound-healing complications. However, the intravitreal injection of low concentrations of anti-VEGF agents limit these systemic effects and numbers of adverse events are often similar between treatment and sham.[30] It remains to be seen whether long-term treatment of anti-VEGF agents in DR patients, who are already at high risk for myocardial infarction and cerebrovascular events, will lead to increased adverse events. Finally, long-term inhibition of VEGF may be detrimental to the health of the retina. VEGF is a survival factor for a number of cell types including retinal neurons, and VEGF inhibition could lead to neurotoxicity.[31] This has been shown in rabbit retinas in which intravitreal injections of bevacizumab increased caspase 3 and 9 expression as well as mitochondrial disruption and photoreceptor damage.[32] Additionally, VEGF is important for maintaining the integrity of the choroidal vasculature, the vessels responsible for providing oxygen and nutrients to the photoreceptors while other vascular beds have been shown to be susceptible to regression after anti-VEGF therapy.[33, 34]

These issues suggest the need for new therapeutics for DR. Ideally, treatment of DR would occur before progression to the stages that result in vision loss. While several signaling pathways have been implicated in DR pathogenesis, inflammation represents a potentially important target for new therapeutics.

Chronic inflammation as a disease state

Inflammation is a complex process involved in numerous biological and pathological functions. Acute inflammation, characterized by heat, swelling, and pain, occurs shortly after injury or infection to promote healing of the damaged tissue. Chronic inflammation, on the other hand, is prolonged inflammation that does not resolve and is a component of a number of diseases including asthma, heart disease, arthritis, and

celiac disease. The primary contributor to inflammation is the endothelium. In response to an injury, endothelial cells in the vasculature are activated and begin expressing leukocyte adhesion molecules on the plasma membrane. The activated endothelial cells also produce pro-inflammatory cytokines and chemokines. These chemokines recruit and activate leukocytes to the injured tissue. Finally, activated leukocytes adhere to the endothelium, eventually transmigrating into the tissue to heal the injury. Besides leukocyte recruitment, the endothelium is also responsible for edema, which is another component of inflammation. In response to inflammatory stimuli, the tight junctions between endothelial cells open. The resulting exudation of fluid into the tissue carries clotting factors stop to blood flow from broken blood vessels and antibodies to protect against microorganisms.

Inflammation in diabetic retinopathy

In 1964 it was reported that diabetic patients taking aspirin for rheumatoid arthritis had a lower incidence of DR.[35] Since then, numerous studies in both diabetic patients as well as experimental models of diabetes have confirmed inflammation as a component of DR. First, the pro-inflammatory cytokines tumor necrosis factor alpha (TNFα) and interleukin-1 beta (IL-1β) are increased in both the serum and vitreous of patients with PDR.[36, 37] Both TNFα and IL-1β are cytokines that are involved in acute inflammation and serve to further activate cells to produce inflammatory chemokines. TNFα is active in PDR, as vitreous levels of soluble TNF receptors I and II, markers for TNFα activity, are increased in patients with PDR.[38] Additionally, TNFα is even increased in the tears of patients with PDR.[39] Finally, TNFα levels correlate with worsening DR. In 2002, Doganay et al found that serum levels of TNFα increased with progression of DR.[40]

Similarly in 2009, Klein et al found that levels of TNFα were associated with increased risk of severe DR in patients with kidney disease.[41]

Further evidence of the activity of TNFα and IL-1β in patients with DR is the upregulation of numerous chemokines and growth factors. Vitreous levels of eotaxin-1 (CCL11), IL-6, IL-8 (CXCL8), MCP-1 (CCL2), endothelin 1, and VEGF are increased in patients with PDR.[37, 42-44] Many of these proteins are chemokines involved in the recruitment of leukocytes. Finally, levels of soluble adhesion molecules are also increased. Soluble intercellular adhesion molecule 1 (ICAM-1), vascular adhesion molecule 1 (VCAM-1) and E-selectin are increased in the vitreous of patients with PDR.[45] The membrane-bound forms of these proteins are responsible for leukocyte adherence to endothelium.

Retinal leukostasis in diabetic retinopathy

One of the main results of retinal vascular inflammation is leukostasis. In response to inflammatory signals such as TNFα, vascular endothelial cells are activated and begin expressing molecules to capture and adhere leukocytes. The selectins (P-selectin, E-selectin, and L-selectin) are responsible for slowing the velocity of leukocytes and causing them to roll along the endothelial wall of a capillary. P- and E-selectins form weak bonds with Sialyl Lewis x glycans on leukocytes. These bonds result in activation of integrins on the leukocytes. Arrest and firm adhesion is triggered by integrins binding to immunoglobulin proteins. On leukocytes, very late antigen 4 (VLA4, also knowns as $\alpha_4\beta_7$ integrin) binds to VCAM-1 on endothelial cells resulting in firm adhesion to the endothelium. B_2 integrins such as lymphocyte function-associated antigen 1 (LFA1, also known as $\alpha_1\beta_2$ integrin) bind to ICAM-1 and also support rolling and adhesion (**Figure 1**).

Additionally, chemokines bind to the surface of endothelial cells and function to activate integrins on the surface of leukocytes, stimulating arrest.[46]

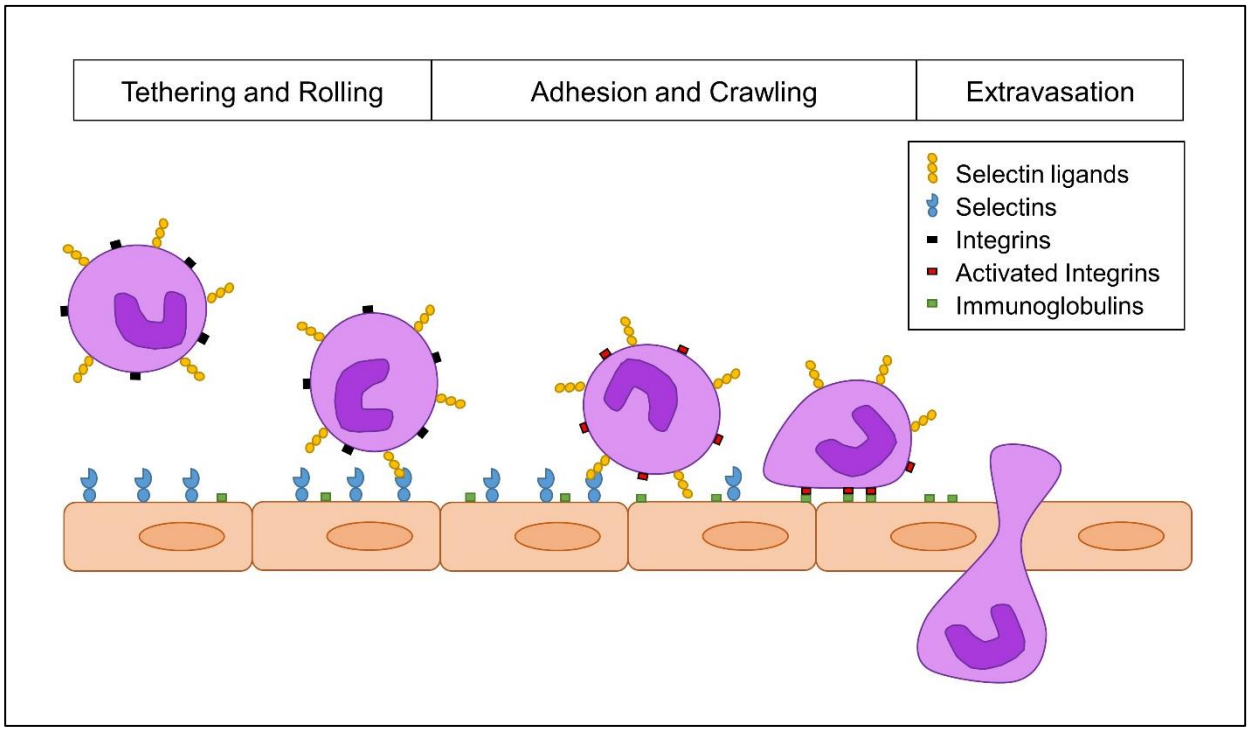

Figure 1. Leukocyte adhesion cascade. Activated endothelium expresses selectins and immunoglobulin superfamily adhesion molecules. Leukocytes flowing through the bloodstream are captured by selectins and roll along the surface of the endothelium. Integrins on the surface of the leukocyte are activated and bind to adhesion molecules (VCAM-1 and ICAM-1) on endothelial cells. The leukocyte crawls along the endothelium and then extravasates into the retinal tissue.

Leukostasis occurs before any other clinical sign of DR. In diabetic rats, retinal leukostasis occurs within 1 week after induction of diabetes and remains constant for at least 4 weeks.[47] Clinically, leukostasis has also been observed in diabetic human patients with NPDR.[48] While leukocyte adhesion is a clear sign that retinal inflammation is occurring in DR, its presence may also cause a significant amount of the damage associated with DR pathology.

First, leukocyte adhesion may contribute to DME by affecting vascular permeability. In an experimental form of diabetes in rats, leukostasis correlated with

retinal vascular permeability and blocking leukostasis with an antibody against ICAM-1 resulted in decreased vascular leakage.[47] In another study using diabetic mice, blocking leukostasis with an antibody for ICAM-1 or an antibody for the integrin CD18 on leukocytes also inhibited blood-retina barrier breakdown.[49] In rat brain vasculature, neutrophil adhesion is associated with lower expression of the tight junction proteins occludin and zonula occludens-1 and redistribution of the adherens junction protein vinculin.[50] These proteins normally form a barrier between endothelial cells, preventing fluid exudation from the vasculature. Finally, in an *in vitro* assay, polymorphonuclear leukocyte cell adhesion to human umbilical vein endothelial cells (HUVEC) resulted in increased endothelial cell permeability.[51]

In addition to contributing to vascular permeability, leukocytes can also affect endothelial cell death and capillary atrophy. Inhibiting leukostasis in mice and rats through a variety of mechanisms results in fewer injured endothelial cells, pericyte ghosts, and acellular capillaries.[49, 52, 53] Additionally, numbers of leukocytes correlate with choroid capillary dropout in human diabetic eyes.[54] *In vitro*, neutrophil co-culture with human dermal microvascular endothelial cells resulted in increased endothelial cell apoptosis involving the proteins Fas and its ligand FasL.[55] Similar results were seen *in vivo* in diabetic rat retinas. Finally, inhibiting the Fas-FasL system also prevented retinal vascular permeability induced by diabetes in rats.[55]

Leukocyte adhesion may contribute to vascular leakage and endothelial apoptosis through two mechanisms: vessel blockage with resulting capillary nonperfusion and extravasation into the tissue with resulting production of inflammatory mediators. In animal models of retinal leukostasis, leukocyte occlusion of capillaries has been shown

to block perfusion, which correlated with the number of acellular capillaries.[47, 52] Capillary degeneration then develops into focal areas of ischemia, eventually resulting in upregulation of growth factors and neovascularization. Further evidence for the importance of leukocytes in vascular remodeling comes from experiments in the developing eye. During development, areas of dense leukocytes correlate with areas of less dense vasculature and the leukocytes are responsible for vascular pruning.[56] They also appear in high oxygen conditions immediately preceding vaso-obliteration.[56]

In addition to blocking capillaries, leukocytes can extravasate into the tissue and produce inflammatory factors. In mice, inhibition of leukostasis resulted in less superoxide generation in the retina.[53] Furthermore, leukocytes isolated from both diabetic cats and diabetic human patients show increased superoxide production compared to isolated healthy leukocytes.[57, 58] In other systems, leukocytes produce cytokines that can contribute to further inflammation. Peritoneal macrophages have been shown to secrete TNFα in response to the endotoxin lipopolysaccharide (LPS).[59] In mice, T cells cause experimental autoimmune encephalitis through production of TNFα and interferon-γ.[60]

If inflammation is truly a causative factor of DR pathology, anti-inflammatory therapies would be expected to reduce DR. This has been the case in experimental diabetes models. In diabetic rats, high dose aspirin, the NSAID meloxicam, and the TNFα inhibitor etanercept all inhibited leukostasis, blood-retina barrier breakdown, acellular capillary formation, and nuclear factor kappa B (NF-κB) activation.[61, 62] In diabetic dogs, aspirin inhibited the formation of acellular capillaries and retinal hemorrhages.[63] In human patients, clinical trials determining the efficacy of aspirin treatment for DR have produced contradictory results. In the DAMAD trial, aspirin reduced the number of

microaneurysms.[64] However, in the ETDRS trial, aspirin had no effect on DR pathology, although this result may have been due to greater DR severity at the start of the trial.[65] Other trials have examined the use of steroids, which have anti-inflammatory properties. Intravitreal injection of the steroid triamcinolone improves visual acuity in both DME and PDR patients, but carries a risk of cataract formation and elevation of intraocular pressure.[66, 67]

Peroxisome proliferator-activated receptors

The peroxisome proliferator-activated receptors (PPARs) are a family of nuclear receptors that function as transcription factors. There are three subtypes with distinct tissue expression patterns and functions. PPARα (NR1C1) is found primarily in liver, heart, intestine, and kidney and is important in fatty acid uptake and oxidation. PPARβ/δ (NR1C2) is ubiquitously expressed and has a primary role in fatty acid catabolism. PPARγ (NR1C3) is found primarily in adipose tissue, colon, and macrophages and is responsible for adipocyte differentiation and energy homeostasis. In addition to these roles, PPARs have been shown to regulate numerous other processes including inflammation, angiogenesis, wound healing, and metabolism.

Like other nuclear hormone receptors, PPARs have a modular structure consisting of a ligand-independent activation domain (AF-1), a zinc-finger DNA-binding domain, hinge region, and a ligand-binding domain that also contains a ligand-dependent activation region (AF-2). The DNA-binding domains of the 3 PPARs are highly conserved, with a sequence homology between 83-86%. The ligand-binding domain is less conserved, with only between 68-72% homology. The ligand binding pockets of the PPARs are much larger and more open than other nuclear receptors which may account

for the wide range of ligands, including fatty acids and fatty acid metabolites, which are able to bind PPARs.[68] PPARs form heterodimers with the retinoid X receptor (RXR), and bind to specific peroxisome proliferator-activated response elements (PPRE) in DNA. These PPREs consist of direct repeats of AGGTCA separated by one base pair.

PPARβ/δ regulation

Probably owing to its ubiquitous expression and lack of specific ligands, the studies on PPARβ/δ have lagged behind those of PPARα and PPARγ. PPARβ/δ was originally discovered in the early 1990s by several groups around the same time and named PPARβ in *Xenopus* and PPARδ in mouse and human.[69-71] It was later discovered that PPARβ/δ is activated by fatty acids, triglycerides, *all-trans* retinoic acid, and prostacyclin.[69, 72-75] Additionally, several specific agonists and antagonists have been developed for PPARβ/δ including the commonly used agonists GW501516 and GW0742, as well as the antagonist GSK0660.[76-78]

Following from its ubiquitous expression, PPARβ/δ activation has been shown to have a role in numerous physiological processes. The main function of PPARβ/δ is fatty acid catabolism in which it promotes fatty acid oxidation in multiple tissues as well as improves lipid profiles in humans.[73, 79-81] Additionally, PPARβ/δ regulates differentiation in a variety of cell types including oligodendrocytes, trophoblasts, and keratinocytes.[82-84] Finally, PPARβ/δ has diverse and sometimes contradictory roles in angiogenesis, tumorigenesis, wound healing, development, and inflammation.

PPARβ/δ regulates these processes through complex interactions with ligands, DNA, and cofactors (**Figure 2**). The most straightforward way PPARβ/δ can regulate protein expression is through direct activation of gene transcription. In this mechanism,

activation of the PPARβ/δ and RXR heterodimer by a ligand results in dissociation of corepressors, recruitment of coactivators, and binding to a PPRE to induce gene transcription. Most of the work identifying coactivators of PPARs have been specific to PPARα and PPARγ, but PPARβ/δ is known to bind the coactivator PGC-1α.[85] Additionally, PPARβ/δ is able to directly repress transcription of genes by binding to corepressors including SMRT, SHARP, and NCoR.[86] In this way, PPARβ/δ may inhibit PPARα and PPARγ signaling by preventing their binding to PPREs.[87] Finally, PPARβ/δ may regulate gene expression through transrepression, which is the inhibition of protein function by protein-protein interaction. PPARβ/δ has been shown to sequester B-cell lymphoma 6 (BCL6), preventing it from influencing gene transcription.[88] Upon ligand activation of PPARβ/δ, BCL6 is released to repress gene transcription. Additionally, PPARβ/δ binds transcription factors such as NF-κB, preventing its effect on gene transcription.[89] Other more indirect mechanisms include competition for binding partners (RXR, corepressors, coactivators). For example, PPARβ/δ inhibits LXR signaling by competing with LXRα for binding to RXR.[90]

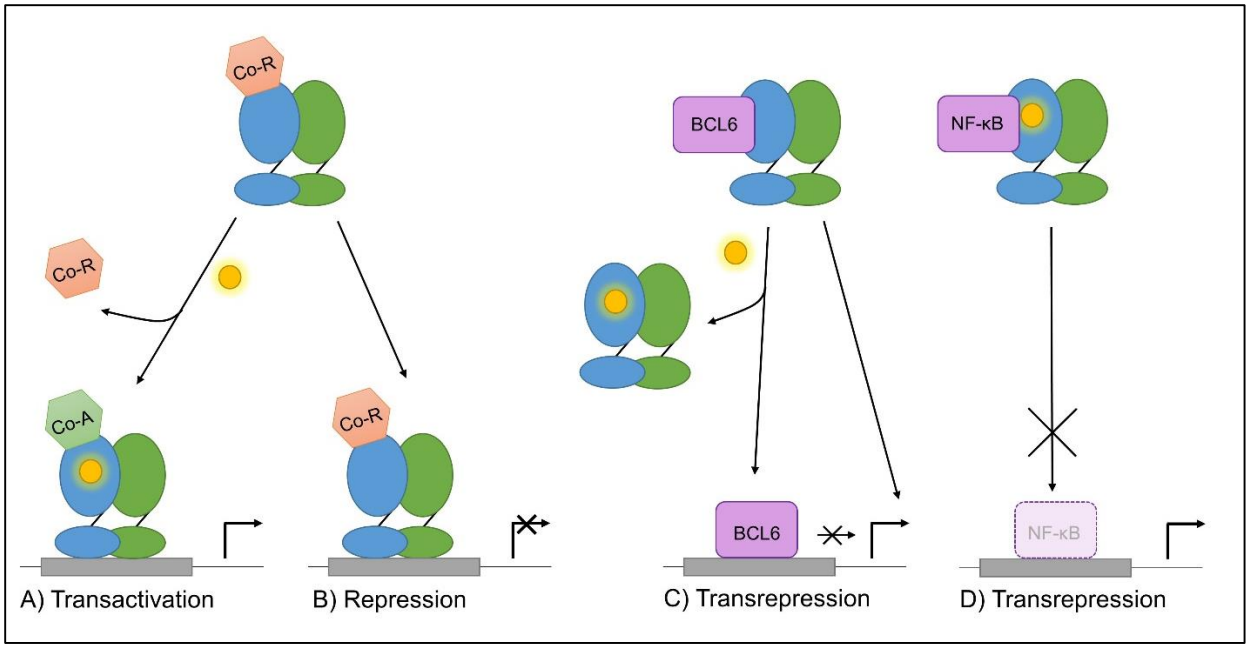

Figure 2. Mechanisms of PPARβ/δ on transcriptional activity. A) Ligand (yellow) binding to PPARβ/δ (blue) causes release of corepressors and recruitment of coactivators. The activated PPARβ/δ and RXR heterodimer binds to PPREs and increases gene transcription. B) Inactive PPARβ/δ and RXR bound to corepressors can inhibit gene transcription. PPARβ/δ can also affect gene transcription through transrepression C-D. C) PPARβ/δ binds BCL6 allowing inflammatory gene transcription. Ligand activation of PPARβ/δ releases BCL6 to repress inflammatory gene transcription. D) PPARβ/δ can bind transcription factors such as NF-κB and prevent their activity. Figure is adapted from Daynes et al 2002 and Tan et al 2005.[91, 92]

PPARs in diabetes and diabetic retinopathy

There is substantial evidence supporting a beneficial effect of PPARα and PPARγ in diabetes and DR. These receptors are useful in reversing the metabolic dysfunction, insulin resistance, and dyslipidemia associated with type 2 diabetes and both are widely considered to be anti-inflammatory and anti-angiogenic. Drugs targeting both of these receptors have been approved for clinical use. Fibrates (bezafibrate, fenofibrate, gemfibrozil, etc) activate PPARα and are used as treatment for hyperlipidemia and dyslipidemia. Additionally, fenofibrate has recently been approved for use in DR in Australia. The Fenofibrate Intervention and Event Lowering in Diabetes (FIELD) and the Action to Control Cardiovascular Risk in Diabetes (ACCORD) studies reported a reduced

need for laser therapy and a slower progression of retinopathy with fenofibrate treatment.[93, 94] Thiazolidinediones (rosiglitazone, pioglitazone, troglitazone, etc) are PPARγ activators and are currently used to increase insulin sensitivity, reduce HbA_{1C}, and improve hyperinsulinemia in diabetic patients. PPARγ agonists have been reported to have a mixed effect on DME with the ACCORD study noting no effect of thiazolidinediones on DME while another group showed thiazolidinediones increased risk of DME.[95, 96]

There is evidence that PPARβ/δ may also be beneficial in type 2 diabetes. PPARβ/δ activation increases insulin sensitivity, islet function, and glucose metabolism and reduces weight in various animal and cell models.[97-99] Furthermore, single-nucleotide polymorphisms of PPARβ/δ have been associated with overall adiposity, BMI, and HDL levels.[100, 101] Phase II clinical trials with the PPARβ/δ agonist, GW501516, also support the role of PPARβ/δ in fat metabolism. In these trials, GW501516 increased HDL levels and triglyceride clearance as well as reduced LDL and insulin levels.[81, 102] However, GlaxoSmithKline discontinued further trials and there are currently no clinically available drugs targeting PPARβ/δ. Additionally, although PPARβ/δ is expressed in the eye, very little is known about PPARβ/δ in the retina. With the possibility of developing pan-PPAR agonists, elucidating the role of PPARβ/δ in DR, particularly in inflammation and angiogenesis, becomes critical.

PPARβ/δ in inflammation

Most of the evidence to date suggests that agonists of PPARβ/δ, like those for PPARα and PPARγ, are anti-inflammatory. Activating PPARβ/δ in a variety of inflammatory environments reverses inflammation. For example, in models of ischemia

and reperfusion, PPARβ/δ prevents upregulation of inflammatory cytokines TNFα, IL-1β, CCL2 and IL-6, as well as the adhesion protein ICAM-1.[103-105] In agreement with this, PPARβ/δ activation also reduces myeloperoxidase staining indicative of leukocyte invasion, and has been shown to inhibit macrophage and monocyte infiltration into tissue after ischemia and reperfusion injury.[103, 104] Similar results have been shown in models of sepsis and chemically-induced organ failure where agonist treatment promoted survival and prevention of an inflammatory response.[89, 106] Further evidence for an anti-inflammatory role of PPARβ/δ comes from animal knockout studies. Deletion of PPARβ/δ worsened organ dysfunction and increased leukocyte infiltration during sepsis.[107] Knockout mice also have an exacerbated inflammatory response to carbon tetrachloride-induced hepatotoxicity.[108]

Finally, PPARβ/δ also prevents inflammation-induced by toxins such as LPS, advanced glycation end products (AGE), and TNFα in cell culture. Agonist treatment prevented the upregulation of TNFα, IL-6, and receptor for advanced glycation end products (RAGE) by AGE in human embryonic kidney cells and inhibited the upregulation of LPS-induced TNFα in cardiomyocytes.[109, 110] Furthermore, a PPARβ/δ agonist inhibited TNFα-induced adhesion molecules VCAM-1 and E-selectin expression in HUVEC, which prevented leukocyte adhesion.[111]

The mechanism through which PPARβ/δ influences inflammation is still not completely understood. One theory is that PPARβ/δ inhibits NF-κB activation. Indeed, activation of PPARβ/δ prevented the induction of NF-κB activity in the heart of high fat diet-fed mice.[112] In human embryonic kidney cells treated with AGE, PPARβ/δ reduced NF-κB (p65 subunit) nuclear localization and increased expression of the NF-κB inhibitor,

IκBα.[109] Another possibility is that PPARβ/δ binds directly to NF-κB to inhibit its transcriptional activity. This has been shown in murine microglia where radiation-induced inflammation was reversed by PPARβ/δ interacting directly with the p65 subunit of NF-κB.[113]

Other systems, however, have shown the role of PPARβ/δ in inflammation to be more complicated. While one study suggested that PPARβ/δ promotes macrophage conversion to the alternative, anti-inflammatory phenotype, another found no effect of PPARβ/δ on macrophage phenotype.[114, 115] A third study found that interestingly, both ligand activation and deletion of PPARβ/δ were anti-inflammatory, resulting in decreased expression of CCL2, IL-1β, and MMP9 in macrophages. Overexpression of PPARβ/δ, however, increased expression of these same genes.[88] This suggested that unliganded PPARβ/δ is responsible for inflammatory gene expression, and the evidence pointed to transrepression of BCL6, an inflammatory suppressor, as the mechanism. When BCL6 is bound to PPARβ/δ, transcription of inflammatory genes is able to occur. However, when PPARβ/δ is removed or when it is activated by a ligand, BCL6 is released, allowing it to repress inflammatory gene transcription. This mechanism was further shown in pancreatic beta cells. Activation of PPARβ/δ did not affect expression of CCL2 in these cells as they do not express BCL6.[116]

Additionally, there are a few reports in the literature suggesting that PPARβ/δ may support a pro-inflammatory action. Treating mice with a toxin along with a PPARβ/δ agonist resulted in increased gastric tumor formation with a pro-inflammatory gene signature.[117] Additionally, overexpression of PPARβ/δ in conjunction with agonist treatment caused an inflammatory psoriasis-like skin condition.[118] Despite these

reports, the majority of evidence points towards PPARβ/δ being anti-inflammatory, and it is likely to perform a similar function in DR.

PPARβ/δ in angiogenesis

Unlike PPARα and PPARγ, PPARβ/δ is believed to be angiogenic and anti-apoptotic. In fact, PPARβ/δ has found to be a “hub node” in angiogenesis, promoting colon cancer growth.[119] PPARβ/δ can affect angiogenesis by promoting both endothelial cell survival and growth. *In vitro*, activation of PPARβ/δ prevents H_2O_2 stress-induced apoptosis of HUVEC and hypoxia-induced apoptosis of endothelial progenitor cells (EPC).[120, 121] In addition to promoting survival, PPARβ/δ also stimulates proliferation of HUVEC and EPC.[121, 122] Furthermore in HUVEC, agonist stimulation increased expression of VEGF.[122]

In vivo, PPARβ/δ promotes angiogenesis. In the tibialis muscle, activation of PPARβ/δ promotes capillary growth, as well as VEGF expression through a process involving the phosphatase calcineurin.[123] Furthermore, PPARβ/δ activation promoted corneal neovascularization through vasculogenesis.[121] Finally, lung tumor growth is inhibited in mice with PPARβ/δ deletion. The vasculature in the tumors of the knockout mice were abnormal and immature, characterized by hyperplasia and reduced patency.[124] Taken together, PPARβ/δ is likely to play a role in DR, both in the components of inflammation and angiogenesis, although its effect remains to be seen.

Chapter 2

The inverse agonist of PPARβ/δ, GSK0660, has a role in TNFα-induced chemokine expression in retinal endothelial cells

**Portions of this chapter have been published previously in Savage SR et al. RNA-seq identifies a role for the PPARβ/δ inverse agonist GSK0660 in the regulation of TNFα-induced cytokine signaling in retinal endothelial cells. Molecular Vision. 2015.[125]*

Introduction

In order to study the role of PPARβ/δ in DR, it is best to start with well-controlled *in vitro* experiments. However, it is difficult to model the long-term, systemic conditions of diabetes and DR in cell culture. A good surrogate stimulus to study the process of inflammation seen in DR is TNFα. TNFα is upregulated in both the serum and vitreous of DR patients, and its levels correlate with DR severity.[36, 40] Use of a TNFα inhibitor, etanercept, reduced endothelial cell death and leukostasis in a short-term model of diabetes in rats.[61, 126] Moreover intravitreal injection of infliximab, a TNFα monoclonal antibody, increased visual acuity in a small cohort of patients with AMD.[127] However, these drugs are not optimized for DR, as other studies using small cohorts indicated neither infliximab nor etanercept had an effect on visual acuity in patients with DME.[128, 129]

TNFα-induced inflammation recapitulates the inflammatory changes seen in DR. TNFα stimulation of retinal endothelial cells increased the expression of chemokines including CXCL8, CCL2, and GROα (CXCL1) which are also increased in the vitreous of DR patients.[42, 130] Additionally in HUVEC, TNFα increased expression of the adhesion molecules ICAM-1, VCAM-1, and E-selectin, which are also upregulated in DR.[45, 131] Together, these proteins result in increased leukocyte adhesion to endothelial cells and leukostasis in the retina. As further proof, human monocyte adhesion to retinal endothelial

cells was stimulated by TNFα.[132] Additionally, TNFα is important in both retinal leukostasis and blood-retinal barrier breakdown as both features were abolished in diabetic TNFα-knockout mice.[133]

TNFα influences signaling by first binding to its receptors TNFR1 and TNFR2, although TNFR2 is activated primarily by membrane-bound TNFα and not by soluble TNFα. TNFR1 signals by recruiting the protein TRADD. TRADD then binds to multiple other proteins to influence signaling. One of these proteins is TRAF2, which activates both the c-Jun N-terminal kinase (JNK) and NF-κB pathways. Through these pathways, TNFα promotes cell proliferation and inflammation. TRADD can also bind to FADD to induce a death-inducing signaling pathway involving caspase 8. While the signaling pathways activated by TNFα are well known, the downstream effect of TNFα on retinal microvascular endothelial cells has not been fully characterized.

Activation of PPARβ/δ has been shown to influence TNFα signaling in cell systems outside of the eye. In HUVEC, PPARβ/δ agonists inhibited TNFα-induced expression of adhesion molecules and subsequently prevented TNFα-induced leukocyte adhesion to endothelial cells.[111, 134] However, few studies have been done using the specific antagonist of PPARβ/δ, GSK0660, which also has inverse agonist effects when used alone.[76] As it is predicted that inhibiting PPARβ/δ will prevent retinal angiogenesis seen in PDR, it is useful to know how inhibiting PPARβ/δ affects vascular endothelial cell inflammation.

To determine the full effect of TNFα on retinal microvascular endothelial cells, as well as the effect that inhibition of PPARβ/δ has on TNFα-induced inflammation, RNA-sequencing technology is a clear choice. RNA-seq is a robust method to determine

differential expression of mRNA transcripts between various treatment groups. Compared to microarray technology, it is more sensitive, has a broader dynamic range, and allows for identification of novel transcripts.[135]

Methods

Culture of human retinal endothelial cells and RNA isolation

Primary human retinal microvascular endothelial cells (HRMEC; catalog #ACBRI 181) were purchased from Cell Systems (Kirkland, WA) and grown in endothelial basal medium (EBM; Lonza; Walkersville, MD) with 10% fetal bovine serum (FBS; Atlanta Biologicals; Flowery Branch, GA) and endothelial growth supplements (EGM SingleQuots; Lonza). Cultures were kept in a humidified cell culture incubator at 37°C in 5% CO_2. Cells were plated in 6-well dishes coated with attachment factor (Cell Systems) and grown to 70% subconfluency. Medium was changed to 2% FBS with one of the following treatment schemes (**Figure 3**): vehicle (0.1% DMSO) for 24 hrs then vehicle for 4 hrs, vehicle for 24 hrs then 1 ng/ml TNFα (Sigma-Aldrich; St. Louis, MO) + vehicle for 4 hrs, or 10 μM GSK0660 (Tocris; Minneapolis, MN) for 24 hrs, then TNFα + GSK0660 for 4 hrs. Cells were lysed and total RNA was isolated from cell lysates using an RNeasy kit (Qiagen; Valencia, CA) according to the manufacturer's directions.

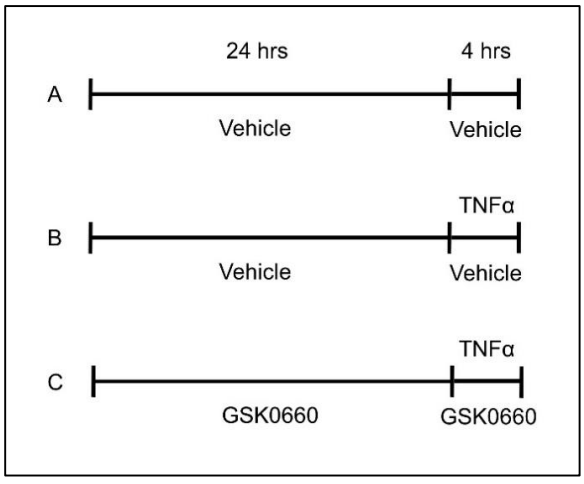

Figure 3. Treatment scheme for RNA-seq. HRMEC samples were treated with vehicle for 24 hrs and then A) vehicle or B) 1 ng/ml TNFα plus vehicle for 4 hrs. C) Other HRMEC samples were treated with 10 μM GSK0660 for 24 hrs and then TNFα plus GSK0660 for an additional 4 hrs.

Library preparation and RNA-sequencing

RNA samples were submitted to the Vanderbilt VANTAGE core for RNA-sequencing. RNA quality was determined using the 2100 Bioanalyzer (Agilent Technologies; Santa Clara, CA). All samples had an RNA-integrity number of 10, which indicates high quality and lack of degradation of the RNA. Libraries were prepared using the TruSeq RNA Sample Prep Kit (Illumina; San Diego, CA) to enrich for poly(A)-containing mRNA and generate cDNA. This kit uses oligo-dT attached to magnetic beads to capture the poly(A) tail of mRNAs. The mRNA was then fragmented and reverse-transcribed into double stranded cDNA. Adapter sequences were ligated to the cDNA and then the cDNA was amplified by PCR. Finally, library quality was confirmed using the 2100 Bioanalyzer. The libraries were sequenced using a 30 million, 50 bp single read protocol on the Illumina HiSeq 2500 (Illumina). Sequence data were deposited at the NCBI Short Read Archive under the accession number SRP053124.

Sequence alignment and differential expression

Sequence alignment and differential expression were performed by the Vanderbilt VANGARD core. TopHat v2.0.9 was used to align sequences to the University of California, Santa Cruz (UCSC) human reference genome hg19 and the transcript annotation of Ensembl's GRCh37 using default parameters.[136] Raw counts of mapped reads were generated using HTSeq and then used by the program MultiRankSeq which utilizes the edgeR algorithm to determine differential expression.[137, 138] Comparisons were made between vehicle and TNFα-treated HRMEC, and between TNFα-treated HRMEC and TNFα-treated HRMEC with GSK0660. Transcripts were considered to be significant with an adjusted p value < 0.05. The list was further reduced to transcripts with

a fold change greater than or equal to 2. The Euler diagram was generated using the R package utility VennDiagram.[139]

Gene ontology, pathway analysis, and network visualization

The lists of differentially expressed genes were submitted to the Database for Annotation, Visualization and Integrated Discovery (DAVID) v6.7 for gene ontology (GO) and pathway analysis.[140, 141] GO was determined using the GOTERM_BP_FAT dataset which includes the lower levels of the biological process ontology. GO terms were considered enriched with an EASE score < 0.05. The EASE score is a modified Fisher Exact P-Value. Pathway enrichment was determined using the Kyoto Encyclopedia of Genes and Genomes (KEGG) Pathway annotation. Pathways were considered enriched with an EASE score < 0.05. Cytoscape v3.2.0 with the PINA4MS v1.1 plugin was used for network visualization.[142, 143] Lists of differentially expressed genes were combined with protein interaction data from the PINA platform to generate a network. Disconnected components of fewer than three nodes were discarded. Nodes of genes differentially expressed by TNFα compared to vehicle were colored green while nodes of genes differentially expressed by TNFα plus GSK0660 compared to TNFα were colored red. Genes found in both lists were colored half green and half red. Nodes were connected by edges based on the protein interaction data. Protein-protein interactions were indicated by blue lines while kinase-substrate interactions were indicated by pink arrows. Node size was correlated to the degree of connectivity, and nodes were arranged by an edge-weighted spring embedded layout.

qRT-PCR validation

RNA was reverse transcribed to cDNA using the High-Capacity cDNA Archive Kit (Applied Biosystems; Carlsbad, CA) according to the manufacturer's directions. Quantitative real-time PCR (qRT-PCR) was performed by amplification of the gene of interest (*ANGPTL4*, *CCL8*, *NOV*, *CXCL10*, or *PDPK1*) vs. *ACTB* (β-actin) using gene-specific TaqMan Gene Expression Assays (Applied Biosystems). Taqman gene expression IDs are found in **Appendix A**. Data were analyzed using the comparative Ct method and Ct values were normalized to *ACTB* levels. Statistical significance was determined using the statistical software JMP (SAS Institute; Cary, NC) and ANOVA with student's t post hoc analysis. Data were considered significant with $p < 0.05$.

Results

RNA-seq quality and alignment

When performing an RNA-seq experiment, several parameters must be taken into consideration. RNA-seq experiments can differ by sample number, sequencing depth, read length, and whether the sequencing is single read or paired end. These parameters are determined by the cell type or tissue being used and the question to be answered, with cost being taken into consideration. As I was interested primarily in differential expression between treatment groups of mammalian cells, sequencing 30 million reads of 50 bp in length for single strands was optimal.

To determine the effect of GSK0660 on TNFα-dependent gene expression in HRMEC, three samples each of mRNA from HRMEC treated with vehicle, TNFα plus vehicle, or TNFα plus GSK0660 were sequenced. Total numbers of reads generated ranged between 28,275,640 and 33,252,277, which covered 32,009 different transcripts

(**Table 1**). There was no difference in the total number of reads across the 9 samples (ANOVA, p = 0.07). Only between 311 and 1084 reads were removed due to low quality before mapping. On average, 96.5% of the reads mapped to the UCSC human genome hg19, assisted by the reference gene annotation from Ensembl's GRCh37.

Treatment	Sample	Total Reads	Reads Removed	% Mapped
Vehicle	1	32,679,282	1084	96.5
	2	30,523,915	702	97.2
	3	32,300,955	849	97
TNFα	1	30,718,657	442	94
	2	32,350,282	981	96.4
	3	33,252,277	438	97.1
TNFα + GSK0660	1	28,275,640	354	97
	2	30,126,192	311	97
	3	30,237,101	807	96.1

Table 1. **Summary of reads mapping to the human genome (UCSC hg19) using TopHat v2.0.9.** Total reads for 3 samples each of vehicle, TNFα, and TNFα + GSK0660 treated HRMEC were generated using RNA-seq and then mapped to the human genome UCSC hg19.

Treatment Comparison	Transcripts with adj p < 0.05	Upregulated Transcripts (≥ 2)	Downregulated Transcripts (≤ -2)
TNFα vs Vehicle	1830	746	1084
TNFα + GSK0660 vs TNFα	273	169	104

Table 2. Summary of RNA-seq differential expression analysis. Differential expression was determined using edgeR and transcripts were considered significantly changed with adjusted p < 0.05 and fold change of at least 2.0.

Differential expression

Differential expression of transcripts was determined using the MultiRankSeq program, which determines differential expression using the edgeR algorithm from raw read counts assembled by HTSeq. Pairwise analyses were performed between the TNFα- and vehicle-treated cells as well as between the TNFα- and TNFα plus GSK0660-treated cells. Transcripts were considered significant with an adjusted p value < 0.05 and a fold

change of at least 2.0 in either direction. Using these parameters, 1830 transcripts were differentially expressed in the TNFα-treated cells compared to vehicle. TNFα plus GSK0660 treatment altered the expression of 273 transcripts compared to TNFα alone (**Table 2**).

Gene Symbol	Log2FoldChange	Adj P Value	Ensembl ID
Upregulated Genes			
LAD1	6.421452313	1.10E-07	ENSG00000159166
CSF2	6.39995987	<0.000001	ENSG00000164400
TNFAIP6	6.358926206	2.18E-154	ENSG00000123610
CX3CL1	6.121874962	<0.000001	ENSG00000006210
CXCL10	5.706389982	6.14E-222	ENSG00000169245
HLA-DOB	5.667011352	5.01E-13	ENSG00000241106
ETV3L	5.616009893	1.07E-05	ENSG00000253831
CCL5	5.487915198	5.76E-257	ENSG00000161570
TNF	5.486418289	4.71E-52	ENSG00000232810
GBP7	5.455106479	1.78E-05	ENSG00000213512
Downregulated Genes			
RBM20	-4.29030613	0.009588413	ENSG00000203867
PAK6	-4.29073104	0.026177447	ENSG00000137843
OR1F1	-4.291371288	0.00855682	ENSG00000168124
MYO18B	-4.474679753	0.004370114	ENSG00000133454
CSRNP3	-4.474760229	0.004370114	ENSG00000178662
CR1	-4.634084683	0.003662894	ENSG00000203710
ARL14	-4.783629776	0.001145234	ENSG00000179674
STOX2	-4.915666474	0.000890805	ENSG00000173320
FAM151A	-4.916414121	0.000585614	ENSG00000162391
MUC20	-5.040180048	0.000485122	ENSG00000176945

Table 3. Top 10 upregulated and downregulated protein-coding genes by TNFα in HRMEC. Transcript fold change and adjusted p value of transcripts expressed by TNFα-treated HRMEC compared to vehicle-treated were determined by the edgeR algorithm.

Effect of TNFα on HRMEC

Stimulation of HRMEC with TNFα resulted in large changes in gene expression, with the top 10 (based on fold change) upregulated and downregulated transcripts of protein-coding genes summarized in **Table 3**. Notably, TNFα increased expression of

CCL5, *CX3CL1*, and *CXCL10*, all of which have roles in leukocyte recruitment. Additionally, TNFα increased transcription of itself.

To determine the function of the transcripts differentially expressed by TNFα, I used the DAVID tool for functional annotation. In terms of gene ontology, 344 GO biological pathway terms were significantly enriched, with the top 20 (based on significance) summarized in **Figure 4**. Significant terms included immune response, response to wounding, and inflammatory response. Another common theme included terms for regulation of endothelial behavior, such as regulation of cell proliferation, vasculature development, cell adhesion, and chemotaxis.

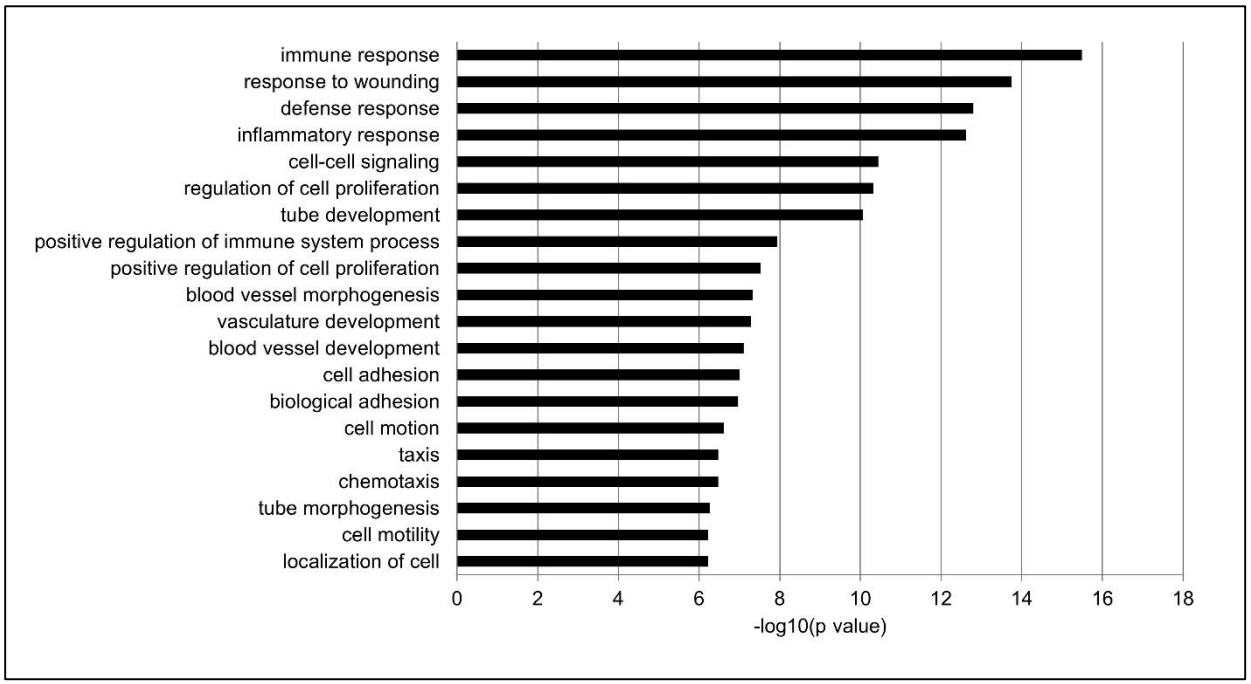

Figure 4. Top 20 biological pathway GO terms enriched in TNFα-treated HRMEC. Biological Pathway GO term enrichment in TNFα-treated HRMEC compared to vehicle-treated HRMEC was determined using DAVID. Terms were considered significant with $p < 0.05$.

To further characterize the transcripts, I used the KEGG database to determine pathway enrichment. The pathways most highly enriched in TNFα-treated cells included cytokine-cytokine receptor interaction (53 transcripts), chemokine signaling pathway (30

transcripts), and Jak-STAT signaling pathway (26 transcripts) (**Figure 5**). Additional pathways through which TNFα may affect HRMEC included calcium signaling, Toll-like receptor signaling, hedgehog signaling, and the complement cascade.

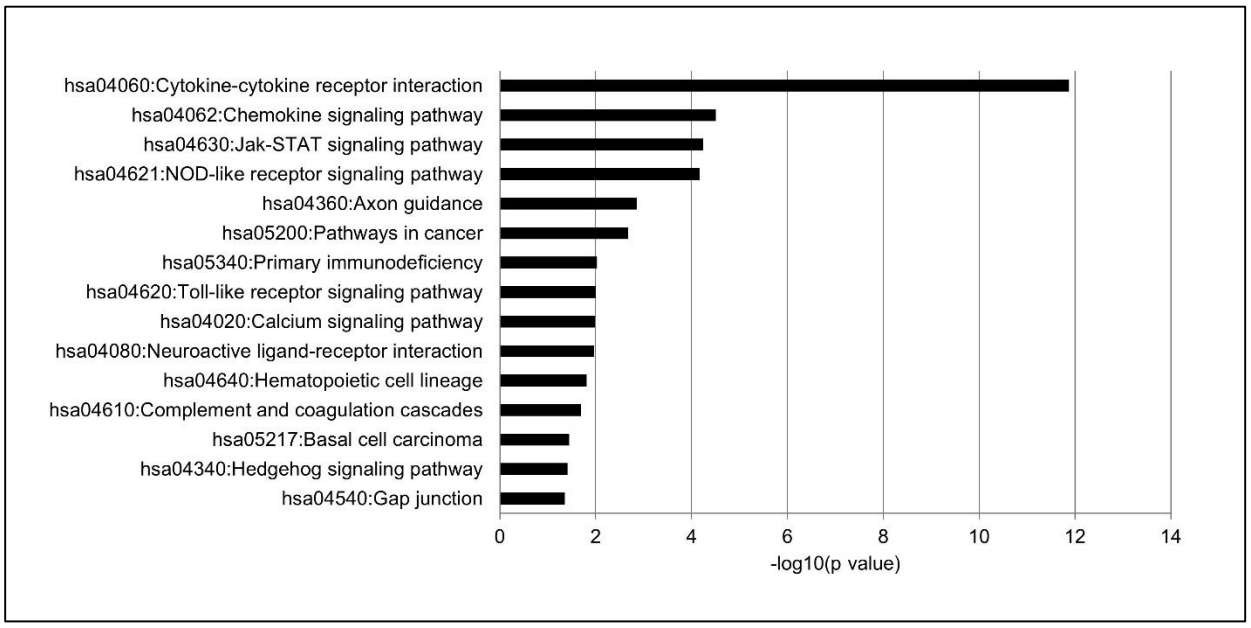

Figure 5. KEGG pathways enriched in TNFα-treated HRMEC. Pathway enrichment was determined for differentially expressed transcripts by TNFα compared to vehicle using DAVID. Pathways were considered enriched with $p < 0.05$.

The effect of GSK0660 on TNFα-treated HRMEC

The effect of GSK0660 on TNFα-regulated gene expression in HRMEC was determined; the top upregulated and downregulated protein-coding transcripts are summarized in **Table 4** while the full dataset can be found in **Appendix B**. Among those most highly downregulated by GSK0660 in TNFα-treated cells, *CCL8* is of interest due to its role in leukocyte recruitment. Also of note, GSK0660 prevented the TNFα-induced downregulation of *FAM151A*, *MUC20*, *STOX2*, and *ARL14*. These four transcripts were among those most highly downregulated by TNFα compared to vehicle. Additionally, GSK0660 affected transcription of 1 (*CXCL10*) of the top 10 genes upregulated by TNFα.

Gene Symbol	Log2FoldChange	Adj P Value	Ensembl ID
Upregulated Genes			
CBFA2T3	4.970269827	0.001038075	ENSG00000129993
FAM151A	4.837332922	0.002008674	ENSG00000162391
MUC20	4.702950855	0.011947675	ENSG00000176945
STOX2	4.133641693	0.027737782	ENSG00000173320
ARL14	4.133638802	0.027737782	ENSG00000179674
BEAN1	3.364047225	0.004043429	ENSG00000166546
WISP2	3.130060871	0.012964106	ENSG00000064205
GPLD1	3.129996475	0.012964106	ENSG00000112293
UBASH3A	2.850826781	0.04000081	ENSG00000160185
GOLGA8R	2.850824538	0.04000081	ENSG00000186399
Downregulated Genes			
KIT	-1.992297751	3.64E-30	ENSG00000157404
PKD2L2	-2.016705824	0.026490386	ENSG00000078795
LCP2	-2.553894739	0.000489648	ENSG00000043462
TMPRSS9	-2.784724078	0.006155424	ENSG00000178297
FOXG1	-2.834209583	0.039176409	ENSG00000176165
CH25H	-3.087262332	0.014984916	ENSG00000138135
CCL8	-3.445451904	0.000244835	ENSG00000108700
HIST1H3J	-4.043009187	0.039661319	ENSG00000197153
CCDC73	-4.252616175	0.022003857	ENSG00000186714
SERPING1	-4.25281999	0.022002453	ENSG00000149131

Table 4. Top 10 protein-encoding genes that were upregulated or downregulated by GSK0660 in TNFα-treated HRMEC. Transcript fold change and adjusted p value were determined using the edgeR algorithm.

Gene ontology revealed 33 GO terms that were significantly enriched. Similar to TNFα treatment alone, TNFα treatment plus GSK0660 affected regulation of cell proliferation and response to wounding (**Figure 6**). The terms also included reproduction, integrin-mediated signaling pathway, regulation of complement activation, and cell recognition. I further split the transcripts into two lists: transcripts upregulated by GSK0660 and transcripts downregulated by GSK0660 in TNFα-treated cells. This revealed that GSK0660 upregulated transcripts particularly related to cell recognition ($p = 0.000266$) and cell-matrix adhesion ($p = 0.001643$). GSK0660 downregulated

transcripts related to the defense response (p = 0.0000603) and the immune response (p = 0.000146). There was only one KEGG pathway enriched in TNFα plus GSK0660 cells compared to TNFα alone: cytokine-cytokine receptor interaction (p = 0.01).

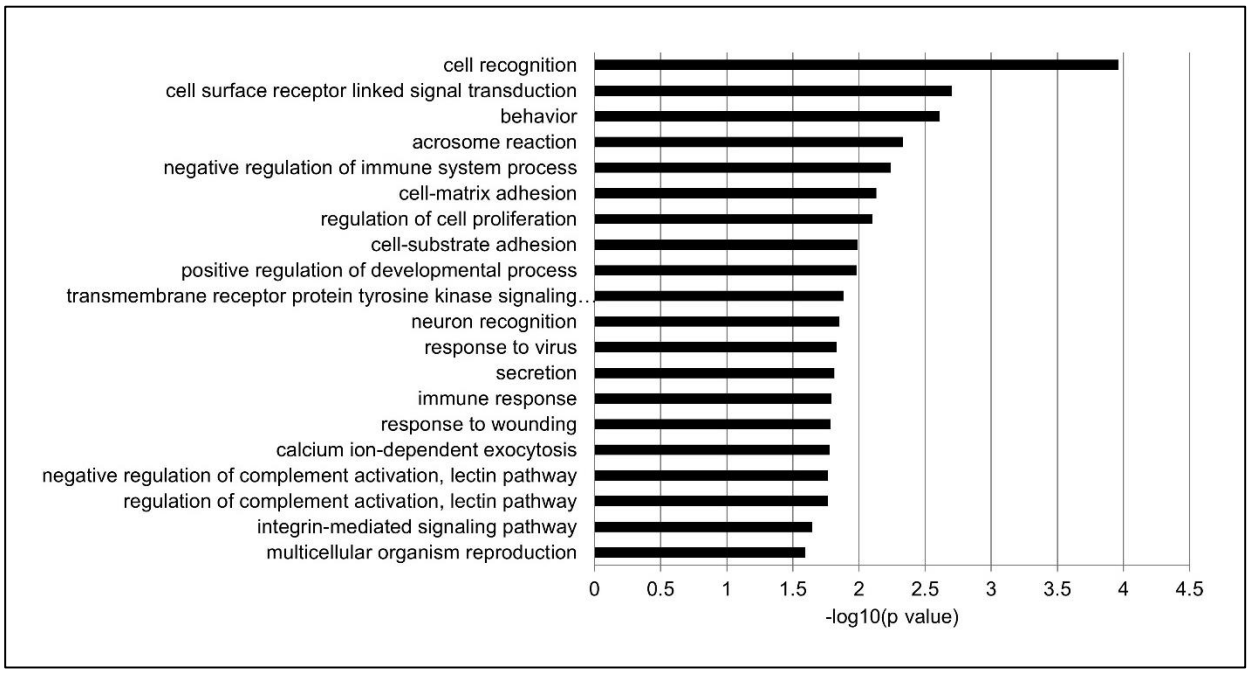

Figure 6. Top 20 GO terms enriched in GSK0660-treated samples. The list of differentially expressed transcripts in TNFα plus GSK0660-treated HRMEC compared to TNFα alone was submitted to DAVID. Terms were considered significant with $p < 0.05$.

Of the 273 genes differentially expressed by TNFα co-treatment with GSK0660, 91 were also differentially expressed by treatment with TNFα compared to vehicle (**Figure 7**). GSK0660 exacerbated the TNFα-induced upregulation of 8 genes (*ATP2C2*, *GATA6*, *GCKR*, *LIF*, *SEMA3A*, *SERPINB2*, *TNFRSF18*, *TSLP*) and TNFα-induced downregulation of 11 transcripts (*A2M*, *CBLN2*, *CH25H*, *MS46A*, *RAP1GAP2*, *RGCC*, *RP11-184M15.1*, *RP11-284F21.10*, *RP11-425L10.1*, *SELPLG*, *SPRY1*). GSK0660 counteracted the effects of TNFα on the remaining 72 transcripts. KEGG pathway analysis of all 91 transcripts included enrichment of cytokine-cytokine receptor interaction (*CCL8*, *CCL17*, *CXCL10*, *LIF*, *TSLP*, *TNFRSF18*) and chemokine signaling (*CCL8*,

CCL17, *CXCL10*, *SHC3*). Finally, the genes differentially expressed by TNFα co-treatment with GSK0660 compared to TNFα alone were combined into a network with the genes differentially expressed by TNFα compared to vehicle based on protein interaction data (**Appendix C**). Of the genes regulated by both treatments, *A2M* was the node with the highest degree of connections.

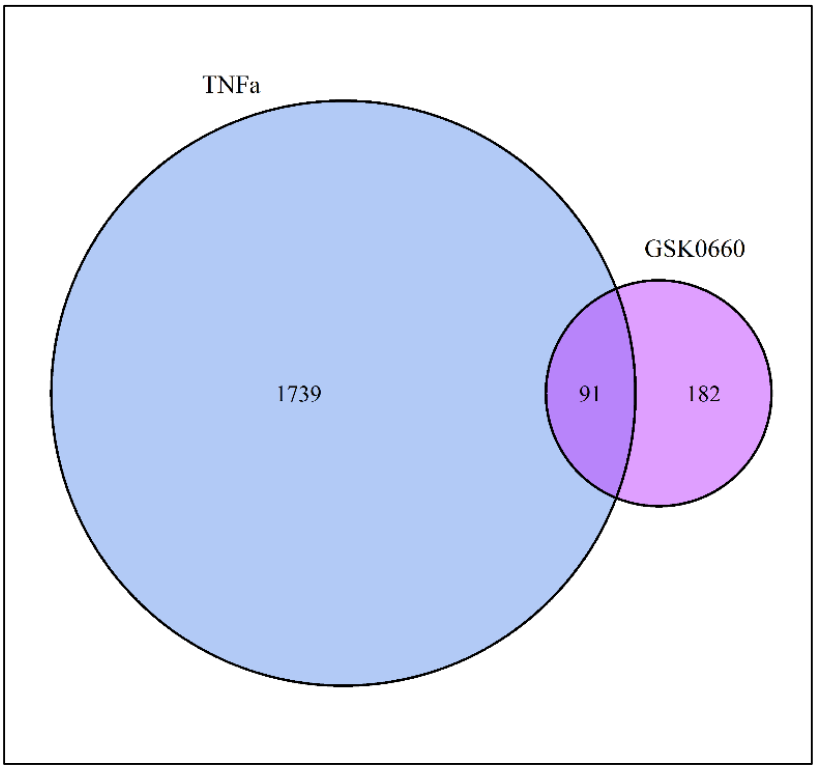

Figure 7. Euler diagram of differentially expressed transcripts by TNFα and GSK0660. TNFα treatment resulted in differential expression of 1830 transcripts compared to vehicle. Addition of GSK0660 regulated 91 of these transcripts. Additionally, co-treatment of GSK0660 and TNFα resulted in differential expression of 182 transcripts that were not affected by TNFα alone.

qRT-PCR validation

For validation of the RNA-seq, we confirmed expression of *ANGPTL4*, *CCL8*, *NOV*, *CXCL10*, and *PDPK1* by qRT-PCR. *ANGPTL4* is a well-known PPARβ/δ target and is known to be downregulated by GSK0660. *CCL8* and *CXCL10* are chemokines and their TNFα-induced expression was blocked by GSK0660 in the RNA-seq. *NOV* was

upregulated by GSK0660 in TNFα-treated HRMEC, but not by TNFα alone in the RNA-seq. In HRMEC, TNFα increased expression of *ANGPTL4*, *CCL8*, and *CXCL10*, but had no effect on *NOV*. GSK0660 reduced expression of *ANGPTL4*, *CCL8*, and *CXCL10* in TNFα-treated cells and increased expression of *NOV*. *PDPK1* expression was not affected by either treatment using RNA-seq or qRT-PCR (**Figure 8**). Taken together, these data confirm gene expression changes seen in RNA-seq.

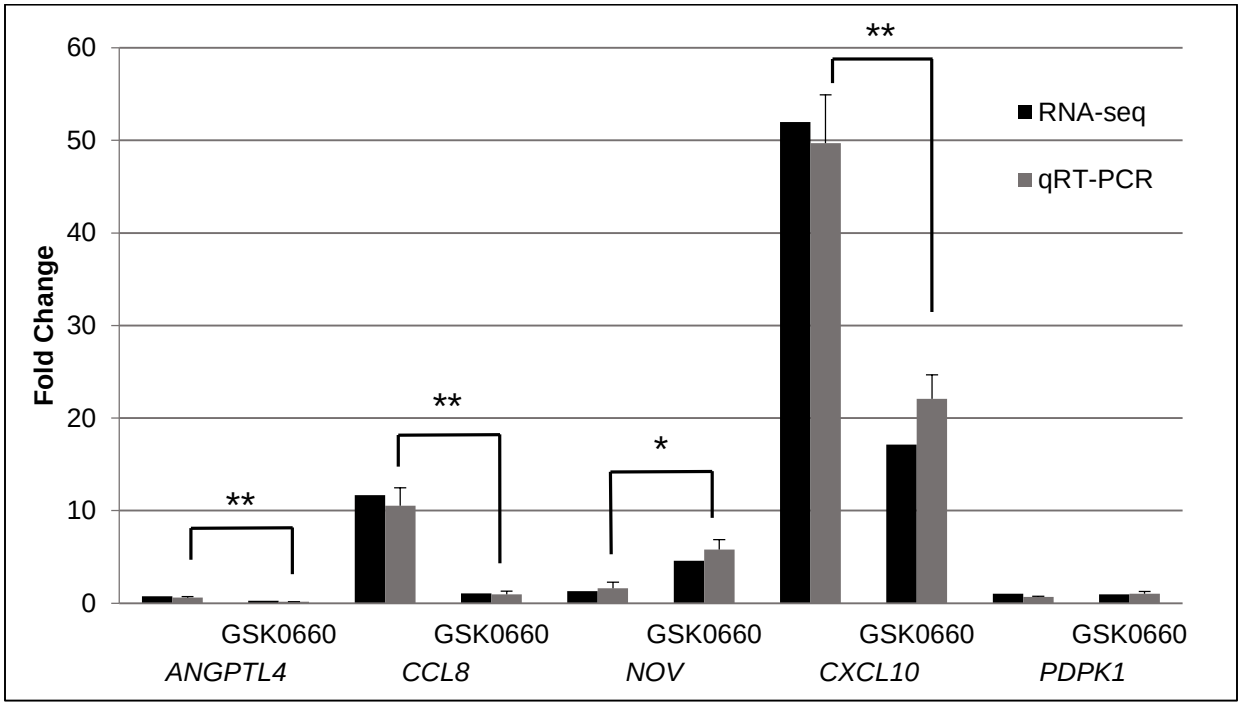

Figure 8. qRT-PCR validation of RNA-seq targets. HRMEC were pre-treated with vehicle or GSK0660 for 24 hrs, then stimulated with 1 ng/ml TNFα for 4 hrs. mRNA expression was evaluated by RNA-seq and qRT-PCR. Fold change for RNA-seq was determined by the edgeR algorithm while fold change for qRT-PCR was determined by the comparative Ct method and is relative to *ACTB* expression levels. All fold changes are relative to HRMEC treated with vehicle alone. Error bars indicate standard deviation for 3 samples in each group. *p = 0.0003, **p < 0.0001

Discussion

Using RNA-seq, this study further confirms the effects of TNFα on HRMEC, as well as the role the PPARβ/δ inverse agonist GSK0660 plays in TNFα-induced inflammation. In our study, TNFα demonstrated an effect on several signaling pathways including the

Jak-STAT pathway, Toll-like receptor pathway, and the complement cascade, replicating findings in other cell types.[144-146] TNFα also differentially expressed a number of genes involved in cytokine-cytokine signaling and chemokine signaling supporting the role of TNFα in retinal inflammation. Further evidence suggests that this role may be tied to retinal leukostasis as TNFα induced the expression of several leukocyte adhesion genes including *VCAM1*, *ICAM1*, and *SELE*, the gene encoding E-selectin. In addition to adhesion protein genes, TNFα also upregulated a number of leukocyte recruiting genes including *CCL8*, *CXCL10*, *CX3CL1*, and *CCL5*. Taken together, these data suggest a role for TNFα-induced inflammation in retinal endothelial cells that is likely to contribute to leukostasis, as seen in DR.

RNA-seq analysis revealed GSK0660 differentially regulated a number of transcripts in TNFα-treated HRMEC. These transcripts have possible diverse roles in cell proliferation, wound response, and cell recognition, which are processes known to be regulated by PPARβ/δ. Importantly, the only pathway significantly enriched was cytokine-cytokine receptor interaction. This finding becomes even more significant when the list of transcripts is limited to those both differentially expressed by TNFα compared to vehicle and by TNFα plus GSK0660 treatment compared to TNFα treatment alone. GSK0660 prevents the TNFα-induced upregulation of *CCL8*, *CCL17*, and *CXCL10*. CCL8, which is also known as MCP-2, CCL17, and CXCL10 are chemokines that attract and activate leukocytes. Interestingly, these data suggest a possible role for GSK0660 in prevention of TNFα-induced leukostasis, particularly related to chemokine recruitment. This result is unexpected as the agonists of PPARβ/δ have been shown to inhibit TNFα-induced cell adhesion through inhibition of VCAM-1 and ICAM-1 expression.[111, 134] These results

suggest that PPARβ/δ may have a contradictory effect on TNFα-induced leukostasis in that its activation inhibits cell adhesion through adhesion molecule expression inhibition while the inhibition of PPARβ/δ prevents leukocyte recruitment.

Chapter 3

GSK0660 affects TNFα-induced chemokine expression in retinal endothelial cells through inhibition of NF-κB activation

Introduction

As confirmed by the RNA-seq experiment, TNFα affects gene transcription of proteins involved in multiple signaling pathways in retinal endothelial cells, but GSK0660, the inverse agonist of PPARβ/δ, specifically regulates TNFα-induced chemokine signaling. There are four main families of chemokines, named by the position of the first cysteine residues found in the protein. The CC family of chemokines has two adjacent cysteines near the N-terminus and it consists of 27 known members. The CXC family of chemokines has an amino acid separating the two cysteines and this family consists of 17 different proteins. Finally, the C family contains only one cysteine at its N-terminus, while the CX3C family has three intervening amino acids between the cysteine residues. There have been only two C chemokines and one CX3C chemokine identified.

Typically, chemokines are produced by cells in response to a stimulus. Secreted chemokines bind to their receptors on endothelial cells or leukocytes to affect downstream signaling. As there are only seven known CXC receptors, 11 CC receptors, one C receptor, and one CXC receptor, some receptors are activated by multiple chemokines. Chemokine receptors are G protein-coupled receptors that primarily activate $G_{\alpha i,}$ which results in inhibition of cAMP synthesis and increased intracellular calcium flux. Receptor activation can lead to a variety of effects on different cell types including proliferation, gene expression, chemotaxis, and cell adhesion. In inflammation, however, the primary function of chemokines is to attract and activate leukocytes.

Leukocytes are circulating immune cells that arise from hematopoietic stem cells and function to protect against infection and to repair injury. The two main types of leukocytes are polymorphonuclear cells (PMN), named for the segmented appearance of their nuclei, and peripheral blood mononuclear cells (PBMC). PMN are also known as granulocytes and consist of basophils, neutrophils, and eosinophils. PBMC consist of lymphocytes (T cells, B cells, and NK cells), monocytes, and dendritic cells. Granulocytes and monocytes in particular are part of the innate immune system and respond rapidly to inflammation while lymphocytes are responsible for adaptive immunity to specific antigens.

In DR, increased leukocyte recruitment and extravasation is a result of a variety of changes to multiple cell types. First, it has been noted that leukocytes in diabetic patients are stiffer and less able to deform than normal. Leukocytes isolated from diabetic patients were more likely to plug microchannels than those isolated from normal patients.[147] As the diameter of leukocytes is larger than the diameter of capillaries, reduced deformability can lead to increased capillary blockage.[148] Additionally, leukocytes are reported to be activated in diabetic patients. Monocytes isolated from patients with uncontrolled diabetes were found to have increased expression of CCL2 and the scavenger receptor CD36. These monocytes were also more likely to adhere to endothelial monolayers compared to monocytes isolated from healthy patients.[149] Neutrophils isolated from type 2 diabetic patients had increased expression of CD66b, which is a marker of neutrophil activation.[150] Specifically in retinal capillaries, monocytes and granulocytes were both found at a higher number in diabetic rats than in controls.[151] Additionally, both the monocytes and granulocytes were more active in terms of free radical generation. Finally,

normal function of leukocytes is impaired in diabetics. In diet-induced diabetic mice, leukocyte recruitment and adherence was increased in the cremaster muscle. Function of the leukocytes was assessed by a subcutaneous injection of *Staphylococcus aureus* and leukocytes were found to have impaired phagocytic ability, which resulted in a prolonged bacterial infection.[152]

Endothelial cell dysfunction is also a component of DR that contributes to leukocyte recruitment. This dysfunction under diabetic stimuli includes production of high numbers of chemokines that recruit leukocytes as well as upregulation of adhesion proteins that facilitate surface binding. PDR epiretinal membranes stain for the chemokines CCL2 and SDF-1 (CXCL12) in association with endothelial cells.[153] Endothelial cells treated for 6 hrs with serum from type 1 diabetic patients increased expression of VCAM-1 compared to cells treated with serum from non-diabetic healthy patients.[154] These changes are reflected in diabetic patients as both chemokines and soluble leukocyte adhesion proteins are increased in the vitreous. Together these changes contribute to increased leukostasis in diabetics.

TNFα is known to stimulate leukostasis through induction of both chemokines and adhesion proteins. From the RNA-seq in HRMEC, TNFα increased transcription of six CCL chemokines and ten CXC chemokines as well as the lone CX3C chemokine, CX3CL1. Additionally, TNFα reduced transcription of one chemokine, CXCL12 (**Table 5**). Chemokine induction by TNFα in other cell types has been well characterized. In neural precursor cells, TNFα stimulated secretion of CCL2 and CXCL10 through TNFR1-mediated activation of p38 MAPK.[155] In pancreatic periacinar myofibroblasts, TNFα increased CXCL8, CCL2, and CCL5 through NF-κB.[156] Indeed, many chemokines have

promoter binding sites for NF-κB, which is a well-known regulator of inflammation. Normally, NF-κB is retained in the cytoplasm bound to its inhibitor IκBα. However, cellular stimulation activates the kinase IKK, which phosphorylates IκBα, leading to its degradation. This causes release of NF-κB to translocate into the nucleus and affect gene transcription.

Gene Symbol	Log2FoldChange	Adj P Value	Ensembl ID
CCL1	2.282005606	0.011116942	ENSG00000108702
CCL2	2.107448057	<0.000001	ENSG00000108691
CCL5	5.487915198	5.76E-257	ENSG00000161570
CCL8	3.543465222	3.02E-05	ENSG00000108700
CCL17	4.963657626	4.20E-10	ENSG00000102970
CCL20	3.819131936	3.45E-213	ENSG00000115009
CX3CL1	6.121874962	<0.000001	ENSG00000006210
CXCL1	2.289362754	2.52E-268	ENSG00000163739
CXCL2	3.626239366	2.88E-284	ENSG00000081041
CXCL3	4.456190761	<0.000001	ENSG00000163734
CXCL5	3.370123795	1.74E-273	ENSG00000163735
CXCL6	2.327383477	6.29E-170	ENSG00000124875
CXCL8	4.007068946	<0.000001	ENSG00000169429
CXCL9	4.613321441	2.37E-11	ENSG00000138755
CXCL10	5.706389982	6.14E-222	ENSG00000169245
CXCL11	2.514448171	6.00E-84	ENSG00000169248
CXCL12	-2.141567522	1.13E-20	ENSG00000107562
CXCL16	0.903039639	1.43E-23	ENSG00000161921

Table 5. TNFα-induced chemokine expression in retinal endothelial cells determined by RNA-seq. All transcripts with an adjusted p value < 0.05 determined by the edgeR algorithm are included regardless of level of fold change.

However, the role of PPARβ/δ in chemokine secretion has not yet been fully evaluated. It has been shown in many cell types and tissues that agonist stimulation of PPARβ/δ inhibits chemokine secretion induced by a variety of stimuli. In HUVEC, the PPARβ/δ agonist GW501516 reduced TNFα-induced release of CXCL1.[134] In the human monocytic cell line THP-1, two agonists of PPARβ/δ, GW501516 and GW0742, prevented VLDL-induced expression of MIP-1α (CCL3) while GW501516 prevented the

angiotensin II-induced expression of MIP-1β (CCL4) in the abdominal aorta of apoE$^{-/-}$ mice.[157, 158] Additionally, agonist stimulation of PPARβ/δ has a history of preventing CCL2 induction. GW0742 prevented diabetes-induced expression of CCL2 in the kidney of streptozotocin (STZ) mice and high glucose-induced CCL2 expression in RAW macrophages.[159] GW501516 decreased high fat diet-induced CCL2 expression in the heart of CD-1 mice while deletion of PPARβ/δ increased baseline expression of CCL2 in the heart.[112] However, very little is known about the effect of GSK0660 on chemokine secretion and to date there have been no reports of any synthetic ligand of PPARβ/δ acting on CCL8, CCL17, or CXCL10.

Methods

Culture and treatment of HRMEC

HRMEC (passages 4-8) were cultured and treated as described in Chapter 2, with the additional treatment groups of 0.1 μM and 1 μM GSK0660. For the parallel plate flow chamber (PPFC) experiment with recombinant proteins, monolayers were pre-treated with 50 ng/ml CCL8 (R&D Systems; Minneapolis, MN) and 50 ng/ml CXCL10 (R&D Systems) for 24 hrs in combination with 10 μM GSK0660. Protein concentrations were chosen from the middle of the reported activity levels from R&D Systems. The R&D Systems recombinant CCL8 has an ED_{50} of 30-100 ng/ml for attracting THP-1 monocytic leukemia cells while the recombinant CXCL10 has an ED_{50} of 30-180 ng/ml for attracting BaF3 mouse pro-B cells transfected with human CXCR3. After 24 hrs, monolayers were stimulated with 1 ng/ml TNFα with CCL8 + CXCL10 + GSK0660, GSK0660 alone, or vehicle for 4 hrs. Additional monolayers were treated with 1 μg/ml anti-CCL8 (R&D Systems), 4 μg/ml anti-CXCL10 (R&D Systems), or 4 μg/ml of anti-CCL8 and anti-

CXCL10 at the time of stimulation with 1 ng/ml TNFα. These concentrations were chosen from the low and high ends of the company-reported Neutralization Dose (ND_{50}) for neutralization of 0.2 μg/ml recombinant protein-induced chemotaxis. For experiments using the MEK inhibitor, cells were pre-treated with 10 μM, 30 μM, or 50 μM PD98059 (Cell Signaling; Danvers, MA) for 1 hr before stimulation with TNFα.

qRT-PCR

Cells were collected and processed as described in Chapter 2. The primers used were *CCL8*, *CCL17*, *CXCL10*, *CCL5*, *CCL2*, *CXCL11*, *CX3CL1*, *VCAM1*, *ICAM1*, *PPARD*, and *ACTB*, which are further described in **Appendix A**.

Parallel plate flow chamber

PBMC (Sanguine Biosciences; Valencia, CA) were resuspended in Hank's Buffered Salt Solution (Life Technologies; Grand Island, NY) at a concentration of $5x10^5$ cells/ml and loaded into a syringe. HRMEC were grown in monolayers on glass slides coated with attachment factor and treated as above. After treatment, slides were mounted in a rectangular parallel plate flow chamber with a silicon rubber gasket (GlycoTech; Gaithersburg, MD). With the gasket, the chamber had a flow width of 1.00 cm and a height of 0.005 inch (**Figure 9**). The chamber was connected to inlet and outlet syringes with Silastic™ tubing (GlycoTech) with an inner diameter of 1/16 inch. A syringe pump (World Precision Instruments; Sarasota, FL) was used to pull PBMC across HRMEC monolayers at a rate of 150 μl/min for 7 min. Non-adherent cells were washed off at 300 μl/min with HBSS for 2 min. Eight fields of view were captured using an IMT-2 inverted microscope (Olympus; Tokyo, Japan) and Q-Color3 digital camera (Olympus) at 20x magnification.

Adherent cell counts were performed by masked observers using ImageJ (NIH; Bethesda, MD) and averaged for each slide.

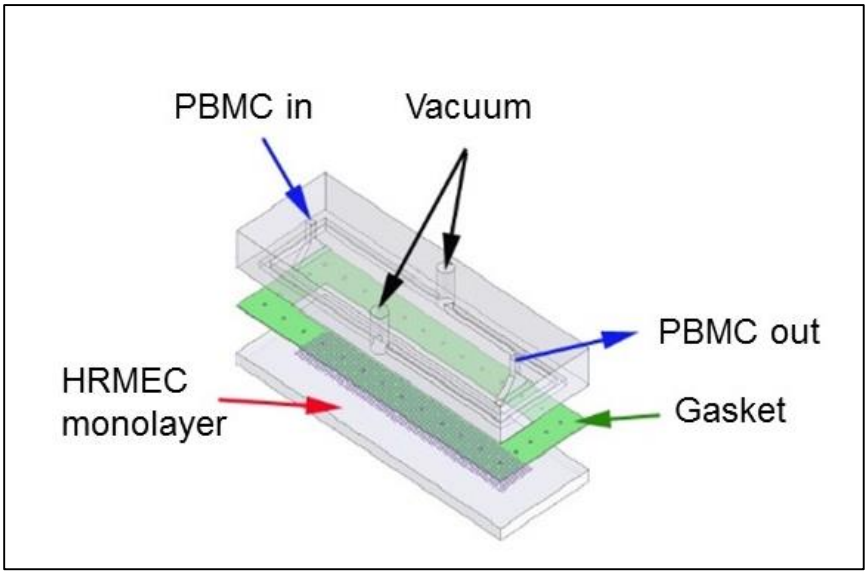

Figure 9. Diagram of the PPFC. The inlet syringe containing PBMC is connected to one end of the chamber. The outlet syringe is connected to a syringe pump. The chamber is held together by vacuum suction. Diagram adapted from T Desai.[160]

HRMEC siRNA transfection

HRMEC were grown in 6-well dishes or in monolayers on glass slides and changed to fresh 10% culture medium 30 min before transfection. Transfection was performed using the Targefect-siRNA kit (Targeting Systems; El Cajon, CA) and control and PPARβ/δ-directed siRNA oligomers (**Appendix D**; Qiagen). Oligomers were administered to cells at a final concentration of 75 nM in a solution of Targefect Solution A, Virofect, and Optimem (Life Technologies). Medium was changed after 12 hrs to 2% FBS medium. After 20 hrs, HRMEC were stimulated with 1 ng/ml TNFα. Knockdown efficacy was confirmed by qRT-PCR.

Western blot

HRMEC were grown in 10 cm dishes and treated as above. Cells were detached using TrypLE™ Express Enzyme (Life Technologies) and pelleted at 4000 x g in 4°C for

5 min. Lysates were washed with PBS and pelleted at 4000 x g in 4°C for 3 min. Nuclear and cytosolic fractions were collected using the NE-PER™ kit (Life Technologies) according to the manufacturer's directions in solutions containing protease (Halt™ Protease Inhibitor Cocktail; Thermo Scientific; Rockford, IL) and phosphatase (Phosphatase Inhibitor Cocktail 2; Sigma-Aldrich) inhibitors. Protein concentration was determined using a bicinchoninic acid assay (Pierce; Rockford, IL). Protein samples were mixed with 4x Laemmli buffer (Bio-Rad; Hercules, CA) containing 355 mM β-mercaptoethanol (Bio-Rad) and then heated for 10 min at 96°C. 15 µg of protein was loaded onto a 10% SDS gel (Bio-Rad). The gel was run at 100 mV for 1 hr. The proteins were transferred onto a PVDF membrane (Life Technologies) using the iBLOT2 system (Life Technologies) P0 protocol (20 mV for 1 min, 23 mV for 4 min, 25 mV for 2 min). Membranes were blocked for 1 hr in 5% milk. Primary antibodies were incubated in 5% milk at 4°C overnight. The primary antibodies used were NF-κB p65 (1:2000; Abcam; Cambridge, MA), lamin B1 (1:1000; Abcam), phospho-p44/42 MAPK (1:1000; Cell Signaling), p44/42 MAPK (1:1000; Cell Signaling), and β-actin (1:5000, Thermo Scientific). Then, membranes were washed in TBST and incubated with horseradish peroxidase-conjugated secondary antibody (Promega; Madison, WI) at 1:2000 in 5% milk for 1 hr at room temperature. After washing, SuperSignal® (Thermo Scientific) was added to membranes and film was exposed and developed.

In vivo leukostasis

All experiments were approved by the Vanderbilt University Institutional Animal Care and Use Committee and were performed in accordance with the ARVO statement for the Use of Animals in Ophthalmic and Vision Research. C57BL/6 mice were

purchased from Charles River Laboratories (Wilmington, MA). Mice were given a 2 µl injection of 50 ng/ml TNFα in PBS with either 0.1% DMSO or 1 µM GSK0660. Twenty-four hrs after injection, mice were anesthetized with ketamine and xylazine and perfused with 0.9% saline at physiological pressures followed by 40 µg/ml FITC-conjugated concanavalin-A (Vector Laboratories; Burlingame, CA). Non-adherent leukocytes were washed out with 0.9% saline. Eyes were enucleated and retinas dissected in 4% paraformaldehyde. Retinas were flat-mounted and fluorescent images captured with an AX70 upright microscope (Olympus) with a DP71 digital camera (Olympus). Lumenal leukocytes were counted by masked observers using ImageJ.

Statistics

For all experiments, statistical significance was determined using ANOVA with a student's t post hoc analysis using the software JMP. Data are reported as means plus or minus the standard deviation, and data are considered significant with $p < 0.05$.

Results

GSK0660 inhibits TNFα-induced chemokine expression

The RNA-seq experiment suggested that GSK0660 inhibits TNFα-induced *CCL8*, *CCL17*, and *CXCL10* expression. To confirm this, I used qRT-PCR with multiple concentrations of GSK0660 for a dose response. In HRMEC, GSK0660 inhibited TNFα-induced expression of *CCL8* and *CXCL10* in a dose-dependent manner (**Figure 10A-B**). However, the effect of GSK0660 on *CCL17* did not repeat over several experiments (**Figure 10C**). Further analysis of the effect of the highest concentration of GSK0660 on the expression of other chemokines revealed a significant effect on TNFα-induced *CCL2*, *CXCL11*, and *CX3CL1* expression (**Figure 10D**). As GSK0660 affects expression of

multiple chemokines, I focused on CCL8 and CXCL10, on which GSK0660 had the largest effect, for further experiments.

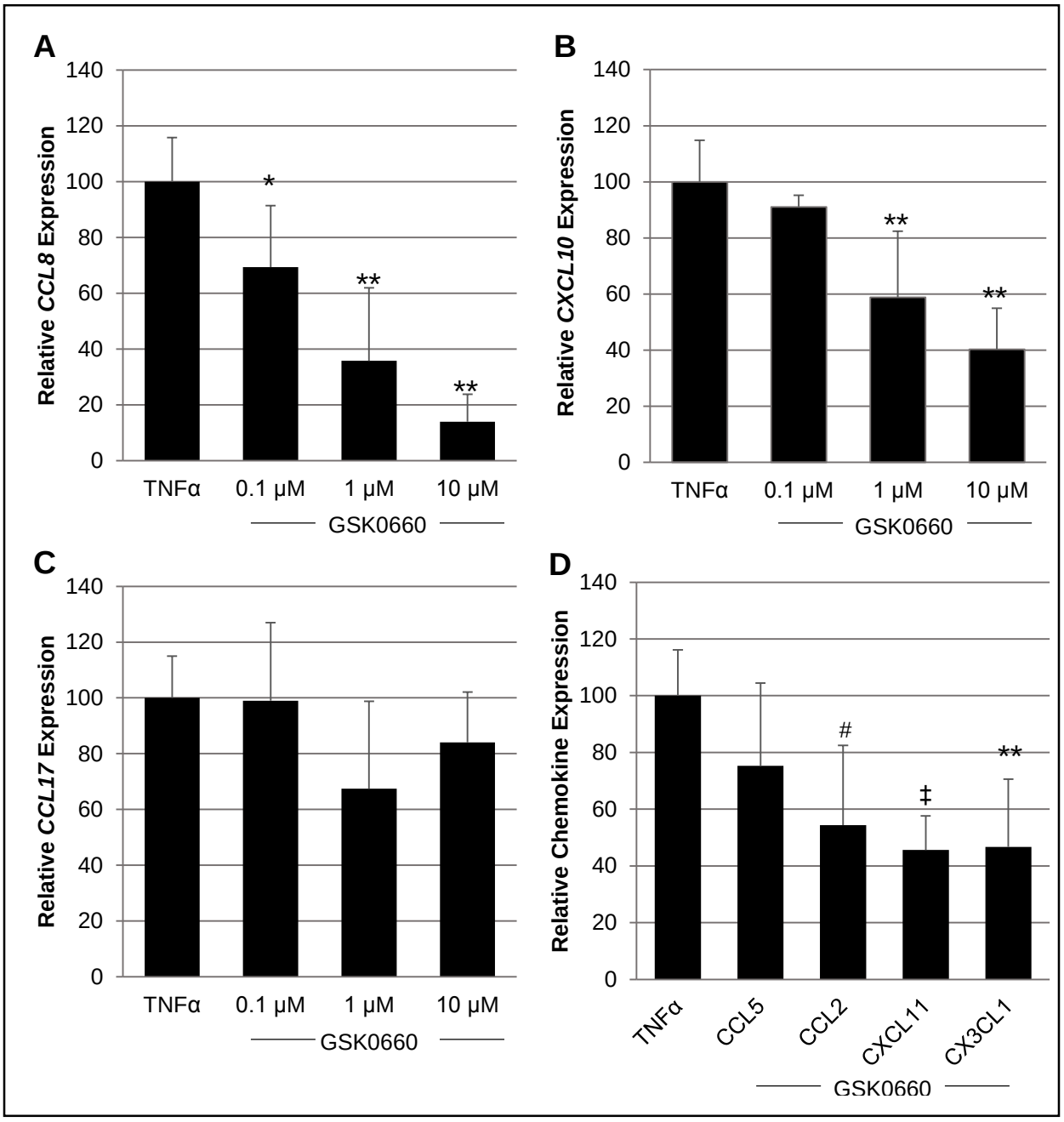

Figure 10. qRT-PCR of the effect of GSK0660 on TNFα-induced chemokine expression in HRMEC. HRMEC were pre-treated with increasing concentrations of GSK0660 for 24 hrs before stimulation with 1 ng/ml TNFα for 4 hrs. GSK0660 dose-dependently decreased TNFα-induced expression of A) *CCL8* and B) *CXCL10* in HRMEC while GSK0660 had no significant effect on TNFα-induced expression of C) *CCL17*. D) GSK0660 at 10 μM significantly reduced TNFα-induced *CCL2*, *CXCL11*, and *CX3CL1* expression. All bars are relative to the TNFα plus vehicle-treated samples. *p = 0.0025, **p < 0.0001, #p = 0.0054, ‡p = 0.0008

GSK0660 has no effect on TNFα-induced adhesion protein expression

Besides inducing chemokine expression, TNFα also increases expression of adhesion proteins that tether and activate leukocytes. This effect is regulated by PPARβ/δ agonists in other cell types.[111] In HRMEC, TNFα induced the expression of *VCAM1* and *ICAM1*. However, GSK0660 did not have any effect on expression of these same transcripts (**Figure 11A-B**).

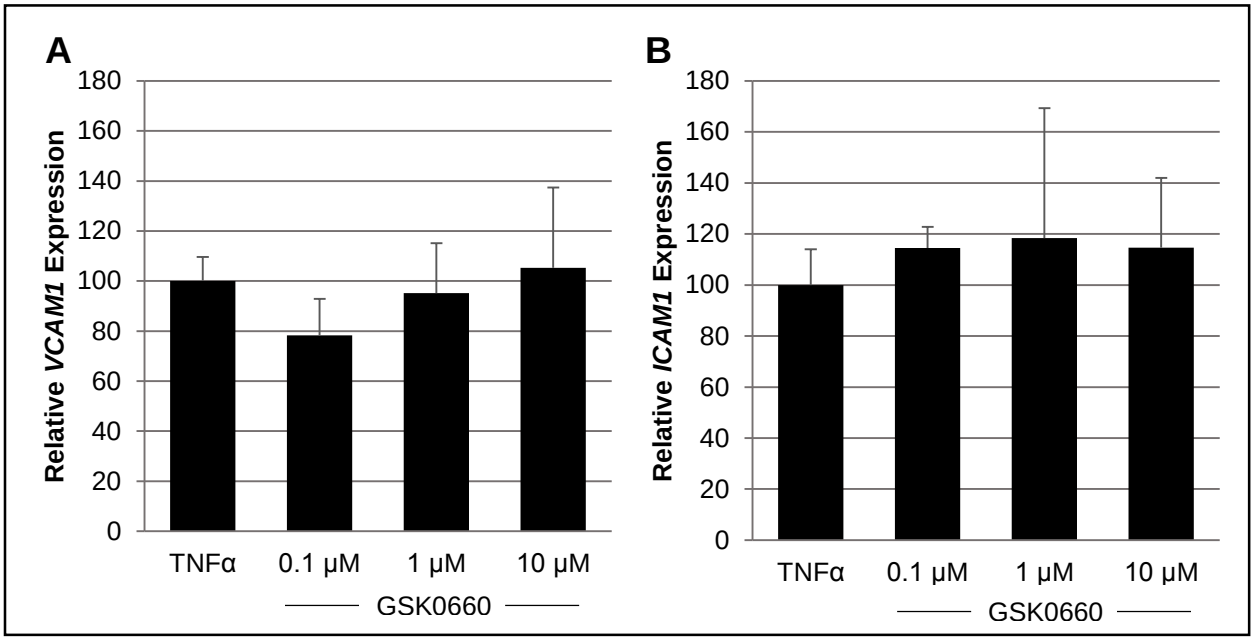

Figure 11. Effect of GSK0660 on TNFα-induced expression of adhesion proteins. HRMEC were pre-treated with GSK0660 for 24 hrs before TNFα stimulation for 4 hrs. GSK0660 treatment had no effect on (A) *VCAM1* or (B) *ICAM1* gene expression. All bars relative to the TNFα plus vehicle-treated samples.

Inhibition of PPARβ/δ reduces TNFα-induced cell adhesion

One effect of chemokines is to activate leukocytes to adhere to endothelial cells. To determine whether GSK0660 had an effect on TNFα-induced cell adhesion, I used a parallel plate flow chamber, which allows for flow of leukocytes over cell monolayers. Slides of HRMEC were treated as before, with a 24 hr pre-treatment of GSK0660 and a 4 hr stimulation with TNFα at 1 ng/ml. PBMC were then flowed across the treated monolayers and adherent cells were counted. TNFα at a concentration of 1 ng/ml strongly

activated HRMEC to capture and adhere PBMC (**Figure 12**). Treatment with both 1 μM and 10 μM GSK0660 significantly inhibited TNFα-induced cell adhesion.

As GSK0660 had no effect on the expression of the major adhesion proteins, but it did affect TNFα-induced chemokine expression in HRMEC, it is likely that GSK0660 affects TNFα-induced cell adhesion through an overall reduction in chemokine secretion. To determine this, HRMEC monolayers were treated with 10 μM GSK0660 in combination with recombinant CCL8 and CXCL10 before and during TNFα stimulation. The addition of CCL8 and CXCL10 prevented the effect of GSK0660 on TNFα-induced cell adhesion (**Figure 12**).

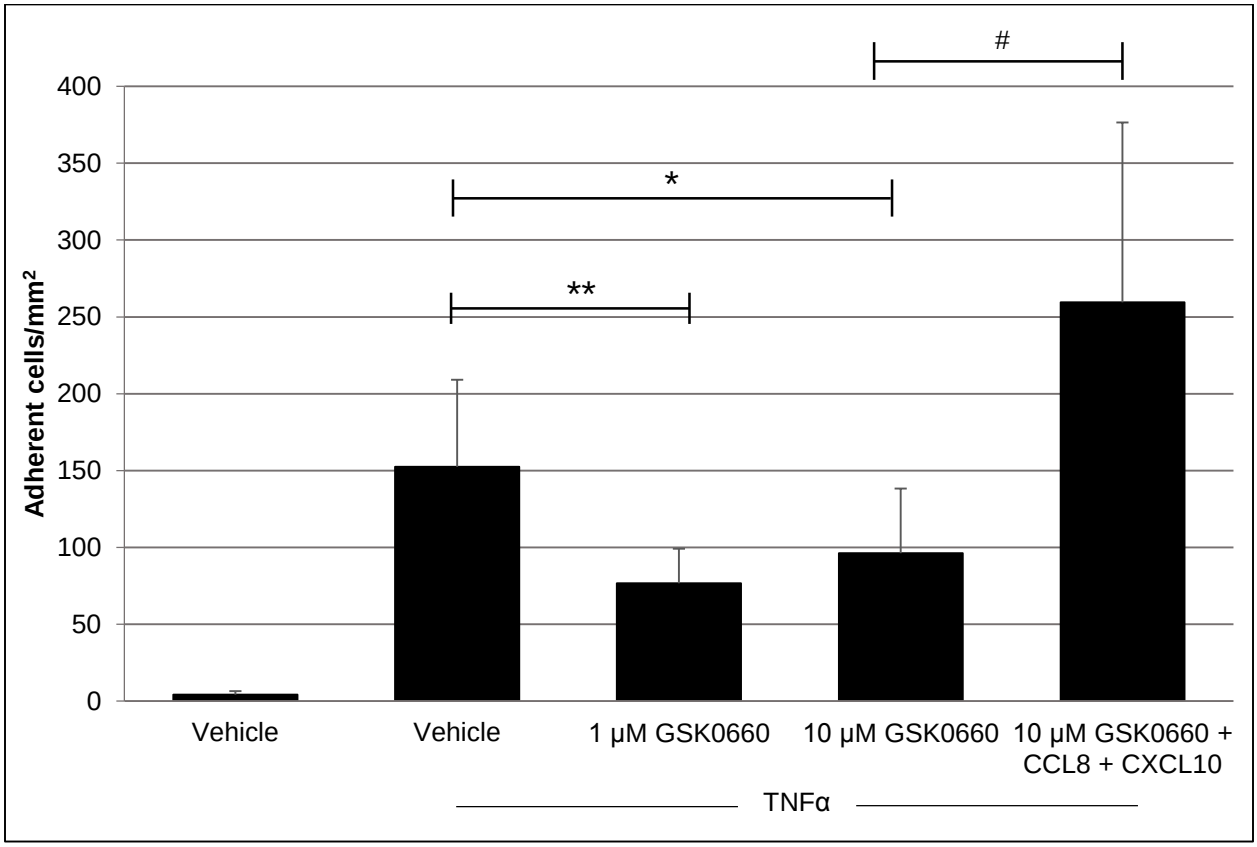

Figure 12. Effect of GSK0660 on TNFα-induced PBMC adhesion to HRMEC. HRMEC monolayers were treated with vehicle or 1 or 10 μM GSK0660 for 24 hrs before stimulation with 1 ng/ml TNFα. An additional group was treated with 50 ng/ml of both CCL8 and CXCL10 in addition to 10 μM GSK0660. TNFα increased PBMC adhesion to HRMEC while GSK0660 at both concentrations significantly reduced this effect. CCL8 and CXCL10 prevented the effect of GSK0660 on TNFα-induced cell adhesion. *$p = 0.0291$, **$p = 0.0083$, #$p < 0.0001$

For further evidence for the roles of CCL8 and CXCL10 in leukocyte adhesion, antibodies against CCL8 and CXCL10 were used in combination with TNFα. Addition of an antibody against CCL8 did not significantly affect TNFα-induced PBMC adhesion to HRMEC monolayers (**Figure 13**). However, addition of 4 μg/ml of anti-CXCL10 significantly reduced TNFα-induced cell adhesion. This effect was increased by using a combination of anti-CCL8 and anti-CXCL10.

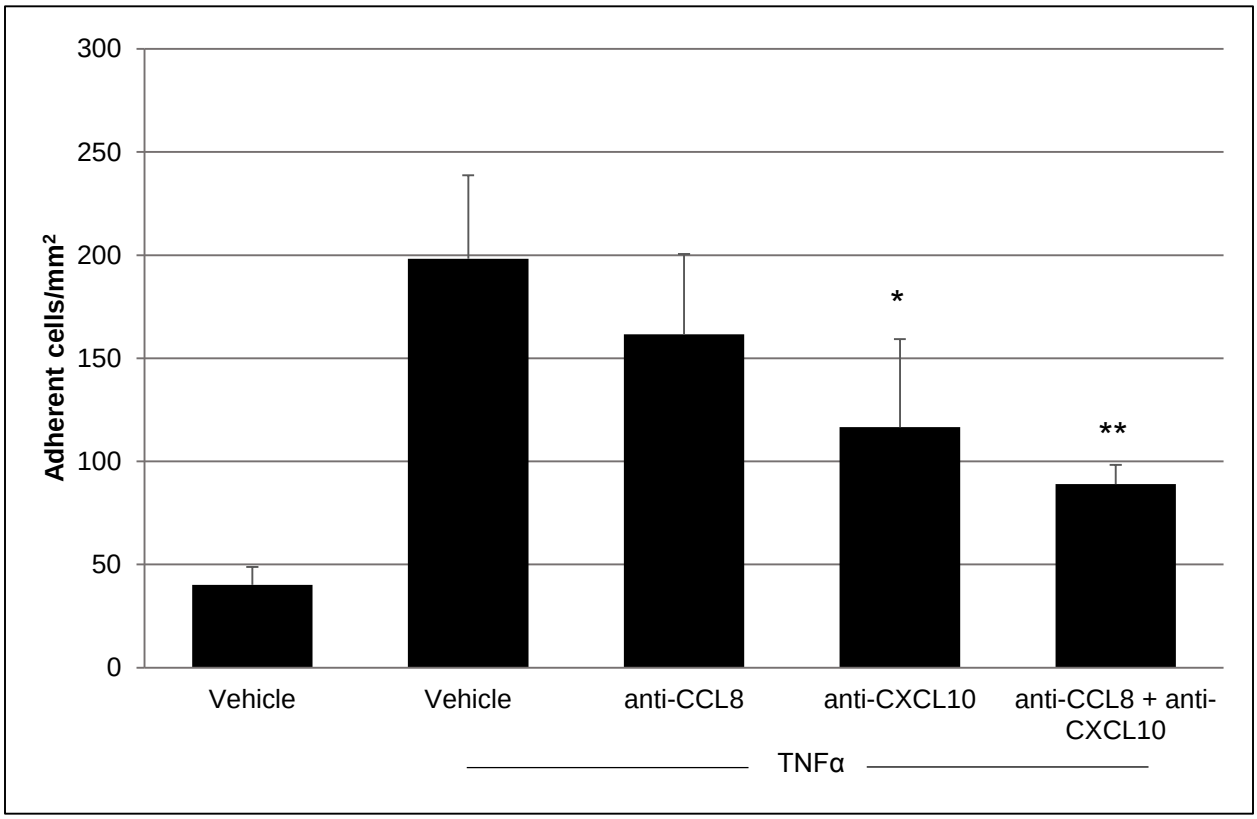

Figure 13. Effect of chemokine antibodies on TNFα-induced PBMC adhesion to HRMEC. HRMEC monolayers were treated with 1 μg/ml anti-CCL8, 4 μg/ml anti-CXCL10, or a combination of 4 μg/ml of both CCL8 and CXCL10 during stimulation with 1 ng/ml TNFα. TNFα increased PBMC adhesion to HRMEC. An antibody against CCL8 had no effect alone, but a combination of anti-CCL8 and anti-CXCL10 inhibited TNFα-induced cell adhesion. Anti-CXCL10 alone also significantly inhibited TNFα-induced cell adhesion. *p = 0.0012, **p = 0.0006

Finally as a proof of concept, the effect of PPARβ/δ knockdown on TNFα-induced cell adhesion was examined. Knockdown of PPARβ/δ with siRNA reduced PPARβ/δ mRNA expression by 72% compared to cells transfected with a control oligomer (**Figure**

14). Similar to the effect of GSK0660, knocking down PPARβ/δ in HRMEC monolayers significantly reduced TNFα-induced cell adhesion (**Figure 15**).

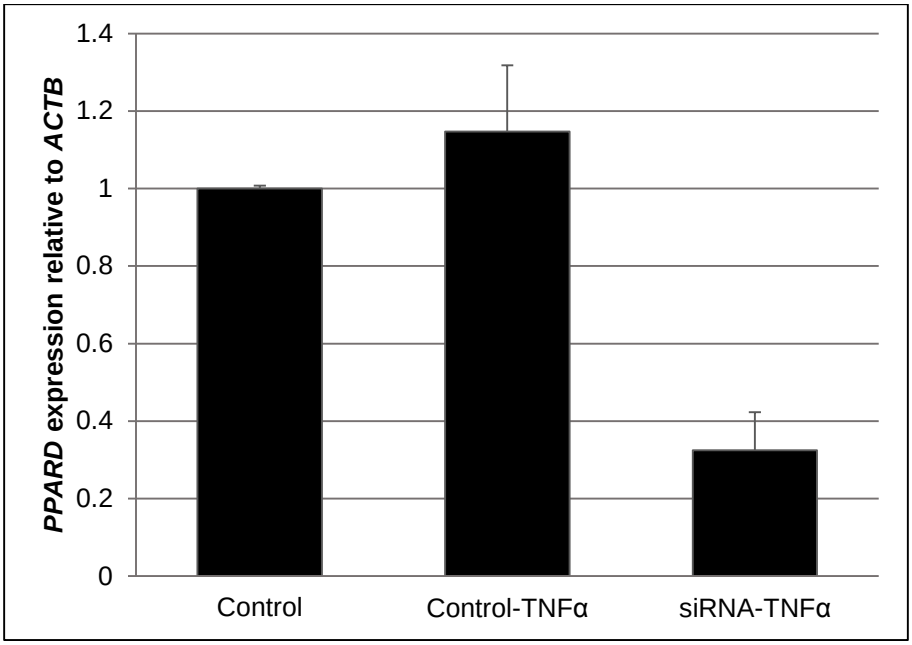

Figure 14. PPARβ/δ siRNA knockdown on PPARβ/δ expression. HRMEC were transfected with either control siRNA or siRNA targeting PPARβ/δ. Knockdown of PPARβ/δ was confirmed using qRT-PCR and resulted in a 72% reduction in PPARβ/δ mRNA expression after 24 hrs.

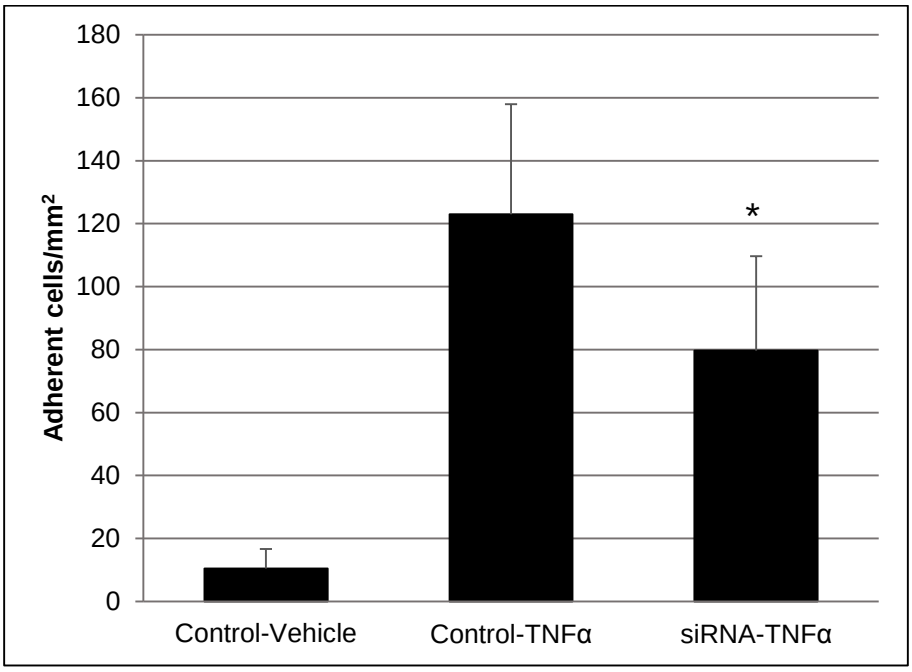

Figure 15. Effect of PPARβ/δ siRNA knockdown on TNFα-induced PBMC adhesion to HRMEC. HRMEC monolayers were transfected with control or PPARβ/δ siRNA for 20 hrs before a 4 hr stimulation with 1 ng/ml TNFα. *p = 0.0029.

GSK0660 inhibits TNFα-induced NF-κB p65 translocation

The expression of chemokines can be induced by a variety of pathways, but the most well-known is through NF-κB activation. TNFα stimulation of cells can activate NF-κB, which translocates to the nucleus to affect transcription of a variety of proteins. While NF-κB consists of a heterodimer of most combinations of the subunits p50, p52, p65 (RelA), c-Rel, and RelB, the dimer consisting of p65 and p50 is the most abundant.[161] In HRMEC, a pilot experiment showed that TNFα induced NF-κB p65 nuclear translocation within 15 minutes of stimulation, which continued at 2 and 4 hrs after the introduction of TNFα. Therefore, HRMEC were pre-treated with 10 μM GSK0660 for 24 hrs and then stimulated by TNFα for 4hrs, as before. The lysate was split into cytosolic and nuclear fractions. GSK0660 reduced the TNFα-induced translocation of the p65 subunit of NF-κB at 4 hrs (**Figure 16**).

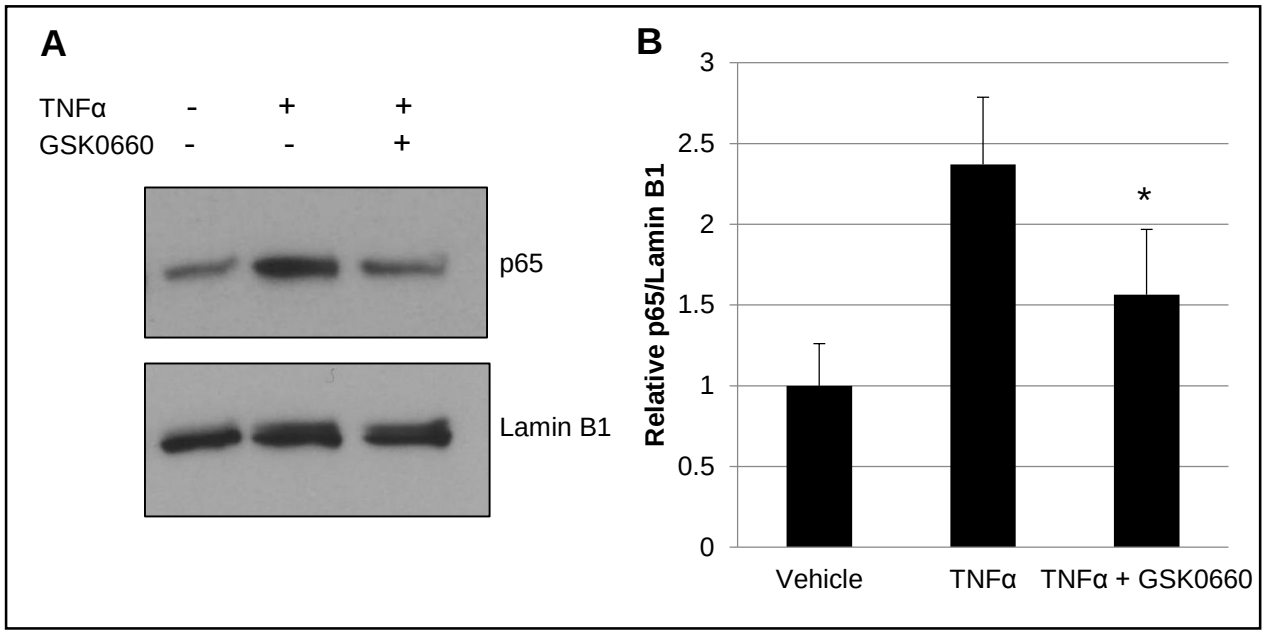

Figure 16. Effect of GSK0660 on TNFα-induced nuclear p65 expression. HRMEC were treated with 10 μM GSK0660 for 24 hrs before 1 ng/ml TNFα stimulation for 4 hrs. Cell lysates were collected and split into nuclear and cytosolic fractions. A) Representative blot of TNFα- and TNFα + GSK0660-treated HRMEC nuclear fractions. TNFα induced p65 localization to the nucleus. Treatment of HRMEC with GSK0660 prevented that effect at 4 hrs. B) Quantification of nuclear p65 compared to lamin B1 and relative to vehicle-treated cells. *p = 0.0361

GSK0660 inhibits the activation of ERK

The activation and translocation of NF-κB can be stimulated by a variety of mechanisms. One mechanism includes mitogen-activated protein kinases (MAPK) pathways. There are several different MAPK networks, but the best studied is the extracellular signal-regulated kinase-1 and 2 (ERK1/2) pathway. ERK1/2 is activated via a signaling cascade starting with a growth factor-induced activation of the GTPase Ras, which in turn leads to the RAF kinase activation. RAF phosphorylates another kinase known as MEK, which then phosphorylates and activates ERK. TNFα induction of the ERK pathway can induce NF-κB activation and nuclear translocation.[162] In HRMEC, TNFα stimulation increased ERK activation within 15 minutes which continued for 4 hrs. GSK0660 reversed cytoplasmic ERK activation, particularly at 4 hrs (**Figure 17**).

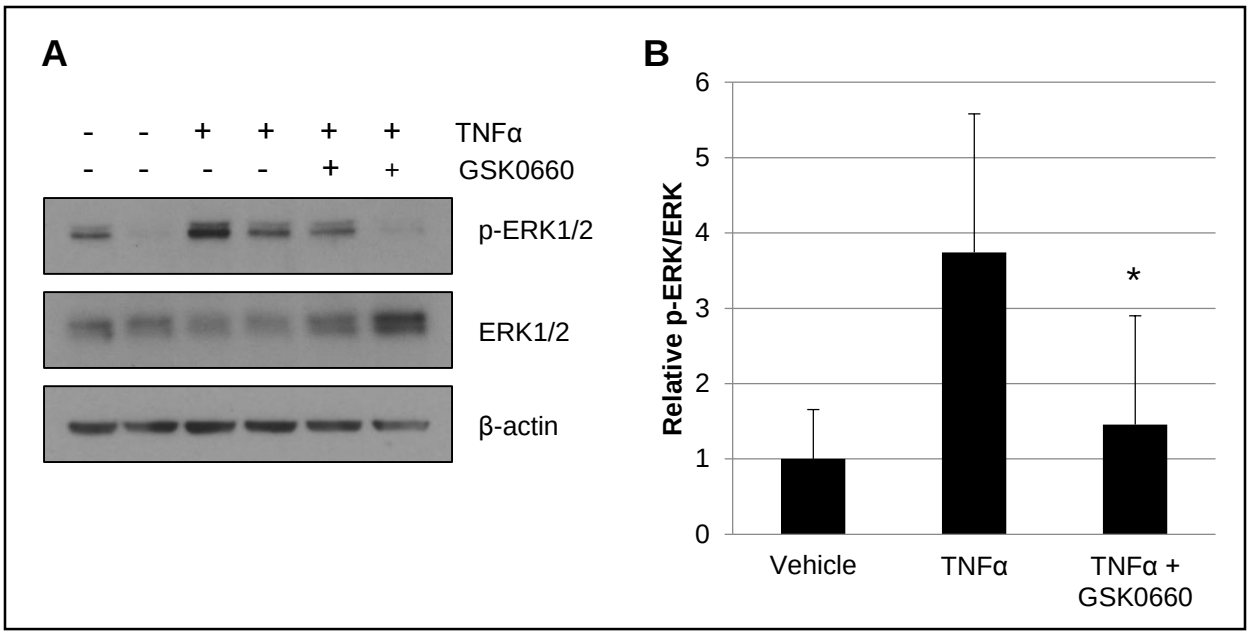

Figure 17. Effect of GSK0660 on TNFα-induced ERK activation. HRMEC were treated with 10 μM GSK0660 for 24 hrs before 1 ng/ml TNFα stimulation for 4 hrs. Cell lysates were collected and split into nuclear and cytosolic fractions. A) Representative blot of TNFα- and TNFα + GSK0660-treated HRMEC cytoplasmic fractions. TNFα increased phosphorylated ERK. Treatment of HRMEC with GSK0660 prevented that effect at 4 hrs. Beta-actin is included as a loading control. B) Quantification of phospho-ERK compared to ERK and relative to vehicle-treated cells. Bars include 4 separate experiments. *p = 0.0465

ERK inhibition mitigates TNFα-induced chemokine expression

To determine whether the ERK pathway plays a role in the TNFα-induced expression of chemokines in HRMEC, I utilized the inhibitor of MEK, PD98059. PD98059 binds to inactive MEK, preventing its activation from upstream kinases. Cells were pre-treated with increasing concentrations of PD98059 for 1 hr before stimulation with TNFα for 4 hrs. PD98059 at 30 and 50 μM significantly inhibited the TNFα-induced expression of *CXCL10* (**Figure 18**).

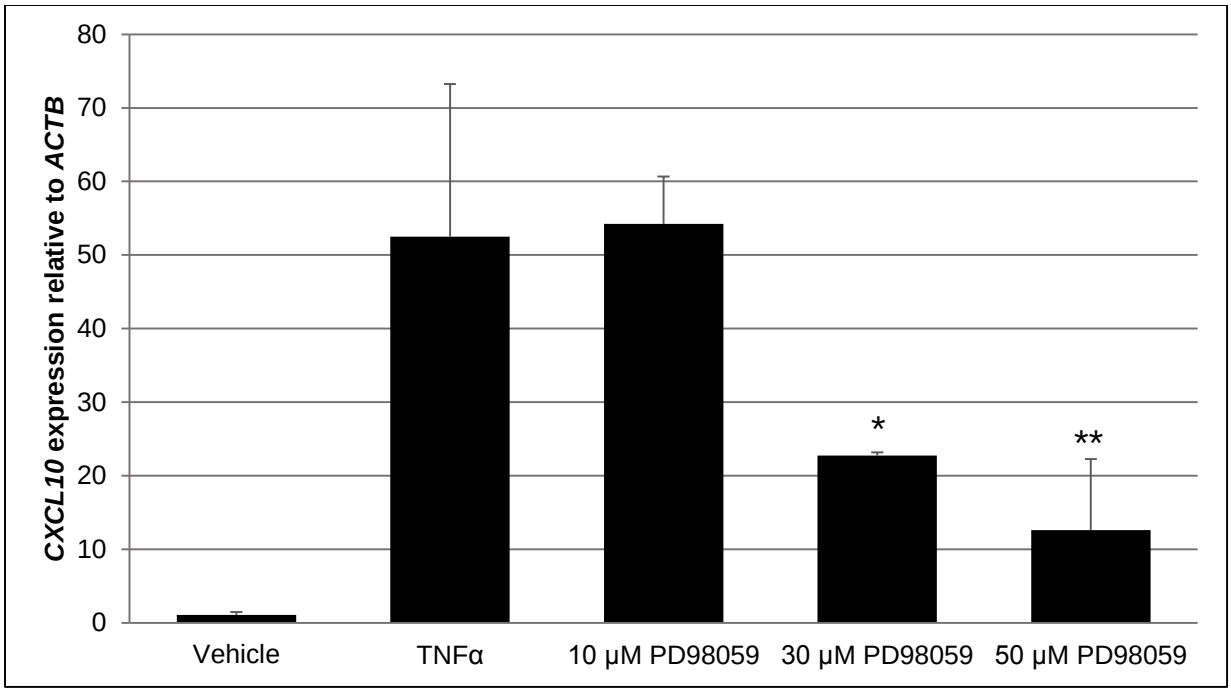

Figure 18. qRT-PCR of the effect of PD98059 on TNFα-induced *CXCL10* expression in HRMEC. HRMEC were pre-treated with increasing concentrations of the MEK inhibitor PD98059 for 1 hr before stimulation with 1 ng/ml TNFα for 4 hrs. PD98059 dose-dependently decreased TNFα-induced expression of *CXCL10* in HRMEC. *p = 0.0235, **p = 0.003

GSK0660 inhibits TNFα-induced leukostasis in vivo

To determine whether GSK0660 affects leukostasis *in vivo*, intravitreal injections of 50 ng/ml TNFα with or without 1 μM GSK0660 were administered to mice. Twenty-four hrs later, animals were perfused with FITC-concanavalin A to label adherent leukocytes and retinas were collected for analysis. TNFα increased lumenal leukostasis in the retinal vasculature in mice (**Figure 19**). GSK0660 treatment reduced this effect by almost 43%.

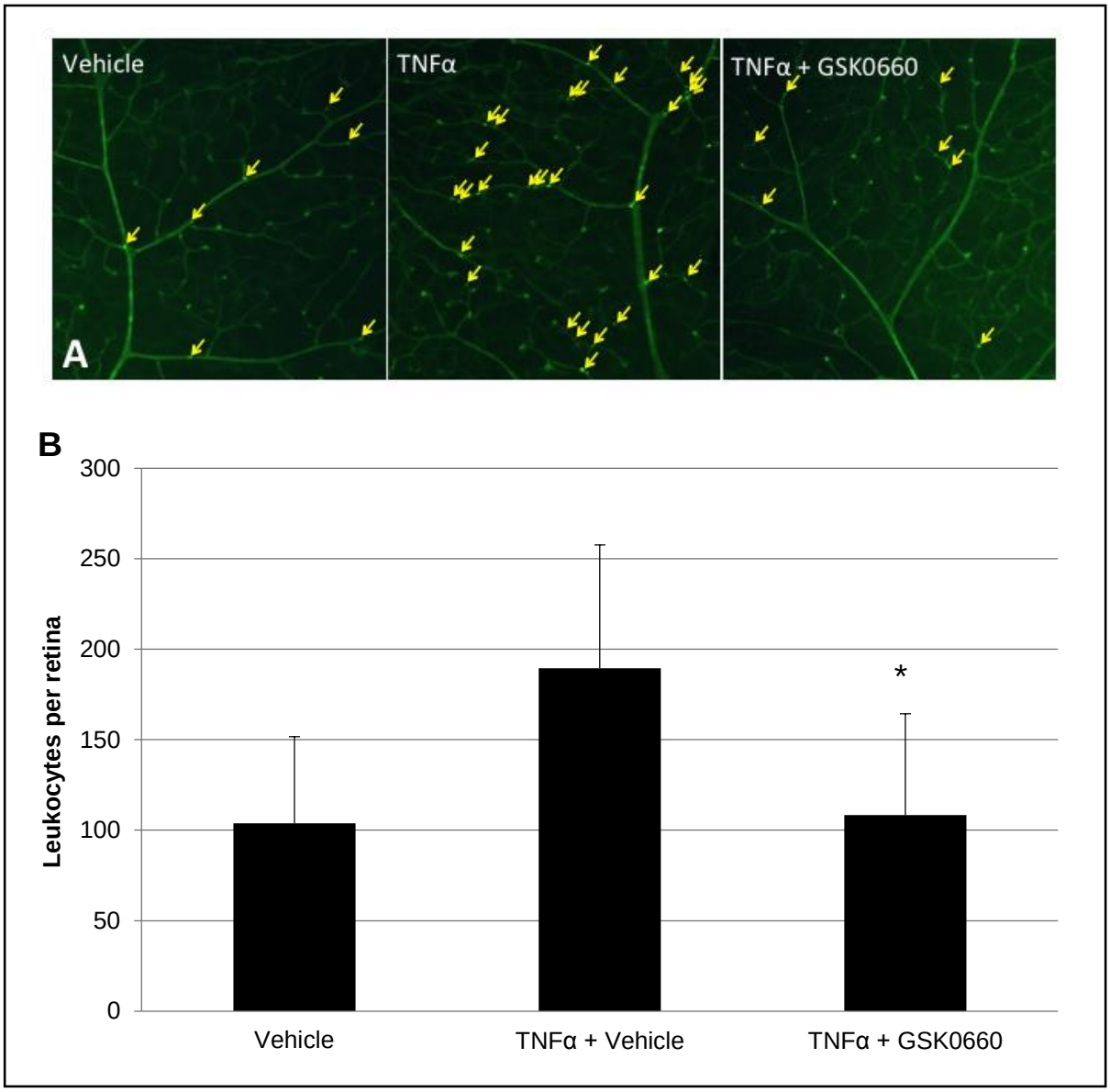

Figure 19. Effect of GSK0660 on TNFα-induced retinal leukostasis. Mice were given intravitreal injections of vehicle or 50 ng/ml TNFα with or without 1 μM GSK0660. Twenty-four hrs later, mice were perfused with FITC-conjugated concanavalin A to label adherent leukocytes. A) Representative images from retinas. B) Quantification of adherent leukocytes. Bars represent at least 5 retinas with the error bars as standard deviation. *p = 0.0158

Discussion

In summary, stimulation of HRMEC with TNFα results in activation of the ERK pathway. In turn, NF-κB is activated, causing its translocation into the nucleus where it is able to affect gene transcription of a number of genes including the chemokines *CCL8* and *CXCL10*. Together these chemokines promote PBMC adhesion to HRMEC.

Treatment with GSK0660 mitigates these occurrences, possibly through inhibition of ERK activation (**Figure 20**).

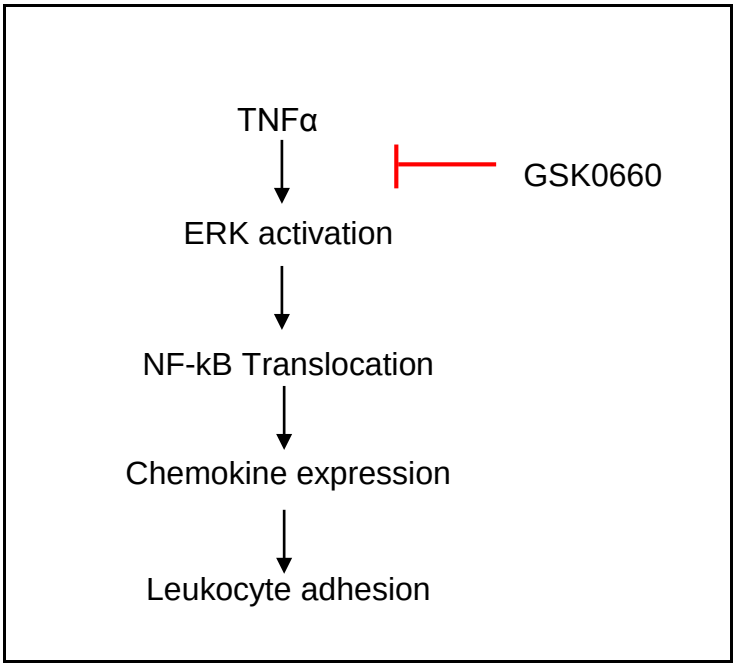

Figure 20. Schematic of the effect of GSK0660 on HRMEC. TNFα induces activation of ERK signaling, which results in translocation of NF-κB to the nucleus. NF-κB increases expression of chemokines, which recruit and activate leukocytes for adherence to the endothelium. GSK0660 treatment prevents ERK activation, preventing all of the downstream effects.

PPARβ/δ has only recently been studied in inflammation, with a majority of work suggesting that PPARβ/δ agonism is anti-inflammatory. Among the studies published, activation of PPARβ/δ prevented TNFα-induced inflammation in adipocytes, human umbilical vein endothelial cells, and proximal tubular cells.[111, 134, 163, 164] Additionally, PPARβ/δ agonists have been shown to be protective against inflammation in both hyperoxia-induced lung injury and spinal cord injury in rodents.[165, 166] There has been little work done, however, on the PPARβ/δ antagonist and inverse agonist GSK0660 and those studies typically co-administer it with the agonist. Despite the clear effects of agonism on reducing inflammation, there also exist reports suggesting that GSK0660 might be anti-inflammatory. In monocytes, GSK0660 reverses the effect of

carbaprostacyclin (a PPARβ/δ agonist) and TNFα on CXCL8 expression.[167] GSK0660 also reduces an inflammatory psoriasis-like skin condition in mice, while also reversing the upregulation of IL-1β.[168]

Inhibition of PPARβ/δ with GSK0660 in retinal endothelial cells has proven to show similar results as agonist treatment in other cell types. Treating HUVEC with the agonist GW501516 prevented TNFα-induced PMN capture and adhesion.[134] This effect was mediated by adhesion protein expression, as GW501516 also prevented the TNFα-induced upregulation of ICAM-1, VCAM-1, and E-selectin. In HRMEC, the effect of GSK0660 is on chemokine expression as GSK0660 had no effect on ICAM-1 or VCAM-1 expression. The effect of GSK0660 was mediated at least partly by reducing ERK activation and NF-κB translocation. The method for the agonist effect on leukocyte adhesion is different. It was noted in HUVEC that PPARβ/δ agonist GW0742 also reduced TNFα-induced VCAM-1, ICAM-1, and E-selectin expression in a BCL6-dependent manner.[111] However, GW0742 had no effect on NF-κB translocation, nor did it affect phosphorylation of the three different MAPK pathways JNK, ERK, or p38 MAPK. Therefore both activation and inhibition of PPARβ/δ may reduce leukocyte adhesion via two separate mechanisms. Activation of PPARβ/δ reduces its association with BCL6, leading to BCL6-induced suppression of adhesion molecule expression. Inhibition of PPARβ/δ with GSK0660, on the other hand, reduces chemokine expression through inhibition of ERK activation.

The exact mechanism by which GSK0660 prevents ERK activation and NF-κB translocation is not yet known. First, inhibition of PPARβ/δ may reduce expression of a component of the ERK signaling pathway. For example, in the RNA-seq, in cells treated

with TNFα and GSK0660, *MAP3K9* was reduced by 3.2 fold compared to cells treated with TNFα alone. MAP3K9 directly phosphorylates MEK to increase ERK signaling.[169] It is also possible that GSK0660 and PPARβ/δ act through a non-genomic mechanism to inhibit ERK signaling. While there have been no reports of PPARβ/δ acting directly on the ERK pathway, PPARβ/δ has been shown to directly activate the Akt signaling pathway by binding to the regulatory subunit of the kinase PI3K.[121] Finally, it should be mentioned that GSK0660 could have PPARβ/δ-independent effects on ERK signaling.

Additionally, GSK0660 may affect NF-κB through mechanisms not involving ERK signaling. One possible mechanism is expression of nephroblastoma overexpressed (NOV), which is also known as CCN3. In our RNA-seq and confirmed by qRT-PCR, GSK0660 increased expression of NOV, a matricellular protein. This protein has been shown to regulate NF-κB in some cell types.[170]

In conclusion, antagonism of PPARβ/δ is anti-inflammatory as it inhibits both TNFα-induced chemokine expression as well as *in vitro* leukocyte adhesion and *in vivo* leukostasis. Thus using a PPARβ/δ inhibitor in DR may be beneficial to prevent leukostasis and its damaging effects.

Chapter 4

PPARβ/δ regulates retinal angiogenesis

**Portions of this chapter have been published previously in Capozzi et al. Peroxisome proliferator-activated receptor-beta/delta regulates angiogenic cell behaviors and oxygen-induced retinopathy. IOVS. 2013.[171]*

Introduction

As shown thus far, PPARβ/δ appears to have a role in the early stage of DR, in which inhibition with GSK0660 results in reduced chemokine expression and leukostasis. However, the later stage of DR, characterized by pathological neovascularization, is the primary cause of irreversible blindness in diabetics. Finding treatments to prevent or treat PDR is important for patients who have already reached that stage of disease.

The canonical pathway of ocular angiogenesis involves development of tissue ischemia that occurs when blood flow is blocked or removed via capillary atrophy. This creates areas of hypoxia in the retinal tissue. Cells respond to hypoxia by increasing production of various growth factors to stimulate endothelial cell growth to the hypoxic tissue. Unfortunately in diabetics, the angiogenic growth induced by hypoxia is fragile and unstable. The new vessels often leak and grow through the surface of the retina into the vitreous.

In the retina, astrocytes, ganglion cells, and RPE can all respond to tissue hypoxia, but the cell type that responds with the greatest production of growth factors is the Müller glia.[172] Müller glia are specialized cells that stretch nearly the entire depth of the retina to form the inner and outer limiting membranes. They are primarily responsible for maintaining retinal homeostasis by mediating the composition of the extracellular fluid, taking up neurotransmitters, and removing cellular debris. In response to hypoxia, Müller cells increase production and secretion of VEGF, among other factors.

VEGF is an important target in DR as it causes both DME and PDR. Once secreted from VEGF-producing cells, it binds to its downstream receptors VEGFR1 and 2 on retinal endothelial cells. This stimulates a signaling cascade to increase retinal endothelial cell growth, migration, and tube formation.

PPARβ/δ has a long history of contradictory effects on angiogenesis and cell proliferation, particularly in the cancer literature. Treatment of the human hepatocellular carcinoma cell line with 0.5 to 50 nM GW501516 increased proliferation after 24 hrs while PPARβ/δ siRNA reduced proliferation.[173] However, no concentration of GW0742 (from 0.01 to 10 μM) had any effect on proliferation of the breast cancer cell lines MDA-MB-231 or MCF7 over 96 hrs of treatment. Meanwhile, treatment of the colon cancer cell line HCT116 with 1 and 10 μM of GW0742 or GW501516 inhibited proliferation by 96 hrs, but the effect was dependent on the presence of serum in the medium.[174] Additionally, cells overexpressing PPARβ/δ had slightly reduced proliferation after 72 hrs, and the combination of overexpression of PPARβ/δ with 10 μM GW0742 reduced proliferation of MCF7 cells but not MDA-MB-231 after 72 hrs.[175]

In angiogenesis, PPARβ/δ has been reported to be a hub node.[119] GW501516 increased proliferation and cell survival of EPC as well as tube formation and migration.[121] GW501516 also increased proliferation and VEGF expression in HUVEC.[122] Owing to the importance of retinal neovascular growth in PDR, we sought to study the effect PPARβ/δ would have on retinal angiogenesis.

Methods

Isolation and culture of mouse Müller Cells

The isolation protocol was adapted from Hicks and Courtois, 1990.[176] Litters of C57BL/6 mice were sacrificed at post-natal day 6 (P6) and eyes were enucleated and placed in serum free Dulbecco's Modified Eagle Medium (DMEM; Life Technologies) containing low glucose (1 g/L), phenol red, and added 1% antibiotic/antimycotic (Hyclone; Thermo Scientific). Eyes were incubated overnight in the dark at room temperature. The following day eyes were digested for 20 min at 37°C in serum free medium containing 1 mg/ml trypsin (Sigma-Aldrich) and 70 U/ml collagenase (Sigma-Aldrich). Eyes were washed with medium containing 10% FBS to stop digestion before being returned to serum free medium. Retinas were carefully dissected and placed in fresh serum free medium. Retinas were dissociated via repeated pipetting and washed once in serum free medium before plating in 10 cm dishes in growth medium consisting of DMEM, 1% antibiotic/antimycotic, and 10% FBS. Medium was changed after 6 days, and then every two days thereafter. Cells not consistent with Müller cell morphology were removed by mechanical dissociation before the first passage. Cultures were maintained at 37°C in a humidified atmosphere with 5% CO_2 and used before passage 7. Müller cell identity was confirmed by immunostaining for four Müller cell markers: vimentin, CRALBP, glutamine synthetase, and GFAP.

Isolation and culture of human Müller cells

Retinas were dissected from human donor tissue obtained from the National Disease Research Interchange (NDRI; Philadelphia, PA) within 24 hrs post-mortem and placed into serum free medium. Müller cell isolation proceeded as above for mouse cells.

Müller cell treatment

Müller cells were plated in 6-well dishes and grown to 80% confluency. Cells were serum starved in medium without FBS for 8 hrs before treatment with 0.01, 0.1, or 1 μM GW0742 (Tocris) or GSK0660 in 2% FBS medium. The cells were maintained in standard culture conditions or in hypoxia (0.1% O_2) for 24 hrs.

ARPE-19 culture and treatment

ARPE-19, an RPE cell line, are grown in DMEM:F12 (Life Technologies) containing 10% FBS and 1% antibiotic/antimycotic. Serum was reduced to 2% FBS for 12 hrs before the experiment. Then ARPE-19 cells were treated as described for Müller cells.

ELISA

Culture medium was collected and stored at -80°C until use. VEGF concentration in the medium was determined using a colorimetric sandwich ELISA (R&D Systems) according to the manufacturer's instructions.

qRT-PCR

Cells were collected and processed for qRT-PCR as described in chapter 2. Primers used were *ANGPTL4* and *ACTB* for the appropriate species and are further described in **Appendix A**.

HRMEC treatment for qRT-PCR

HRMEC were cultured as described in chapter 2. For assessment of *ANGPTL4*, HRMEC were serum starved in 0.5% FBS EBM medium for 12 hrs. HRMEC were then treated with 0.01, 0.1, or 1 μM GW0742 on a background of 0.5% FBS. Other samples

were treated with 0.01, 0.1, or 1 μM GSK0660 on a background of 2% FBS. Cells were collected after 6 hrs as described before in chapter 2.

Isolation and culture of rat retinal endothelial cells (RRMEC)

Litters of Sprague-Dawley rats (Charles River) were sacrificed at P15 and retinas were extracted and placed in serum free medium (EBM with 1% Hyclone antibiotic/antimycotic). Retinas were dissociated with enzyme free cell dissociation buffer (Invitrogen) for 10 min at 37°C. Retinas were washed in isolation buffer (PBS containing 2% FBS and 5 mM EDTA) and homogenized by repeated pipetting. Endothelial cells were isolated using a phycoerythrin (PE)-conjugated antibody against PECAM (BD Pharmingen; San Jose, CA) and an EasySep™ PE positive selection kit (STEMCELL Technologies; Vancouver, BC, Canada) according to the manufacturer's instructions. Cells were plated on attachment factor-coated plates in endothelial growth medium containing 20% FBS until cultures were established and then grown in endothelial growth medium containing 10% FBS thereafter. Culture purity was confirmed by staining for VE-Cadherin.

Isolation and culture of human choroidal endothelial cells (HCEC)

This protocol was adapted from established methods.[177] Human eyes were received from the NDRI within 24 hrs post-mortem. Retinas were removed and discarded and RPE brushed off. The choroid was dissected away from the sclera, cut into 1 mm^2 pieces, and washed 3x in minimal essential medium (MEM; Life Technologies) containing 30 mM HEPES and 1% antibiotic/antimycotic. The choroid was digested in MEM containing 0.1% collagenase for 1 hr at 37°C and then neutralized in MEM containing 10% FBS. The tissue was then washed 3x with isolation buffer and homogenized by

repeated pipetting. Cells were isolated and cultured following the same protocol as that for RRMEC except that an FITC-conjugated antibody for PECAM (BD Pharmingen) was used with the EasySep™ kit for FITC selection (STEMCELL).

Endothelial cell proliferation

Cells were plated in attachment factor-coated 96-well plates at a density of 3 x 10^3 cells/well for HRMEC, 2 x 10^3 cells/well for RRMEC, and 1.7 x 10^3 cells/well for HCEC. After 8 hrs to allow for attachment, cells were serum starved in EBM containing 1% antibiotic/antimycotic for 12 hrs. Cells were then treated with increasing concentrations of GW0742 on a background of 0.5% FBS or increasing concentrations of GSK0660 on a background of 2% FBS (HRMEC and HCEC) or 10% FBS (RRMEC) for 24 hrs. Additional treatment groups of HCEC were treated with GSK0660 on a background of 50 ng/ml recombinant VEGF (Millipore; Billerica, MA) in 0.5% FBS medium. Cells were labeled with bromodeoxyuridine (BrdU) and staining was assayed with a colorimetric BrdU kit (Roche). Cell number and stimulating FBS concentration were optimized for the growing rate of each cell type.

Endothelial cell tube formation

HRMEC were plated in 24-well plates coated with Matrigel™ (BD Biosciences; San Jose, CA) at a density of 2.5 x 10^4 cells/well. After 1 hr for attachment, cells were treated in serum free medium with increasing concentrations of GW0742 or in 2% FBS medium with increasing concentrations of GSK0660. Twenty-four hrs later, images of tubes were captured using an IMT-2 inverted microscope and Q-Color 3 digital camera. The length of the capillary-like formations were measured using ImageJ.

Rat model of oxygen-induced retinopathy (OIR)

The protocol for rat OIR is well established.[178] Briefly, pregnant rats were purchased from Charles River Laboratories. Within hrs after birth, pups and their mothers were placed in oxygen exposure chambers and subjected to periods of 50% and 10% oxygen alternating every 24 hrs. On P14, rats were returned to room air. Animals received 5 µl intravitreal injections of vehicle (0.1% DMSO in PBS) or 0.02, 0.1, or 0.5 µM GW0742 or GSK0660 upon removal from oxygen and three days later. Seven days after initial removal from oxygen, retinas were carefully dissected, stained for adenosine diphosphatase (ADPase) activity, flatmounted, and images were captured. Neovascularization was quantified by outlining with an irregular polygon in Adobe Photoshop (Adobe Systems Incorporated; San Jose, CA), counting the number of pixels inside of the polygons, and converting to square millimeters.

Mouse model of OIR

The protocol for mouse OIR is also well established.[179] Briefly, pregnant mice were purchased from Charles River Laboratories. Seven days after birth, mouse pups and their mothers were placed in 75% oxygen for 5 days. Mice were given 2 µl intravitreal injections of 0.1 and 1 µM GSK0660 in PBS on P13, which was one day after removal from oxygen. Eyes were collected on P17, retinas were carefully dissected, stained for isolectin B4, flatmounted, and fluorescent images were captured. Neovascularization was quantified as described above for the rat model.

Results

Effect of PPARβ/δ manipulation on VEGF production

Growth factor production is an important component of DR and Müller cells are one of the main producers of growth factors in the retina. Therefore, I assayed Müller cells isolated from mice to determine whether the PPARβ/δ antagonist affects VEGF secretion. This species was initially chosen over human cells for the ability to assess cells isolated from PPARβ/δ knockout mice. When placed in hypoxic conditions, Müller cells increased their production of VEGF by 3 fold. However, treatment with increasing doses of GSK0660 had no effect on VEGF production in mouse Müller cells in hypoxic or normoxic conditions (**Figure 21A**). As Müller cells are not the only producers of VEGF in the retina, I also assayed VEGF production by ARPE-19, an RPE cell line. In hypoxia, ARPE-19 increased their production of VEGF by 2 fold. Here, GSK0660 at a concentration of 1 μM had a minimal (21% reduction) but significant effect on VEGF production. (**Figure 21B**). To determine whether activation of PPARβ/δ had any effect in these cells, the agonist GW0742 was used only in normoxic conditions because Müller cells in hypoxia are already producing a near-maximal amount of VEGF. GW0742 had no effect on VEGF secretion from Müller cells (**Figure 21C**) or ARPE-19 (**Figure 21D**).

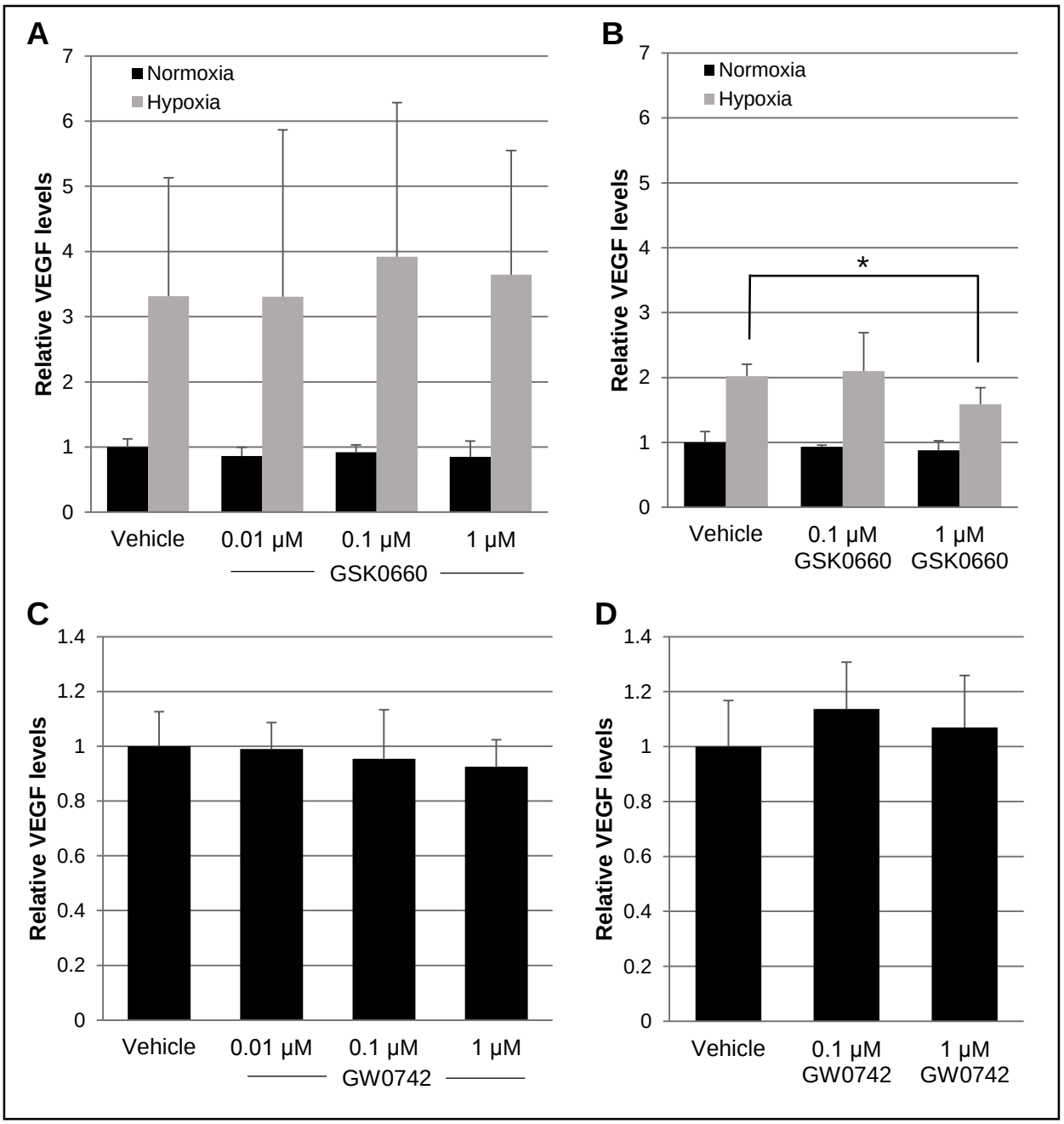

Figure 21. Effect of pharmacologic manipulation of PPARβ/δ on VEGF production. A) Mouse Müller cells were placed in normoxia (20.9% O_2) or hypoxia (0.1% O_2) and treated with vehicle or increasing concentrations of GSK0660 for 24 hrs. Medium was collected and assayed for VEGF concentration. While VEGF production was increased 3 fold in hypoxia, GSK0660 had no effect on VEGF levels. B) ARPE-19 cells were treated as Müller cells and increased production of VEGF by 2 fold in hypoxia. GSK0660 at 1 μM reduced hypoxia-induced VEGF secretion. C) GW0742 had no effect on VEGF production in mouse Müller cells. D) GW0742 had no significant effect on VEGF secretion from ARPE-19. VEGF concentration was normalized to vehicle-treated cells cultured in normoxia. *p = 0.003.

Effect of PPARβ/δ manipulation on ANGPTL4 expression

While VEGF has been one of the most well-studied proteins regarding DR pathology, it is not the only secreted protein that is both hypoxia-responsive and angiogenic. Recently, angiopoietin-like protein-4 (ANGPTL4) has also been implicated in PDR.[180] ANGPTL4 is also a well-recognized PPARβ/δ target gene.[181] Therefore, I determined whether GSK0660 had an effect on ANGPTL4 expression in Müller cells. Mouse Müller cells were treated with increasing concentrations of GSK0660 in either hypoxia or normoxia and *Angptl4* expression was assayed by qRT-PCR. Hypoxia induced expression of *Angptl4* by 2 fold. (**Figure 22A**). In hypoxia, 0.01, 0.1, and 1 μM GSK0660 all significantly reduced *Angptl4* expression. In normoxia, 0.1 and 1 μM GSK0660 also reduced *Angptl4* expression. On the other hand, 0.01 μM GSK0660 slightly increased *Angptl4* expression.

ANGPTL4 produced by Müller cells can act as a paracrine factor acting on endothelial cells. However, endothelial cells can also produce ANGPTL4 that acts in an autocrine fashion. Therefore, HRMEC were also assayed for the effect of GW0742 and GSK0660 on *ANGPTL4* expression. Human endothelial cells were chosen for their relevance to human disease and because of the difficulty in isolating mouse retinal endothelial cells. HRMEC were treated with GW0742 or GSK0660 at increasing concentrations for 6 hrs. Activation of PPARβ/δ with 0.01, 0.1, and 1 μM GW0742 increased *ANGPTL4* expression in HRMEC (**Figure 22B**). Meanwhile, GSK0660 at all concentrations tested reduced baseline expression of *ANGPTL4* at 6 hrs of treatment (**Figure 22C**).

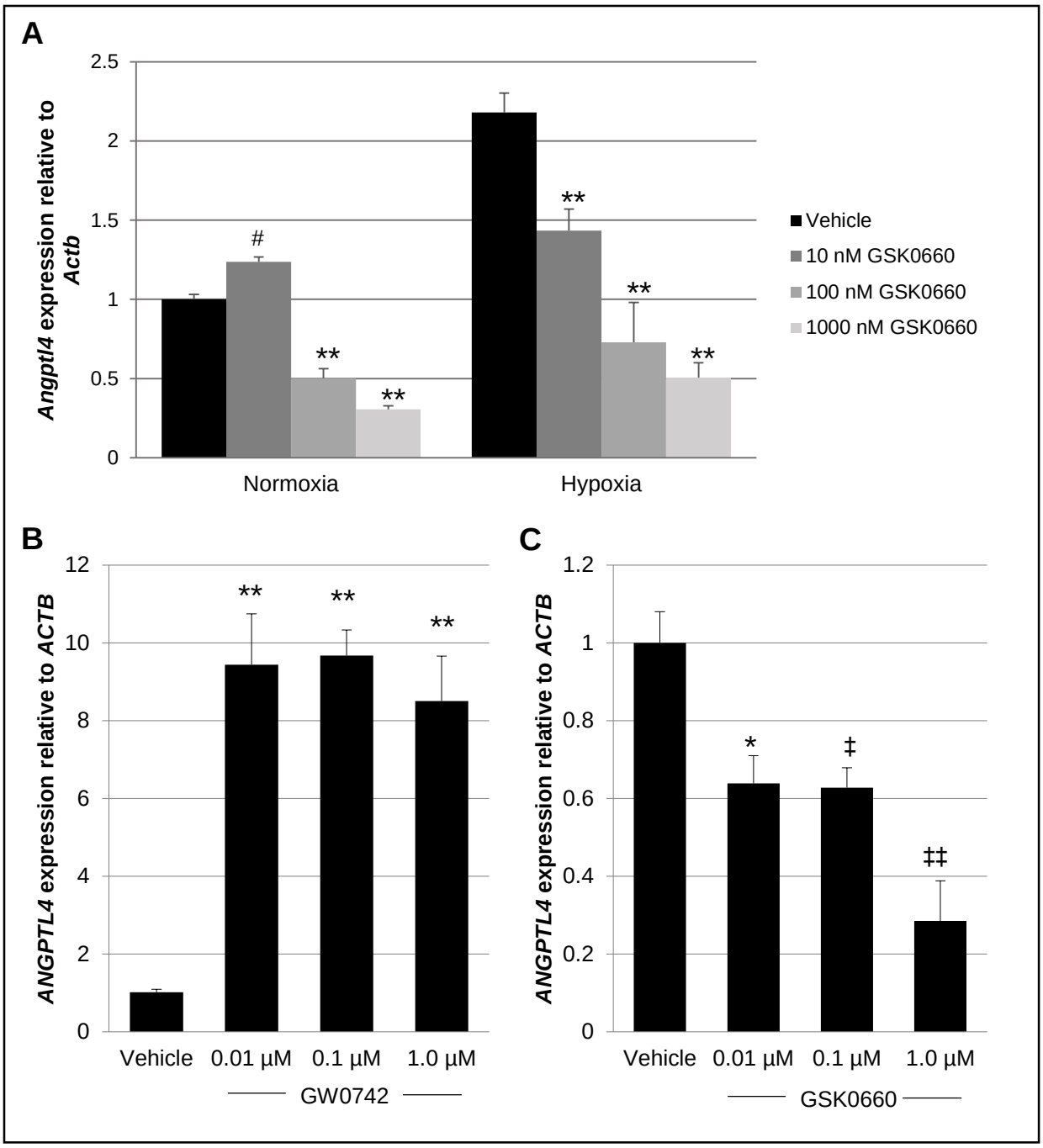

Figure 22. Effect of PPARβ/δ manipulation on *ANGPTL4* expression. A) Mouse Müller cells were placed in normoxia (20.9% O_2) or hypoxia (0.1% O_2) and treated with vehicle or increasing concentrations of GSK0660 for 24 hrs. Cell lysates were processed for qRT-PCR analysis. Hypoxia increased expression of *Angptl4*. GSK0660 significantly reduced this expression in hypoxia at all concentrations tested. GSK0660 at 0.01 µM slightly increased expression of *Angptl4* in normoxia, but reduced expression at 0.1 µM and 1 µM. B) HRMEC cells were treated in 0.5% FBS medium with 0.01, 0.1, or 1 µM GW0742. All concentrations increased expression of *ANGPTL4* compared to vehicle at 6 hrs. C) HRMEC were treated in 2% FBS medium with 0.01, 0.1, or 1 µM GSK0660. All concentrations reduced expression of *ANGPTL4* compared to vehicle at 6 hrs Significance is reported for treatment compared to the vehicle treatment of the same condition. #p = 0259, ‡p = 0.0092, ‡‡p = 0.0002, *p = 0.0035, **p < 0.0001.

Effect of GSK0660 on endothelial cell behaviors

Secreted factors from Müller cells such as VEGF and ANGPTL4 activate endothelial cells to proliferate, migrate, and form tubes to create new capillaries. Previously, we showed that inhibition of PPARβ/δ reduced endothelial cell proliferation and tube formation. Complimentary to my research, other members of the laboratory determined the effect of GW0742 and GSK0660 on HRMEC behaviors. In HRMEC, proliferation is stimulated by addition of FBS to the medium. To determine whether activation of PPARβ/δ stimulates proliferation, GW0742 was added to HRMEC in the presence of 0.5% FBS serum. GW0742 had no effect on proliferation at any concentration tested (**Figure 23**). To determine whether inhibition of PPARβ/δ could inhibit proliferation, GSK0660 was added in the presence of 2% FBS serum. GSK0660 inhibited serum-induced proliferation only at 1 μM.

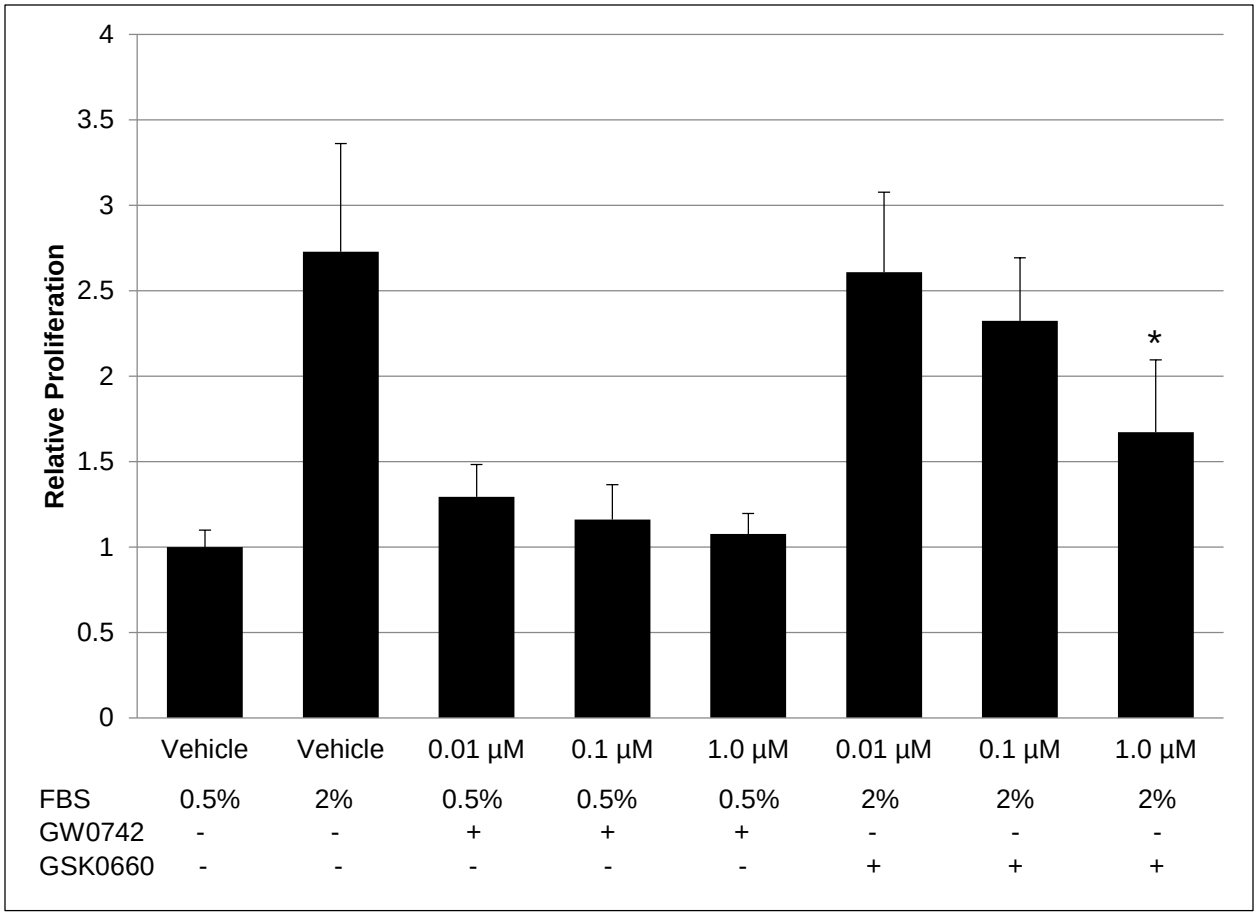

Figure 23. Effect of PPARβ/δ manipulation on HRMEC proliferation. HRMEC were treated with 0.01 to 1 µM GW0742 on a background of 0.5% FBS serum or with 0.01 to 1 µM GSK0660 in the presence of 2% FBS serum for 24 hrs before labeling with BrdU for 12 hrs. GSK0660 reduced cell proliferation at 1 µM while GW0742 had no effect on proliferation. *p = 0.0034

Tube formation is another endothelial cell behavior required for the growth of new blood vessels. To assay tube formation *in vitro*, endothelial cells are placed on Matrigel, which stimulates the formation of connections and tube-like structures between individual endothelial cells. In this experiment, HRMEC were treated with increasing concentrations of GW0742 in serum free conditions to prevent the effect of serum on tube formation. Other samples of HRMEC were treated with increasing concentrations of GSK0660 in the presence of 2% FBS. GW0742 at 0.1 and 1 µM increased the length of tubes produced by HRMEC (**Figure 24**). GSK0660, on the other hand, inhibited serum-induced tube formation at 0.1 and 1 µM.

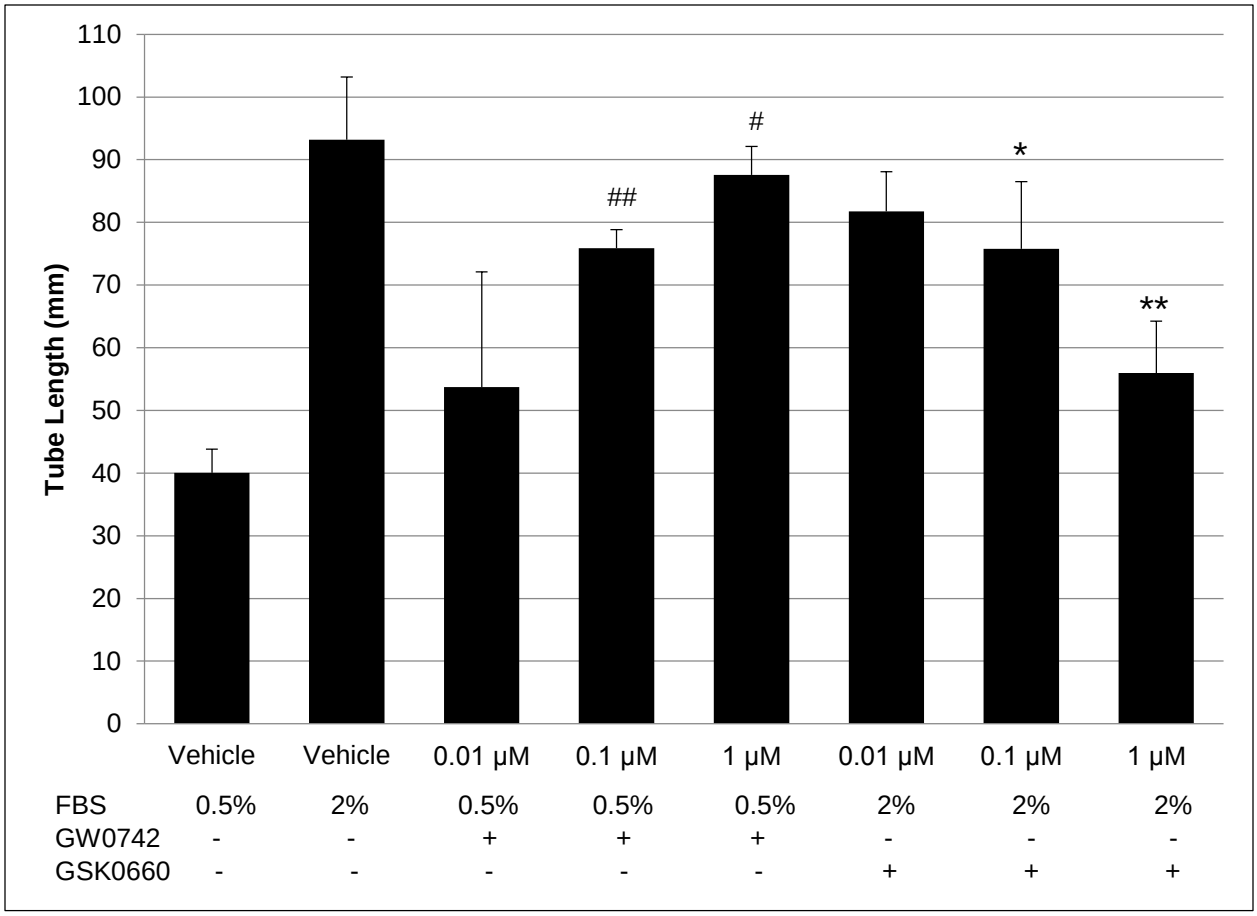

Figure 24. Effect of PPARβ/δ manipulation on HRMEC tube formation. HRMEC were treated with 0.01 to 1 μM GW0742 on a background of 0.5% FBS serum or with 0.01 to 1 μM GSK0660 in the presence of 2% FBS serum for 24 hrs before assaying tube length. GW0742 increased tube formation compared to the 0.5% FBS vehicle control while GSK0660 reduced tube formation compared to the 2% FBS vehicle control. #p = 0.0028, ##p < 0.0001, *p = 0.04, **p = 0.0067

Furthermore, I examined the effect of GSK0660 on the proliferation of additional endothelial cell types with an extended dose response. I found that the inhibition of endothelial cell proliferation by GSK0660 was not limited to HRMEC, but that other endothelial cell types required higher concentrations of GSK0660 to inhibit proliferation. For RRMEC, proliferation was stimulated with 10% FBS. On this background, GSK0660 significantly inhibited RRMEC proliferation at 5 μM and 10 μM (**Figure 25A**). For HCEC, proliferation was stimulated with 50 ng/ml VEGF or 2% FBS. As the baseline proliferation rate of HCEC is very high even in 0.5% FBS medium, the stimulation of proliferation by

FBS or VEGF was minimal. However, GSK0660 significantly reduced proliferation on both of these backgrounds (**Figure 25B**).

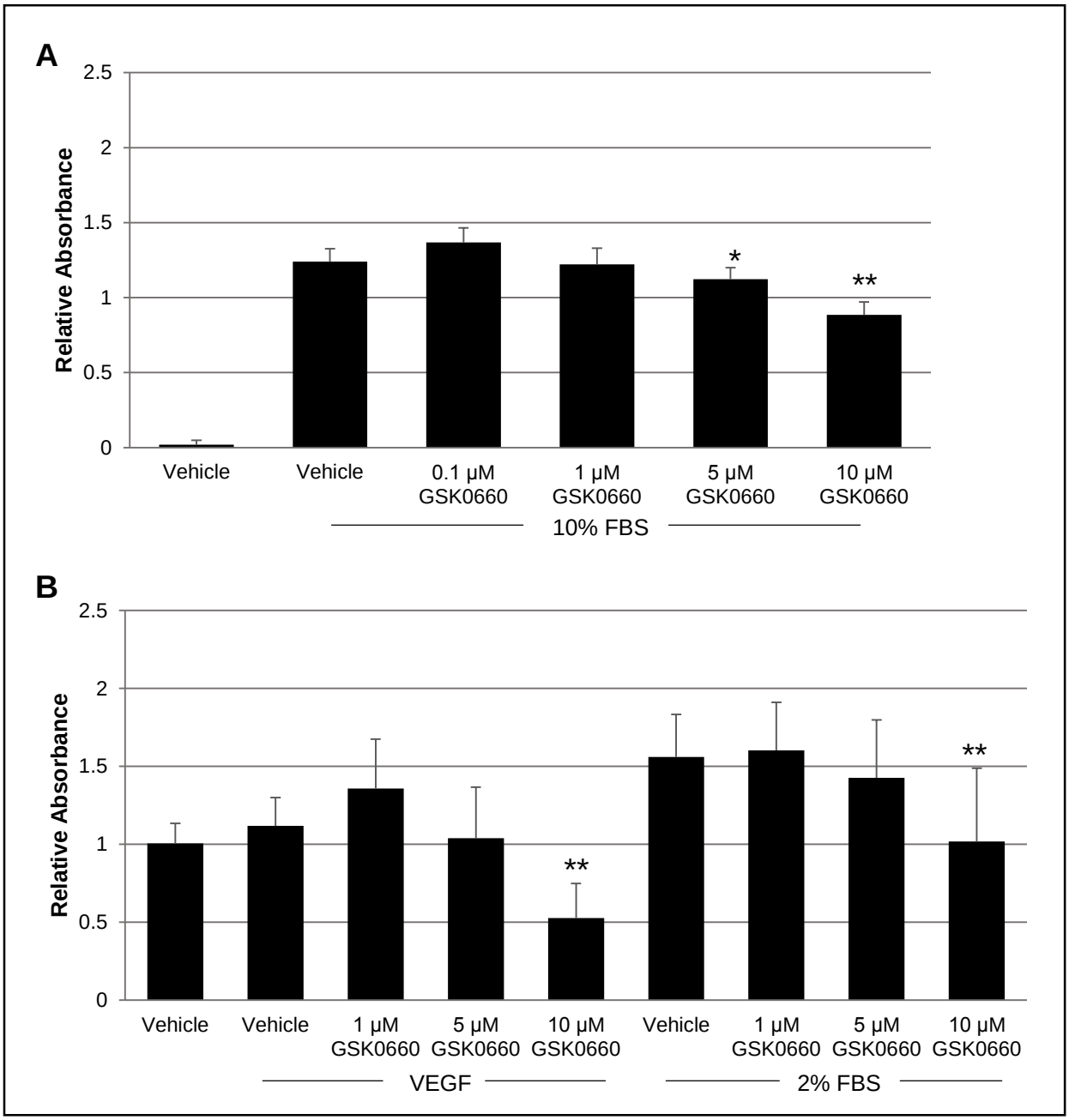

Figure 25. Effect of GSK0660 on endothelial cell proliferation. A) RRMEC were treated with 1 to 10 μM GSK0660 in the presence of 10% FBS for 24 hrs before labeling with BrdU for 12 hrs. GSK0660 reduced cell proliferation at 5 and 10 μM. B) HCEC were treated with GSK0660 in either 0.5% containing 50 ng/ml VEGF or in 2% FBS medium. GSK0660 reduced cell proliferation at 10 μM. *p = 0.0083, **p < 0.0001.

Effect of GSK0660 on models of OIR

Unfortunately there has not yet been a model developed to recapitulate PDR as no animal model of diabetes reliably produces retinal neovascularization. The best *in vivo* model available to measure retinal neovascularization is the OIR model, although it is not related to diabetes. There are two types of rodent OIR models: the rat and the mouse, which have slightly different features. In the rat model of OIR, rat pups are placed in alternating 50% and 10% oxygen levels for the first fourteen days of life. During this time their retinal vasculature is still developing and this protocol stunts growth. Upon return to room air, the avascular peripheral retina becomes hypoxic and upregulates growth factors, resulting in the type of neovascularization seen in PDR. In this model, we administered GW0742 or GSK0660 by intravitreal injections upon removal from oxygen, as well as 3 days later. Three days after the second injection, retinas were collected and analyzed for neovascularization. In this model, GW0742 significantly increased neovascular area compared to a vehicle control, while GSK0660 significantly decreased neovascular area.

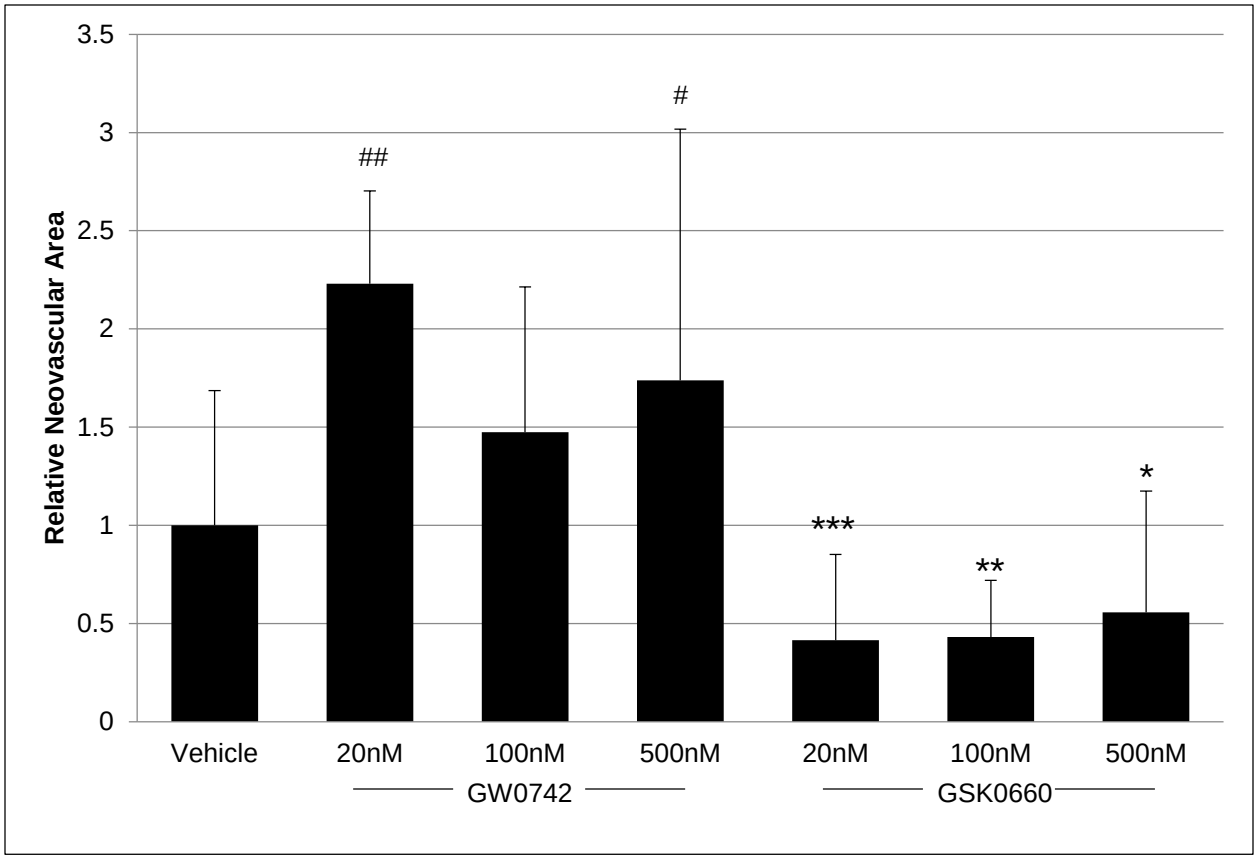

Figure 26. Effect of GW0742 and GSK0660 on rat OIR. Litters of rats are placed in alternating 10% and 50% oxygen from P0 to P14. Upon removal from oxygen, rats were given two intravitreal injections of vehicle, GW0742, or GSK0660 three days apart. Neovascular area was assessed on P20. GW0742 increased neovascular area while GSK0660 inhibited neovascular area. #p = 0.0077, ##p = 0.002, *p = 0.0142, **p = 0.0109, ***p = 0.0084.

The effect of GSK0660 was confirmed in the mouse model of OIR. In this model, litters of seven day old mice are placed in a high oxygen (75%) environment for five days. This environment results in obliteration of capillaries in the central retina of these mice. Upon removal from oxygen at P12 to a room air environment (20.9% O_2), the central retina becomes hypoxic. In response, angiogenic growth occurs in which abnormal vessels grow out of the retina into the vitreous, similar to the neovascular growth seen in patients with PDR. In this model, an intravitreal injection of GSK0660 at a concentration of 1 μM inhibited neovascular growth.

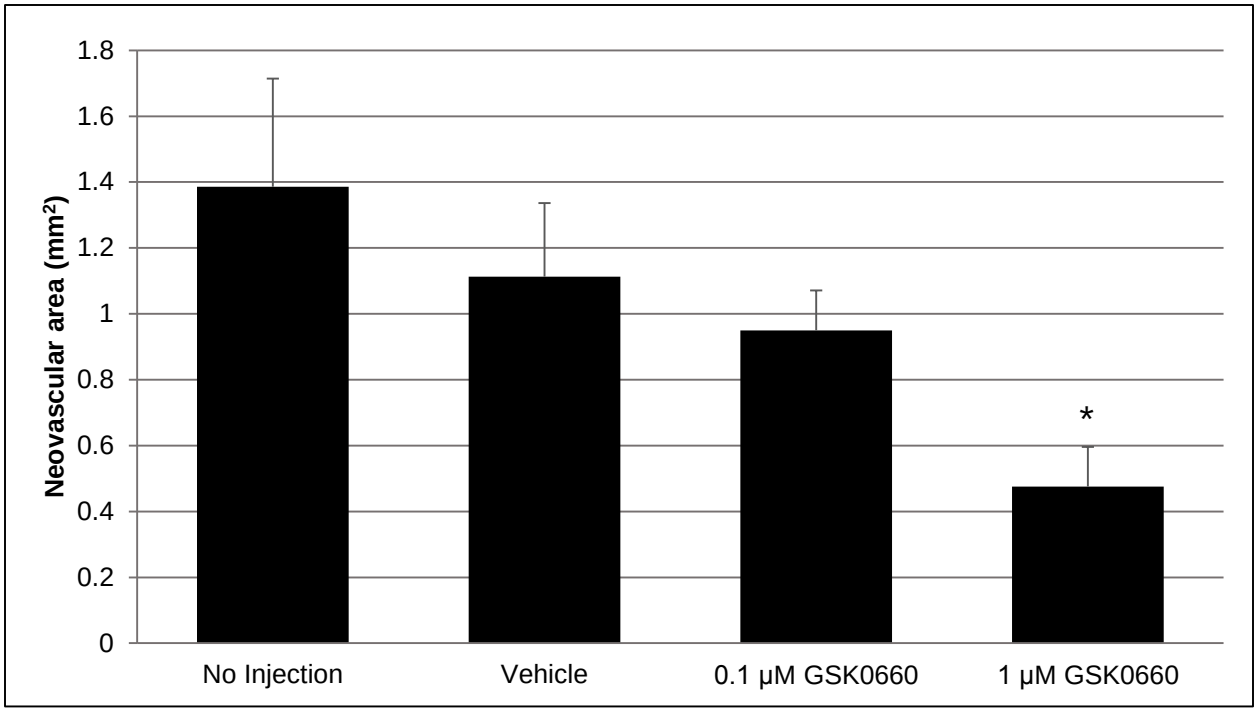

Figure 27. Effect of GSK0660 on mouse OIR. Litters of mice are placed in high oxygen from P7 to P12. Upon removal from oxygen, mice were given intravitreal injections of vehicle, 0.1 or 1 μM GSK0660 and areas of neovascular lesions were counted. GSK0660 at 1 μM significantly reduced neovascular area. Bars represent the mean ± standard error of the mean. *p = 0.0183.

Discussion

In summary, the effect of PPARβ/δ on retinal angiogenesis was consistent with the hypothesis that inhibition of PPARβ/δ is antiangiogenic while activation of PPARβ/δ is angiogenic. In retinal cell types, activation of PPARβ/δ with GW0742 increased production of ANGPTL4 and increased tube formation, ultimately resulting in increased neovascular area in the rat model of OIR. Conversely, inhibition of PPARβ/δ with GSK0660 inhibited production of ANGPTL4, as well as endothelial cell proliferation and tube formation. *In vivo*, GSK0660 inhibited neovascular growth in two rodent OIR models. These results follow well from previous reports in the literature suggesting that PPARβ/δ is angiogenic in a variety of contexts.

The exact mechanism by which PPARβ/δ affects retinal angiogenesis is not yet known although our work suggests at least two possible mechanisms. Upstream, PPARβ/δ affects expression of ANGPTL4, a secreted protein that has a role in lipid metabolism. ANGPTL4 has also recently been reported to play a role in retinal angiogenesis. In a study by Babapoor-Farrokhran et al in 2015, aqueous fluid isolated from patients with PDR stimulated tube formation in immortalized human dermal microvascular endothelial cells that was not affected by addition of anti-VEGF therapy.[180] However, these samples were found to contain ANGPTL4, and when these aqueous samples were pre-incubated with an ANGPTL4 antibody their stimulation of tube formation was eliminated. In the same study, recombinant ANGPTL4 increased corneal neovascularization, further indicating its angiogenic effects. Finally in the mouse OIR model, ANGPTL4 deficiency inhibited neovascularization.[182]

ANGPTL4 is known to be a direct target gene of PPARβ/δ as it contains three PPREs in the third intron and its expression is increased by PPARβ/δ agonists.[183] GSK0660 reduces ANGPTL4 by recruiting corepressors to prevent transcription.[184] By inhibiting production of ANGPTL4, GSK0660 would prevent the angiogenic effects of ANGPTL4 in the retina. On the other hand, the increased expression of ANGPTL4 induced by GW0742 likely contributes to the angiogenic effect of GW0742 in the retina. Our evidence for this includes the robust effect of GW0742 on retinal endothelial tube formation, on which ANGPTL4 also has strong effects.

Besides an effect on the production of angiogenic factors, PPARβ/δ can also contribute directly to the endothelial cell angiogenic response. The likely mechanism for GSK0660 inhibiting endothelial cell behavior and retinal angiogenesis is the inhibition of

ERK. As described in chapter 3, GSK0660 inhibits TNFα-induced ERK activation. Similarly, our laboratory has shown that GSK0660 also inhibits VEGF-induced ERK activation, therefore suggesting that the effect of GSK0660 on ERK activation is not specific to certain stimuli.[185] The activation of ERK is well known to have a significant role in proliferation of endothelial cells. Specifically in OIR, PD98059 significantly inhibits retinal neovascularization.[186]

One other notable discovery from these experiments is that both GW0742 and GSK0660 appear to affect angiogenesis *in vivo* at lower concentrations than *in vitro*. In the rat model of OIR, GW0742 significantly increased neovascularization at an injected concentration of 0.02 μM. The vitreous volume is approximately five times the injection volume, so the effective administered concentration of GW0742 is only 4 nM. Conversely, GW0742 had no effect on *in vitro* proliferation at concentrations ranging from 0.01 to 1 μM and it did not have an effect on *in vitro* tube formation below 0.1 μM. Similarly an effective dose of 4 nM of GSK0660 inhibited retinal neovascularization *in vivo*, but had no effect on proliferation below 1 μM and no effect on tube formation below 0.1 μM. One possibility for these differences could include different ligand potency on PPARβ/δ in different species. Additionally, the effect of PPARβ/δ ligands could be compounded *in vivo* as they hit multiple cell types and points along the angiogenic cascade.

In summary, PPARβ/δ has a role both upstream and downstream in the retinal angiogenic processes. Upstream, inhibiting PPARβ/δ reduces production of the angiogenic factor ANGPTL4. Downstream, PPARβ/δ also inhibits angiogenic endothelial cell behavior. Together, these effects result in inhibition of retinal neovascularization.

Chapter 5

Conclusions and Future Directions

Experimental considerations and the effect of TNFα on retinal endothelial cells

In undertaking this project, my goal was to determine the role of PPARβ/δ in retinopathy, and to discover whether inhibition of PPARβ/δ could be a possible therapeutic avenue for DR. Ultimately, we have learned more about retinal endothelial cell inflammation, PPARβ/δ in the eye, and insights into the mechanisms by which the PPARβ/δ antagonist GSK0660 works.

We were initially led to study TNFα-induced inflammation as a surrogate for DR-induced inflammation as TNFα signaling plays such an important role in DR pathology. TNFα, and its downstream targets, are all upregulated in DR. Additionally, TNFα can cause or contribute to leukostasis, pericyte and endothelial cell death, and retinal inflammation. However, the RNA-seq study performed here in addition to a similar experiment for another project in the laboratory were the first to fully characterize the transcriptional effect of TNFα on human retinal microvascular endothelial cells. This is important because the effect of TNFα on endothelial cells differs between specific types of endothelial cells.[187] HRMEC were chosen as the main cell of study because DR is primarily a disease of microvascular complications and, as primary human cells, HRMEC are the most relevant to human disease.

To be objective, we should consider the parameters chosen for the inflammation-related experiments and the drawbacks to the RNA-seq experiment. First, it can be argued that proteomic changes are more important than mRNA changes since proteins are mainly responsible for cell behaviors. However, to date RNA-sequencing has proven

to be more robust than protein identification and is likely to reflect changes in protein production. Additionally, the RNA-seq experiment and the *in vitro* expression and cell adhesion assays that follow focused on very short periods of stimulation with 1 ng/ml of TNFα. These acute conditions do not reflect DR, since eyes of patients with DR are expected to experience chronic upregulation of low levels of inflammatory factors over a long period of time. Indeed, literature values for serum levels of TNFα in patients with DR, while significantly different from patients without DR, range from 0.8 to 15 pg/ml.[40, 43, 188, 189] Unfortunately these conditions are difficult to mimic in cell culture experiments as longer treatment times result in cell death. For example, direct addition of 20 ng/ml TNFα to cell culture medium leads to apoptosis of 40% of bovine pulmonary artery endothelial cells after only 24 hrs.[190] Therefore, for these experiments care was taken to minimize cell death while maximizing cell inflammation. The concentration of 1 ng/ml for 4 hrs for *in vitro* experiments was chosen because in our PPFC experiments lower concentrations produced very little cell adhesion and higher concentrations produced noticeable phenotypic changes in endothelial monolayer.

In the course of our RNA-seq study, we confirmed transcriptional changes on chemokine and adhesion molecules in HRMEC seen by other groups using other methods. Additionally, the RNA-seq showed that TNFα changed transcripts related to several different inflammatory and immune system pathways, including NOD-like receptor signaling, Toll-like receptor signaling, RIG-I-like receptor signaling, and transcripts related to primary immunodeficiency. Interestingly, TNFα also had an effect on complement and coagulation cascades, calcium signaling pathways, and axon guidance. There has been some work done on the TNFα-induced regulation of these

pathways, but each of these could be interesting areas of further study in retinal endothelial cells.

The role of PPARβ/δ in retinal inflammation

The RNA-seq experiment also served the function of characterizing the role of PPARβ/δ inhibition on TNFα-induced transcriptional changes in HRMEC. Before the studies performed in our laboratory, there had been no reports on pharmacologic manipulation on PPARβ/δ in the retina. In fact, there are few reports of pharmacologic *inhibition* of PPARβ/δ in any context. The main reason for this is that specific antagonists of PPARβ/δ were not developed until 2008, and reports of their use did not appear until 2010. Additionally, the antagonist of PPARβ/δ has been primarily used in co-administration with the agonist. While co-administration serves to confirm specificity of the synthetic agonists, it does not indicate how inhibition of PPARβ/δ might affect cell behavior induced by endogenous agonists.

Endogenous ligands of PPARβ/δ include free fatty acids, retinoic acid, and prostacyclin. Serum levels of free fatty acids have long been known to be increased in both type 1 and type 2 diabetic patients. Additionally, retinal endothelial cells produce free fatty acids, including docosahexaenoic acid and linoleic acid, both of which are ligands for PPARβ/δ.[191, 192] TNFα also increases serum concentrations of free fatty acids.[193] Therefore, there may already be a high level of activation of PPARβ/δ in retinal endothelial cells, particularly in diabetes.

To determine how PPARβ/δ inhibition affects TNFα-induced expression changes in retinal endothelial cells, we used the inverse agonist GSK0660. This drug was developed in 2008 by GlaxoSmithKline using a high-throughput ligand displacement

screen. It was determined to reduce baseline expression of ANGPTL4 and CPT1a, known PPARβ/δ target genes, and to antagonize gene expression changes induced by PPARβ/δ agonists. It was suggested that GSK0660 works by inducing a different conformation of helix 12 in the ligand binding domain of PPARβ/δ than do agonists. This change in conformation reduced the association of the PPARβ/δ ligand binding domain with an LxxLL coactivator peptide while increasing association with a corepressor peptide.[76]

A surprising effect of GSK0660 on HRMEC determined by RNA-seq is the inhibition of TNFα-induced chemokine expression, since agonist effects on other cell types would lead one to expect GSK0660 to exacerbate inflammation. However, in HRMEC, PPARβ/δ inhibited TNFα-induced chemokine expression by varying degrees. According to the RNA-seq, GSK0660 repressed the TNFα-induced effect on 10 chemokines, although the majority of this effect was less than 2 fold. Confirmation of expression changes was determined by qRT-PCR for a subset of these to save resources. GSK0660 was confirmed to reduce the TNFα-induced expression of CCL8, CXCL10, CCL2, CXCL11, and CX3CL1. GSK0660 had a minimal, but ultimately non-significant, effect on CCL17 and CCL5. The reason for the differential effect of GSK0660 on different chemokines could include differences in chromatin conformation or different modes of signaling for inducing various chemokines. For example, allergan-induced expression of CCL17 was STAT6-dependent in lungs, while expression of other chemokines including CCL8 and CXCL10 was not.[194]

Chemokine expression leads to leukostasis through two methods: recruitment of leukocytes and activation of leukocytes. In my studies I chose to focus on CCL8 and CXCL10 as GSK0660 induced the greatest change in their expression with the greatest

consistency between experiments. We evaluated the effect of PPARβ/δ inhibition on both *in vitro* and *in vivo* leukocyte adhesion assays. GSK0660 did inhibit TNFα-induced cell adhesion and this effect *in vitro* was ameliorated by addition of recombinant CCL8 and CXCL10. However, it should also be noted that other chemokines also have a role in the PPFC and their effect is likely to be additive, as seen with the combination of the anti-CCL8 and anti-CXCL10 antibodies on TNFα-induced cell adhesion. For example, CX3CL1, which is also known as fractalkine, has both a transmembrane component as well as a soluble form. Leukocytes can adhere to the transmembrane form of CX3CL1, and this effect is increased by co-expression of VCAM-1.[195] CCL2, another chemokine regulated by GSK0660, regulates monocyte activation for firm adhesion to endothelial cell monolayers.[196] Meanwhile a gradient of CXCL11 in bronchial epithelial cells promotes T cell egression.[197] Thus a combined effect of less overall chemokine production by GSK0660 treated cells is likely responsible for the inhibition of leukostasis.

Besides leukostasis, chemokines can regulate other cell processes. For example, CXCL10 is anti-proliferative and anti-tumorigenic while CX3CL1 mediates neuronal responses to stress.[198] Therefore GSK0660 is almost certain to affect processes other than leukocyte adhesion.

Mechanisms by which GSK0660 inhibits chemokine production

GSK0660 appears to regulate chemokine production and cell adhesion through manipulation of NF-κB translocation. This effect was possibly mediated through inhibition of ERK activation because GSK0660 inhibited TNFα-induced phosphorylation of ERK. Additionally, inhibition of ERK signaling prevented TNFα-induced *CXCL10* expression, further connecting the ERK pathway to chemokine production. Through this, GSK0660

may be responsible for fine-tuning TNFα-induced signaling. The exact mechanism by which PPARβ/δ inhibition affects ERK activation and NF-κB translocation is yet to determined. There are a few hints in the literature for how PPARβ/δ agonism could affect NF-κB activation, but the mechanism remains speculative. In multiple cell types PPARβ/δ prevents degradation of IκBα, the inhibitor of NF-κB. Therefore it is possible that GSK0660 also regulates expression of a regulator of ERK or NF-κB signaling. PPARβ/δ also prevents NF-κB binding to DNA, possibly through a direct interaction between PPARβ/δ and NF-κB. In hearts of mice that underwent endotoxic shock, GW0742 treatment increased phosphorylation of Akt and GSK-3β, which results in inhibition of GSK-3β.[107] Inhibition of GSK-3β resulted in reduced NF-κB activation, as GSK-3β is reported to activate p65 via phosphorylation. Finally in HaCaT cells, GW501516 did not affect IκBα protein levels or TNFα-induced p65 translocation.[199] However, GW501516 did reduce p65 acetylation, thus showing that PPARβ/δ can affect NF-κB activation through a variety of mechanisms in different cell types.

Additionally, PPARβ/δ inhibition could act in ways that are not related to NF-κB. For example, PPARβ/δ could directly repress chemokine expression. However, this seems unlikely as there have been no reported PPREs found in the promoter regions of chemokines including CCL2 and CXCL10. The regulation of chemokine expression by other signaling mechanisms, however, cannot be ruled out. In other cell types, the p38-MAPK and the JNK signaling pathways contribute to chemokine expression. Ligands of PPARβ/δ have been shown to regulate these pathways in other cell types, but it is yet to be determined whether GSK0660 can affect these pathways in HRMEC stimulated with TNFα.

Future directions regarding inflammation

Beyond additional experiments to determine mechanisms by which GSK0660 affects chemokine production, there are several avenues for future studies. One clear extension of these studies is to further characterize the cell adhesion studies, as well as the role of PPARβ/δ in the adhesion process. For our studies we purchased PBMC from Sanguine Biosciences. Depending on the particular donor, a vial of PBMC contains between 70-90% lymphocytes, 10-30% monocytes, and 1-2% dendritic cells. It would be interesting to further characterize which population of cells is being affected both by TNFα and by GSK0660 treatment. The literature suggests that monocytes in particular have a large role in DR. Therefore narrowing the population of cells to a particular type of leukocyte, or even a specific subpopulation of leukocytes, could provide interesting insights into DR. An additional extension could include using PMN. PMN, particularly neutrophils, are also a known component of DR pathology. Furthermore, it would be interesting to see whether using diabetic leukocytes would affect results. As diabetic leukocytes are more highly activated and less likely to deform, it is possible that diabetic leukocytes could overcome the inhibitory effect of GSK0660 on cell adhesion.

Next, our studies regarding inflammation have focused entirely on the effect of GSK0660 on endothelial cells. However, it would be interesting to see whether GSK0660 has an effect on inflammation in other cell types. The first type to study would be leukocytes**.** While few studies have examined the effect of PPARβ/δ manipulation on leukocytes, there have been reports of PPARβ/δ manipulation on platelets and endothelial progenitor cell populations. This could be another important avenue for study as angioblasts are reported to be impaired in diabetes.

Additionally, other retinal cell types, such as Müller cells, also play a role in secretion of inflammatory factors. As chemokine secretion from those cell types would exacerbate retinal inflammation seen in DR, it would be useful to note whether GSK0660 has an effect on expression in those cell types or whether GSK0660 has similar effects using different inflammatory stimuli.

Lastly, the final step regarding inhibition of PPARβ/δ in retinal inflammation would be to evaluate the effect of GSK0660 in a model of diabetes, such as STZ-induced diabetes, to determine whether inhibition of PPARβ/δ has an effect on microvascular changes seen in NPDR. Since chemokine production is elevated in models of diabetes, and that upregulation can lead to leukostasis, further cytokine production, vascular permeability, and endothelial apoptosis, it is likely that PPARβ/δ regulation will have an effect on those downstream targets.

Finally, a clear extension of these studies would include using an agonist of PPARβ/δ to compare the effects of activation vs. inhibition on retinal inflammation. While there have been no studies performed on retinal endothelial cells and inflammation with GW0742, the literature reports on other cell types suggest that GW0742 would show similar anti-inflammatory effects as was seen with GSK0660. Confirming whether GW0742 and GSK0660 have similar effects on TNFα-induced cell adhesion through different mechanisms would give insights into the mechanism of PPARβ/δ activity.

The role of PPARβ/δ in retinal angiogenesis

While inflammation plays a major role in early DR, growth factor-induced angiogenesis is a major component of later DR progression. One contributing growth factor is VEGF, which promotes both DME and PDR. Previous reports of PPARβ/δ

affecting VEGF production have been somewhat contradictory. GW501516 at 10 and 25 nM for 22 hrs increased VEGF mRNA less than 2 fold in HUVEC.[122] Similarly in the EAHy926 endothelial cell line, GW501516 at 100 nM increased VEGF mRNA after 6 hrs and protein secretion after 24 hrs, although both were less than 2 fold.[200] Meanwhile in the human colon cancer cell line KM12C, GW501516 from 1 to 8 μM reduced VEGF secretion while PPARβ/δ knockdown increased VEGF expression.[201] However, neither GW0742 nor GW501516 from 0.1 to 10 μM affected VEGF protein levels in the human colon cancer cell line HCT116.[174]

In mouse Müller cells, neither GW0742 nor GSK0660 had an effect on VEGF production. It should be noted, however, that here and throughout this section the highest concentration of GSK0660 was 1 μM while in other experiments GSK0660 was used up to 10 μM. These experiments were performed first, while later experiments discovered greater effects using 10 μM GSK0660. Therefore it is possible that Müller cell VEGF may be affected by higher concentrations of GSK0660. However, this effect does appear to be cell-type specific. In the RPE cell line ARPE-19, GSK0660 at 1 μM did significantly affect VEGF secretion. It should also be noted that in pilot experiments performed by myself and other laboratory members, neither GW0742 nor GSK0660 had any effect on Müller cell mRNA or retinal VEGF production, nor did siRNA against PPARβ/δ have any effect on VEGF mRNA in Müller cells. As Müller cells are the primary producers of VEGF in DR, I am confident in stating that PPARβ/δ does not have a role in the upregulation of VEGF in DR.

VEGF is not the only important angiogenic factor in DR. Indeed, it has been noted that only 50% of patients with DR respond to anti-VEGF therapy. For further study,

ANGPTL4 was chosen as it is both known to be a direct PPARβ/δ target gene and it has recently been reported to be a therapeutic target for PDR. In the paper by Babapoor-Farrokhran et al 2015, it was noted that aqueous fluid isolated from PDR patients stimulated tube formation of endothelial cells independent of VEGF levels and regardless of the presence of anti-VEGF therapy.[180] ANGPTL4 was discovered to be the factor responsible for tube formation induced by PDR aqueous fluid. ANGPTL4 is a glycosylated protein with a fibrinogen domain that acts primarily in lipid metabolism and glucose homeostasis. In addition to these functions, ANGPTL4 is induced by hypoxia and stimulates angiogenesis. In our cells, GSK0660 is a robust inhibitor of ANGPTL4 expression. The mechanism by which PPARβ/δ modulates ANGPTL4 expression is well known. PPARβ/δ occupancy of the PPRE in ANGPTL4 does not change with addition of GW0742 or GSK0660. GW0742, however, does reduce occupancy of SMRT, a corepressor, thus leading to an increase in ANGPTL4 expression. GSK0660 has no effect on either the corepressors SMRT or NCOR, but it does increase binding of HDAC3, a third corepressor.[76, 184] An additional function of ANGPTL4 promotes vascular permeability.[202] Since increased retinal vascular permeability is a driving force behind development of DME, it is possible that through this mechanism GSK0660 may inhibit DME.

Through inhibition of the production of growth factors such as ANGPTL4, GSK0660 can inhibit angiogenic cell behaviors. However, in our studies we also showed that GSK0660 directly inhibited proliferation of several types of endothelial cells, as well as tube formation of HRMEC. The most likely mechanism by which GSK0660 affects endothelial cell behaviors is through inhibition of ERK activation. However, there are a

few additional possible mechanisms that could be explored. One possibility is that GSK0660 inhibits production of regulators of the cell cycle. In human thyroid epithelial cells, overexpression of PPARβ/δ increased the cell cycle regulators cyclin E1 and cyclin A2.[203] Additionally, GSK0660 may regulate signaling pathways that influence angiogenic responses. For example, GW501516 regulates EPC proliferation via activation of the Akt signaling pathway. GW501516 increased phosphorylation of Akt in EPC within 15 min, which extended to 8 hrs.[121] These effects were PPARβ/δ-dependent as confirmed by using PPARβ/δ siRNA which abolished the effects of GW501516 on Akt signaling.

Future directions

Finally, the main extension of these studies would be to further characterize the signaling mechanisms of PPARβ/δ agonism, antagonism, and knockdown in retinal endothelial cells. Determining the effect of all three methods of PPARβ/δ manipulation on retinal endothelial cell proliferation and inflammation will help to further elucidate PPARβ/δ signaling mechanisms. It would be ideal to use a combination of ChIP-seq and RNA-seq with PPARβ/δ agonism, antagonism, and knockdown to determine which genes are directly targeted by PPARβ/δ in retinal endothelial cells.

In summary, PPARβ/δ inhibition is both anti-inflammatory and anti-angiogenic. PPARβ/δ is likely to have a multi-faceted role in DR. Early in NPDR, inhibition of PPARβ/δ would result in lower chemokine production, reducing the inflammatory environment in the retina. The lowered chemokine production would prevent retinal leukostasis as well as further complications including vascular permeability and capillary degeneration. Finally, inhibition of PPARβ/δ will also affect later issues seen in PDR, as it both prevents

the upregulation of angiogenic factors, and inhibits the downstream response of endothelial cells to those factors. However, because PPARβ/δ is a pleiotrophic transcription factor and is likely to have a number of unexpected side effects, it is not an optimal target for treatment of DR. Still, these studies have been useful to elucidate and underscore the unusual effects of GSK0660.

APPENDIX A

Taqman gene expression IDs used in qRT-PCR.

Gene Name	ID	Species
ACTB	Hs99999903_m1	Human
actb	Mm00607939_s1	Mouse
ANGPTL4	Hs01101127_m1	Human
angptl4	Mm00480431_m1	Mouse
CCL17	Hs00171074_m1	Human
CCL2	Hs00234140_m1	Human
CCL5	Hs00982282_m1	Human
CCL8	Hs99999026_m1	Human
CX3CL1	Hs00171086_m1	Human
CXCL10	Hs01124251_g1	Human
CXCL11	Hs04187682_g1	Human
ICAM1	Hs00164932_m1	Human
NOV	Hs00159631_m1	Human
PDPK1	Hs00176884_m1	Human
PPARD	Hs00602622_m1	Human
VCAM1	Hs01003372_m1	Human

APPENDIX B

List of transcripts differentially expressed in HRMEC treated with TNFα plus GSK0660 compared to treatment with TNFα alone.

Ensembl Gene ID	Official Gene Symbol	log2FoldChange (edgeR)	pValue(edgeR)	pAdj(edgeR)
ENSG00000211966	IGHV5-51	-8.727674012	2.11E-05	0.000390645
ENSG00000251992	SCARNA17	-5.423768796	0.00279933	0.025223908
ENSG00000252139	SCARNA18	-5.201283967	0.002265246	0.021159505
ENSG00000204789	ZNF204P	-4.753134339	0.000638317	0.007420528
ENSG00000225840	AC010970.2	-4.635988029	3.16E-18	8.18E-16
ENSG00000236252	RP11-15J10.8	-4.443198647	0.001611872	0.015977097
ENSG00000256566	RP4-734P14.4	-4.435953441	0.001161682	0.012174777
ENSG00000273338	RP11-386I14.4	-4.435953441	0.001161682	0.012174777
ENSG00000225580	RP1-159M24.1	-4.253932247	0.003071978	0.027235634
ENSG00000149131	SERPING1	-4.25281999	0.002377576	0.022002453
ENSG00000214803	RP11-37N22.1	-4.25281999	0.002377576	0.022002453
ENSG00000186714	CCDC73	-4.252616175	0.002378854	0.022003857
ENSG00000213468	RP11-453F18__B.1	-4.232099694	0.005742193	0.044909935
ENSG00000242154	RP4-778K6.3	-4.04304053	0.004903583	0.039661319
ENSG00000273419	RP4-751H13.7	-4.04304053	0.004903583	0.039661319
ENSG00000197153	HIST1H3J	-4.043009187	0.004903933	0.039661319
ENSG00000259146	RP1-261D10.2	-4.043009187	0.004903933	0.039661319
ENSG00000270068	RP4-761J14.9	-4.042947585	0.004904621	0.039661319
ENSG00000257322	RP11-511B23.2	-4.042916179	0.004904972	0.039661319
ENSG00000213701	SETP22	-4.042822982	0.004906013	0.039661319
ENSG00000225918	AC073331.2	-4.042791492	0.004906364	0.039661319
ENSG00000254990	RP11-108O10.2	-4.042791492	0.004906364	0.039661319
ENSG00000108700	CCL8	-3.445451904	1.23E-05	0.000244835
ENSG00000273374	RP11-383I23.2	-3.200183356	0.000736964	0.008352812
ENSG00000202198	RN7SK	-3.134625795	0.001571152	0.015644466
ENSG00000138135	CH25H	-3.087262332	0.001488116	0.014984916
ENSG00000225764	LEPREL1-AS1	-2.966753533	0.002586032	0.023603472
ENSG00000215304	RP13-395E19.3	-2.838103722	0.005906315	0.045951833
ENSG00000203688	RP11-351J23.1	-2.834471459	0.005102866	0.040915522
ENSG00000176165	FOXG1	-2.834209583	0.004826978	0.039176409
ENSG00000178297	TMPRSS9	-2.784724078	0.000515083	0.006155424
ENSG00000265150	RN7SL2	-2.725060208	3.76E-05	0.000647093
ENSG00000203914	HSP90B3P	-2.572705945	0.000185197	0.002577702
ENSG00000043462	LCP2	-2.553894739	2.74E-05	0.000489648
ENSG00000273190	RP11-255C15.4	-2.509378032	0.002556017	0.023350597
ENSG00000270145	CTD-2267D19.6	-2.496572548	0.000122043	0.001798623
ENSG00000258486	RN7SL1	-2.248076207	0.000627941	0.007325173
ENSG00000237548	TTLL11-IT1	-2.179533373	0.005818334	0.045411752
ENSG00000269720	CTD-2521M24.5	-2.097821581	0.004854009	0.03937472
ENSG00000201678	Y_RNA	-2.062251493	0.003523998	0.030366493
ENSG00000272048	RP11-458N5.1	-2.02884	0.000861249	0.009498798
ENSG00000078795	PKD2L2	-2.016705824	0.002970452	0.026490386
ENSG00000157404	KIT	-1.992297751	3.36E-33	3.64E-30
ENSG00000154188	ANGPT1	-1.991680506	0.000365579	0.004598924
ENSG00000102760	RGCC	-1.972667995	2.83E-92	4.30E-88
ENSG00000137033	IL33	-1.930205781	0.000199892	0.002757035

ENSG00000185860	C1orf110	-1.880363924	6.00E-21	2.26E-18
ENSG00000251562	MALAT1	-1.874628612	0.000102945	0.001557263
ENSG00000255382	RP11-718B12.2	-1.844438925	0.00265657	0.024138339
ENSG00000242242	PVRL3-AS1	-1.71861625	0.003254249	0.028406022
ENSG00000206532	RP11-553A10.1	-1.682434845	1.88E-11	1.48E-09
ENSG00000254481	PTP4A2P2	-1.674905222	0.000550585	0.006532184
ENSG00000171388	APLN	-1.654467587	3.86E-124	1.17E-119
ENSG00000006432	MAP3K9	-1.652772602	0.005127529	0.041066269
ENSG00000169245	CXCL10	-1.638192095	4.53E-45	1.15E-41
ENSG00000116194	ANGPTL1	-1.631997894	0.006477455	0.049498922
ENSG00000268355	AC006129.1	-1.622595142	0.001476529	0.014881284
ENSG00000163687	DNASE1L3	-1.604902697	0.002464155	0.022661557
ENSG00000246777	RP11-61A14.4	-1.594146902	0.001247062	0.01292665
ENSG00000131203	IDO1	-1.587907616	0.001680284	0.016578341
ENSG00000167772	ANGPTL4	-1.537119445	1.70E-05	0.000324657
ENSG00000163362	C1orf106	-1.46621162	0.00048797	0.005887087
ENSG00000261594	TPBGL	-1.423612562	0.001527855	0.015303778
ENSG00000141668	CBLN2	-1.392336412	1.24E-05	0.000246294
ENSG00000135114	OASL	-1.390038229	1.03E-15	1.72E-13
ENSG00000134326	CMPK2	-1.388834822	2.51E-15	3.96E-13
ENSG00000200693	U3	-1.313267744	0.005103311	0.040915522
ENSG00000248187	RP11-184M15.1	-1.310172825	0.001498982	0.01506932
ENSG00000134321	RSAD2	-1.299138388	3.55E-16	6.37E-14
ENSG00000109193	SULT1E1	-1.284115918	8.73E-06	0.000180688
ENSG00000229164	TRAC	-1.25182113	0.000413648	0.005118699
ENSG00000147160	AWAT2	-1.241580923	0.002489182	0.022858847
ENSG00000257511	RP11-278C7.1	-1.223914039	0.002111974	0.019942766
ENSG00000258808	RP11-255G12.3	-1.222035621	0.000751924	0.0085033
ENSG00000227260	AC116035.1	-1.208634063	0.004399307	0.036372202
ENSG00000102970	CCL17	-1.196675084	0.004668547	0.038217825
ENSG00000152503	TRIM36	-1.187138103	0.000215744	0.002943557
ENSG00000117289	TXNIP	-1.185460745	1.03E-21	4.33E-19
ENSG00000236824	BCYRN1	-1.167869083	1.01E-09	5.39E-08
ENSG00000272405	RP11-284F21.10	-1.156997497	0.001610345	0.015971805
ENSG00000267374	LINC00669	-1.156193659	0.005170225	0.041310039
ENSG00000183032	SLC25A21	-1.151709685	1.33E-05	0.000260074
ENSG00000164056	SPRY1	-1.141323776	6.56E-06	0.000140993
ENSG00000104043	ATP8B4	-1.135364158	0.00087439	0.009601828
ENSG00000111335	OAS2	-1.134234458	2.07E-22	9.53E-20
ENSG00000175899	A2M	-1.131419069	0.002888858	0.025884506
ENSG00000224411	RP11-1033A18.1	-1.107350885	0.005652567	0.044395355
ENSG00000183395	PMCH	-1.099326651	1.57E-05	0.000302056
ENSG00000171840	NINJ2	-1.087687072	0.001977525	0.018920613
ENSG00000183196	CHST6	-1.086499625	9.55E-05	0.001462788
ENSG00000103044	HAS3	-1.082886724	3.20E-05	0.000561057
ENSG00000157601	MX1	-1.079236132	2.82E-21	1.12E-18
ENSG00000244313	RP11-425L10.1	-1.069235678	0.00238838	0.022078498
ENSG00000169860	P2RY1	-1.049774256	0.000113878	0.00169559
ENSG00000189120	SP6	-1.044801606	3.58E-18	9.13E-16
ENSG00000183486	MX2	-1.041643685	1.37E-08	5.81E-07
ENSG00000120217	CD274	-1.037932772	3.21E-50	1.08E-46
ENSG00000110876	SELPLG	-1.026503183	0.00022598	0.00306528
ENSG00000178343	SHISA3	-1.009392496	1.34E-05	0.000261553

ENSG00000110077	MS4A6A	-1.007387541	0.004964744	0.04000081
ENSG00000185745	IFIT1	-1.007129479	1.43E-11	1.15E-09
ENSG00000132359	RAP1GAP2	-1.005523953	0.00194879	0.018692852
ENSG00000228495	LINC01013	-1.004984423	8.16E-19	2.31E-16
ENSG00000226053	RP5-1070A16.1	-1.00225345	2.73E-06	6.55E-05
ENSG00000168675	LDLRAD4	1.000308978	3.72E-06	8.58E-05
ENSG00000140044	JDP2	1.00201249	7.04E-06	0.00014948
ENSG00000196517	SLC6A9	1.00266614	0.005701599	0.044692532
ENSG00000223764	RP11-54O7.3	1.00594169	0.000353928	0.004467177
ENSG00000160323	ADAMTS13	1.008450033	5.32E-05	0.000879617
ENSG00000072954	TMEM38A	1.010311279	0.000849942	0.009384322
ENSG00000121895	TMEM156	1.011497973	1.51E-05	0.000292683
ENSG00000075213	SEMA3A	1.013984708	9.48E-70	7.19E-66
ENSG00000162337	LRP5	1.017096212	6.38E-53	2.77E-49
ENSG00000130702	LAMA5	1.025355528	1.33E-34	1.75E-31
ENSG00000006016	CRLF1	1.029327157	7.45E-06	0.000156453
ENSG00000184986	TMEM121	1.033017649	0.004956704	0.039972572
ENSG00000141448	GATA6	1.033351774	5.45E-49	1.65E-45
ENSG00000266176	RP11-855A2.5	1.035499954	0.001028307	0.010993494
ENSG00000162591	MEGF6	1.039404873	5.71E-70	5.78E-66
ENSG00000047648	ARHGAP6	1.040261917	0.000109503	0.001641739
ENSG00000196421	LINC00176	1.043596814	0.00106257	0.011308969
ENSG00000205444	RP4-529N6.1	1.049401774	0.006304414	0.048518869
ENSG00000140465	CYP1A1	1.051285633	3.91E-13	4.35E-11
ENSG00000268297	CLEC4GP1	1.051564554	0.001181247	0.012354214
ENSG00000100191	SLC5A4	1.055374371	0.00400034	0.033674803
ENSG00000100078	PLA2G3	1.062195706	0.00017298	0.002432308
ENSG00000247809	NR2F2-AS1	1.064882326	3.05E-05	0.000537746
ENSG00000130751	NPAS1	1.06585841	0.001019396	0.010908394
ENSG00000169418	NPR1	1.065940394	5.70E-25	3.53E-22
ENSG00000139725	RHOF	1.078399997	4.04E-09	1.90E-07
ENSG00000251705	RNA5-8SP6	1.080796521	0.000224743	0.003049868
ENSG00000146469	VIP	1.081115403	0.002098003	0.019854111
ENSG00000185615	PDIA2	1.088387137	0.004009857	0.033736186
ENSG00000124212	PTGIS	1.099593534	5.15E-33	5.20E-30
ENSG00000115257	PCSK4	1.110444208	0.000603608	0.007097535
ENSG00000142920	ADC	1.110971989	0.001282103	0.013240108
ENSG00000130222	GADD45G	1.112737881	0.000843617	0.009331469
ENSG00000260910	LINC00565	1.114426942	0.002347428	0.021780122
ENSG00000163040	CCDC74A	1.122129837	0.000316716	0.004088802
ENSG00000108602	ALDH3A1	1.142517045	0.000101101	0.001537808
ENSG00000114270	COL7A1	1.146977566	2.93E-07	9.02E-06
ENSG00000177106	EPS8L2	1.15178556	4.31E-18	1.06E-15
ENSG00000105672	ETV2	1.157124664	0.005634431	0.04430705
ENSG00000161328	LRRC56	1.158597274	0.005862551	0.045686325
ENSG00000109452	INPP4B	1.17045071	3.54E-08	1.35E-06
ENSG00000235919	ASH1L-AS1	1.172001118	0.000240438	0.003236793
ENSG00000245532	NEAT1	1.174965781	1.44E-19	4.69E-17
ENSG00000153714	LURAP1L	1.182650865	5.31E-07	1.52E-05
ENSG00000178814	OPLAH	1.190999755	5.04E-10	2.92E-08
ENSG00000203836	NBPF24	1.210988598	0.005777484	0.045127762
ENSG00000181754	AMIGO1	1.214553389	5.52E-05	0.000906924
ENSG00000145777	TSLP	1.220676867	2.77E-06	6.63E-05

ENSG00000183117	CSMD1	1.232736564	0.003197575	0.028053935
ENSG00000248098	BCKDHA	1.235192595	0.000931466	0.010122313
ENSG00000147434	CHRNA6	1.237503345	0.000932095	0.01012552
ENSG00000084734	GCKR	1.253259234	1.72E-13	2.08E-11
ENSG00000137809	ITGA11	1.258065799	4.00E-20	1.35E-17
ENSG00000123384	LRP1	1.260067029	3.11E-21	1.23E-18
ENSG00000089847	ANKRD24	1.277819306	0.004505615	0.037074145
ENSG00000115468	EFHD1	1.279415364	0.000306915	0.00399003
ENSG00000162572	SCNN1D	1.286454459	2.03E-06	5.01E-05
ENSG00000128342	LIF	1.312116752	2.04E-16	3.79E-14
ENSG00000178695	KCTD12	1.327544797	6.09E-60	3.08E-56
ENSG00000212864	RNF208	1.336661658	1.22E-07	4.15E-06
ENSG00000148082	SHC3	1.343667488	0.00041306	0.005113511
ENSG00000064270	ATP2C2	1.3450103	4.90E-19	1.46E-16
ENSG00000065054	SLC9A3R2	1.345759721	6.82E-36	9.85E-33
ENSG00000141314	RHBDL3	1.348728835	4.27E-05	0.000726324
ENSG00000128298	BAIAP2L2	1.353267114	0.003240386	0.028339361
ENSG00000104611	SH2D4A	1.356738118	0.000396434	0.004937929
ENSG00000250999	RP11-1379J22.5	1.361187479	0.004574419	0.037579125
ENSG00000135547	HEY2	1.383838905	0.000378801	0.004743609
ENSG00000249637	CTC-329D1.2	1.390565715	0.003303616	0.028743167
ENSG00000272523	LINC01023	1.394230877	0.001180134	0.012346835
ENSG00000187479	C11orf96	1.461264178	1.53E-05	0.000296392
ENSG00000186891	TNFRSF18	1.472313767	0.004445196	0.036701053
ENSG00000184363	PKP3	1.47633057	0.001205291	0.012558043
ENSG00000144485	HES6	1.477813165	6.49E-08	2.37E-06
ENSG00000243696	RP5-966M1.6	1.484453596	0.002695028	0.024421931
ENSG00000236671	PRKG1-AS1	1.497148149	0.000303063	0.003945024
ENSG00000205038	PKHD1L1	1.520282927	0.000718394	0.008182083
ENSG00000066248	NGEF	1.538868112	6.72E-22	2.88E-19
ENSG00000197632	SERPINB2	1.5427125	4.27E-48	1.18E-44
ENSG00000213363	RPS3P6	1.546600182	0.001750743	0.017140106
ENSG00000163884	KLF15	1.548445763	8.28E-07	2.25E-05
ENSG00000169583	CLIC3	1.54986604	1.68E-06	4.22E-05
ENSG00000202318	Y_RNA	1.559156601	0.006500818	0.049551703
ENSG00000205177	C11orf91	1.574294182	0.003388452	0.029396955
ENSG00000178226	PRSS36	1.57450385	0.004286487	0.035599436
ENSG00000258791	LINC00520	1.5789369	4.80E-07	1.40E-05
ENSG00000142235	LMTK3	1.585059528	0.004848828	0.039343217
ENSG00000267163	AC084219.3	1.585565748	0.001959946	0.018782039
ENSG00000225783	MIAT	1.603305874	0.000497728	0.005978651
ENSG00000249593	CTB-46B19.2	1.62371141	0.006502334	0.049551703
ENSG00000128965	CHAC1	1.624836076	1.49E-12	1.45E-10
ENSG00000254602	AP000662.4	1.634791531	0.002109629	0.019938332
ENSG00000213413	PVRIG	1.63982315	0.001111322	0.011776842
ENSG00000183971	NPW	1.642394488	8.89E-05	0.001377856
ENSG00000101188	NTSR1	1.65762332	7.73E-07	2.12E-05
ENSG00000224950	RP5-1086K13.1	1.681857839	7.42E-06	0.000155987
ENSG00000131650	KREMEN2	1.693316787	0.001980019	0.018932526
ENSG00000235373	RP11-206L10.3	1.695842017	0.005652979	0.044395355
ENSG00000132470	ITGB4	1.699117839	9.84E-33	9.04E-30
ENSG00000131620	ANO1	1.720690373	6.48E-14	8.43E-12
ENSG00000226935	LINC00161	1.737641293	0.000661117	0.007630015

ENSG00000042832	TG	1.755907633	0.003436135	0.029725602
ENSG00000184163	FAM132A	1.762363487	0.000114256	0.001698849
ENSG00000251414	RP11-843P14.1	1.768924293	0.002861621	0.025678392
ENSG00000165795	NDRG2	1.77133057	0.004244831	0.03533088
ENSG00000263588	RP11-595B24.2	1.771553984	9.80E-05	0.001495741
ENSG00000164651	SP8	1.784681087	0.005452295	0.043165779
ENSG00000197301	RP11-366L20.2	1.784701546	0.00545184	0.043165779
ENSG00000229816	DDX50P1	1.784743951	0.005450652	0.043165779
ENSG00000139193	CD27	1.834793126	0.005158483	0.04124882
ENSG00000136999	NOV	1.835132752	7.40E-07	2.04E-05
ENSG00000126217	MCF2L	1.859671792	7.86E-07	2.15E-05
ENSG00000231997	FAM27D1	1.910203846	0.0057622	0.045043175
ENSG00000068078	FGFR3	1.929038415	1.74E-18	4.74E-16
ENSG00000166823	MESP1	1.932664789	0.001724125	0.016914402
ENSG00000161031	PGLYRP2	1.967244702	0.000601801	0.007082901
ENSG00000162009	SSTR5	1.995270822	0.003527239	0.030366493
ENSG00000100312	ACR	1.995283674	0.003527037	0.030366493
ENSG00000232564	RP4-591N18.2	1.995385562	0.003525324	0.030366493
ENSG00000168453	HR	2.010419397	0.002233903	0.020905364
ENSG00000231172	AC007099.1	2.076282993	0.006497851	0.049551703
ENSG00000255559	ZNF252P-AS1	2.080880863	0.002021242	0.019253855
ENSG00000101276	SLC52A3	2.087235666	6.66E-05	0.001069091
ENSG00000151322	NPAS3	2.132837193	5.91E-09	2.69E-07
ENSG00000243056	EIF4EBP3	2.159851995	0.001807995	0.017570166
ENSG00000129451	KLK10	2.180241603	0.003934419	0.03321206
ENSG00000092850	TEKT2	2.278122047	0.002323419	0.021609721
ENSG00000187021	PNLIPRP1	2.347095758	0.006311915	0.048564279
ENSG00000167037	SGSM1	2.3635829	0.001987981	0.018990693
ENSG00000264569	RP13-650J16.1	2.468671389	0.003453404	0.029840953
ENSG00000175315	CST6	2.468774926	0.003381004	0.029340731
ENSG00000243055	GK-AS1	2.468804587	0.003380511	0.029340731
ENSG00000262039	RP11-81K2.1	2.470181191	0.004445752	0.036701053
ENSG00000115339	GALNT3	2.580785122	0.003623198	0.031060368
ENSG00000214389	RPS3AP26	2.580912972	0.001799682	0.017511822
ENSG00000259887	RP11-923I11.5	2.611661691	0.00020068	0.00276344
ENSG00000250122	CTD-2013M15.1	2.85078885	0.004965481	0.04000081
ENSG00000186399	GOLGA8R	2.850824538	0.004964895	0.04000081
ENSG00000160185	UBASH3A	2.850826781	0.004964859	0.04000081
ENSG00000260190	RP11-229P13.25	2.851126706	0.006280258	0.048345238
ENSG00000224261	RP11-179G5.1	3.001864509	0.004797582	0.039053973
ENSG00000112293	GPLD1	3.129996475	0.001252385	0.012964106
ENSG00000064205	WISP2	3.130060871	0.001252086	0.012964106
ENSG00000231943	RP11-395L14.4	3.25171359	0.000626375	0.007313023
ENSG00000269194	AC006942.4	3.251836684	0.000626048	0.007313023
ENSG00000166546	BEAN1	3.364047225	0.000312489	0.004043429
ENSG00000254270	ERHP1	3.656041917	4.28E-05	0.000728868
ENSG00000273449	RP11-218F10.3	3.739328092	7.04E-05	0.001123971
ENSG00000227969	NPM1P22	4.12540086	0.006072136	0.046981603
ENSG00000267136	RP11-53B2.3	4.133589929	0.003156968	0.027737782
ENSG00000179674	ARL14	4.133638802	0.003156595	0.027737782
ENSG00000240210	RP11-204K16.1	4.133638802	0.003156595	0.027737782
ENSG00000173320	STOX2	4.133641693	0.003156573	0.027737782
ENSG00000175772	AC112229.7	4.133641693	0.003156573	0.027737782

ENSG00000244558	RP11-445H22.4	4.133641693	0.003156573	0.027737782
ENSG00000180610	ZBTB12P1	4.133684738	0.003156244	0.027737782
ENSG00000254671	STT3A-AS1	4.133687626	0.003156222	0.027737782
ENSG00000258378	RP11-517O13.1	4.133687626	0.003156222	0.027737782
ENSG00000268593	CTD-2611O12.6	4.133687626	0.003156222	0.027737782
ENSG00000261693	RP13-467H17.1	4.141426441	0.005336214	0.04241283
ENSG00000272027	RP11-529E15.1	4.330679806	0.005557729	0.043851698
ENSG00000264175	MIR3189	4.344228465	0.001430619	0.014487704
ENSG00000260126	RP11-14N9.2	4.347276198	0.001938855	0.018620112
ENSG00000259780	RP11-304L19.12	4.347401868	0.001942383	0.018637296
ENSG00000268470	DNAH17-AS1	4.527256344	0.000717531	0.008175321
ENSG00000252759	Y_RNA	4.52945	0.002896753	0.025939926
ENSG00000176945	MUC20	4.702950855	0.001130952	0.011947675
ENSG00000162391	FAM151A	4.837332922	0.000138746	0.002008674
ENSG00000129993	CBFA2T3	4.970269827	6.43E-05	0.001038075

APPENDIX C

Network of differentially expressed genes in the RNA-seq.

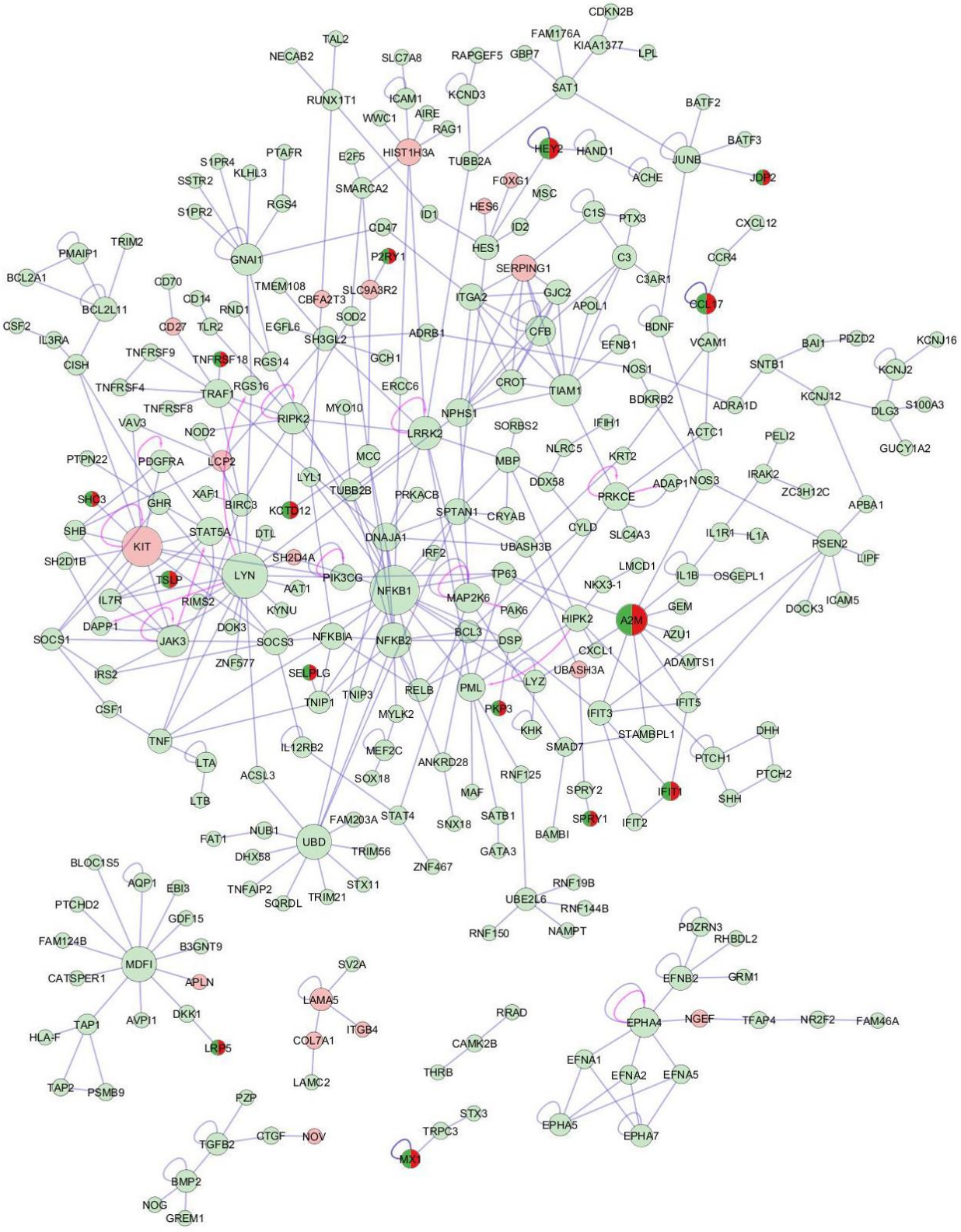

APPENDIX D

siRNA oligomer sequences.

Name	Strand	Sequence
Control	Sense	5'-UUCUCCGAACGUGUCACGUTT-3'
Catalog: 1022076	Antisense	5'-ACGUGACACGUUCGGAGAATT-3'
PPARD	Sense	5'-GUGAUAUCAUUGAGCCUAATT-3'
Catalog: SI00086058	Antisense	5'-UUAGGCUCAAUGAUAUCACTG-3'

REFERENCES

1. Kirtland KA, Burrows NR, Geiss LS. Diabetes Interactive Atlas. Preventing chronic disease. 2014;11:130300.
2. American Diabetes A. Diagnosis and classification of diabetes mellitus. Diabetes care. 2014;37 Suppl 1:S81-90.
3. The effect of intensive treatment of diabetes on the development and progression of long-term complications in insulin-dependent diabetes mellitus. The Diabetes Control and Complications Trial Research Group. The New England journal of medicine. 1993;329(14):977-86.
4. Intensive blood-glucose control with sulphonylureas or insulin compared with conventional treatment and risk of complications in patients with type 2 diabetes (UKPDS 33). UK Prospective Diabetes Study (UKPDS) Group. Lancet. 1998;352(9131):837-53.
5. Fong DS, Aiello L, Gardner TW, King GL, Blankenship G, Cavallerano JD, et al. Retinopathy in diabetes. Diabetes care. 2004;27 Suppl 1:S84-7.
6. Yau JW, Rogers SL, Kawasaki R, Lamoureux EL, Kowalski JW, Bek T, et al. Global prevalence and major risk factors of diabetic retinopathy. Diabetes care. 2012;35(3):556-64.
7. The relationship of glycemic exposure (HbA1c) to the risk of development and progression of retinopathy in the diabetes control and complications trial. Diabetes. 1995;44(8):968-83.
8. Klein R, Klein BE. Blood pressure control and diabetic retinopathy. The British journal of ophthalmology. 2002;86(4):365-7.
9. Toussaint D, Cogan DG, Kuwabara T. Extravascular lesions of diabetic retinopathy. Archives of ophthalmology. 1962;67:42-7.
10. Schmidt D. The mystery of cotton-wool spots - a review of recent and historical descriptions. European journal of medical research. 2008;13(6):231-66.
11. Nunes S, Pires I, Rosa A, Duarte L, Bernardes R, Cunha-Vaz J. Microaneurysm turnover is a biomarker for diabetic retinopathy progression to clinically significant macular edema: findings for type 2 diabetics with nonproliferative retinopathy. Ophthalmologica Journal international d'ophtalmologie International journal of ophthalmology Zeitschrift fur Augenheilkunde. 2009;223(5):292-7.
12. Garner A. Histopathology of diabetic retinopathy in man. Eye. 1993;7 (Pt 2):250-3.
13. Eisma JH, Dulle JE, Fort PE. Current knowledge on diabetic retinopathy from human donor tissues. World journal of diabetes. 2015;6(2):312-20.
14. Boulton ME, McLeod D, Garner A. Vasoproliferative retinopathies: clinical, morphogenetic and modulatory aspects. Eye. 1988;2 Suppl:S124-39.
15. Forrester JV, Shafiee A, Schroder S, Knott R, McIntosh L. The role of growth factors in proliferative diabetic retinopathy. Eye. 1993;7 (Pt 2):276-87.
16. Crawford TN, Alfaro DV, 3rd, Kerrison JB, Jablon EP. Diabetic retinopathy and angiogenesis. Current diabetes reviews. 2009;5(1):8-13.
17. Davidson JA, Ciulla TA, McGill JB, Kles KA, Anderson PW. How the diabetic eye loses vision. Endocrine. 2007;32(1):107-16.
18. Kozak I, Luttrull JK. Modern retinal laser therapy. Saudi journal of ophthalmology : official journal of the Saudi Ophthalmological Society. 2015;29(2):137-46.
19. Ferris FL, 3rd. How effective are treatments for diabetic retinopathy? Jama. 1993;269(10):1290-1.
20. Park YG, Kim EY, Roh YJ. Laser-based strategies to treat diabetic macular edema: history and new promising therapies. Journal of ophthalmology. 2014;2014:769213.
21. Morgan CM, Schatz H. Atrophic creep of the retinal pigment epithelium after focal macular photocoagulation. Ophthalmology. 1989;96(1):96-103.

22. Frank RN. Visual fields and electroretinography following extensive photocoagulation. Archives of ophthalmology. 1975;93(8):591-8.
23. Fong DS, Girach A, Boney A. Visual side effects of successful scatter laser photocoagulation surgery for proliferative diabetic retinopathy: a literature review. Retina. 2007;27(7):816-24.
24. McDonald HR, Schatz H. Macular edema following panretinal photocoagulation. Retina. 1985;5(1):5-10.
25. Ferrara N. Vascular endothelial growth factor and age-related macular degeneration: from basic science to therapy. Nature medicine. 2010;16(10):1107-11.
26. Adamis AP, Miller JW, Bernal MT, D'Amico DJ, Folkman J, Yeo TK, et al. Increased vascular endothelial growth factor levels in the vitreous of eyes with proliferative diabetic retinopathy. American journal of ophthalmology. 1994;118(4):445-50.
27. Funatsu H, Yamashita H, Noma H, Mimura T, Yamashita T, Hori S. Increased levels of vascular endothelial growth factor and interleukin-6 in the aqueous humor of diabetics with macular edema. American journal of ophthalmology. 2002;133(1):70-7.
28. Brown DM, Nguyen QD, Marcus DM, Boyer DS, Patel S, Feiner L, et al. Long-term outcomes of ranibizumab therapy for diabetic macular edema: the 36-month results from two phase III trials: RISE and RIDE. Ophthalmology. 2013;120(10):2013-22.
29. Mirshahi A, Roohipoor R, Lashay A, Mohammadi SF, Abdoallahi A, Faghihi H. Bevacizumab-augmented retinal laser photocoagulation in proliferative diabetic retinopathy: a randomized double-masked clinical trial. European journal of ophthalmology. 2008;18(2):263-9.
30. Sultan MB, Zhou D, Loftus J, Dombi T, Ice KS, Macugen Study G. A phase 2/3, multicenter, randomized, double-masked, 2-year trial of pegaptanib sodium for the treatment of diabetic macular edema. Ophthalmology. 2011;118(6):1107-18.
31. Nishijima K, Ng YS, Zhong L, Bradley J, Schubert W, Jo N, et al. Vascular endothelial growth factor-A is a survival factor for retinal neurons and a critical neuroprotectant during the adaptive response to ischemic injury. The American journal of pathology. 2007;171(1):53-67.
32. Inan UU, Avci B, Kusbeci T, Kaderli B, Avci R, Temel SG. Preclinical safety evaluation of intravitreal injection of full-length humanized vascular endothelial growth factor antibody in rabbit eyes. Investigative ophthalmology & visual science. 2007;48(4):1773-81.
33. Baffert F, Le T, Sennino B, Thurston G, Kuo CJ, Hu-Lowe D, et al. Cellular changes in normal blood capillaries undergoing regression after inhibition of VEGF signaling. American journal of physiology Heart and circulatory physiology. 2006;290(2):H547-59.
34. Saint-Geniez M, Maldonado AE, D'Amore PA. VEGF expression and receptor activation in the choroid during development and in the adult. Investigative ophthalmology & visual science. 2006;47(7):3135-42.
35. Powell ED, Field RA. Diabetic Retinopathy and Rheumatoid Arthritis. Lancet. 1964;2(7349):17-8.
36. Demircan N, Safran BG, Soylu M, Ozcan AA, Sizmaz S. Determination of vitreous interleukin-1 (IL-1) and tumour necrosis factor (TNF) levels in proliferative diabetic retinopathy. Eye. 2006;20(12):1366-9.
37. Zhou J, Wang S, Xia X. Role of intravitreal inflammatory cytokines and angiogenic factors in proliferative diabetic retinopathy. Current eye research. 2012;37(5):416-20.
38. Limb GA, Hollifield RD, Webster L, Charteris DG, Chignell AH. Soluble TNF receptors in vitreoretinal proliferative disease. Investigative ophthalmology & visual science. 2001;42(7):1586-91.
39. Costagliola C, Romano V, De Tollis M, Aceto F, dell'Omo R, Romano MR, et al. TNF-alpha levels in tears: a novel biomarker to assess the degree of diabetic retinopathy. Mediators of inflammation. 2013;2013:629529.
40. Doganay S, Evereklioglu C, Er H, Turkoz Y, Sevinc A, Mehmet N, et al. Comparison of serum NO, TNF-alpha, IL-1beta, sIL-2R, IL-6 and IL-8 levels with grades of retinopathy in patients with diabetes mellitus. Eye. 2002;16(2):163-70.

41. Klein BE, Knudtson MD, Tsai MY, Klein R. The relation of markers of inflammation and endothelial dysfunction to the prevalence and progression of diabetic retinopathy: Wisconsin epidemiologic study of diabetic retinopathy. Archives of ophthalmology. 2009;127(9):1175-82.
42. Schoenberger SD, Kim SJ, Sheng J, Rezaei KA, Lalezary M, Cherney E. Increased prostaglandin E2 (PGE2) levels in proliferative diabetic retinopathy, and correlation with VEGF and inflammatory cytokines. Investigative ophthalmology & visual science. 2012;53(9):5906-11.
43. Yuuki T, Kanda T, Kimura Y, Kotajima N, Tamura J, Kobayashi I, et al. Inflammatory cytokines in vitreous fluid and serum of patients with diabetic vitreoretinopathy. Journal of diabetes and its complications. 2001;15(5):257-9.
44. Murugeswari P, Shukla D, Rajendran A, Kim R, Namperumalsamy P, Muthukkaruppan V. Proinflammatory cytokines and angiogenic and anti-angiogenic factors in vitreous of patients with proliferative diabetic retinopathy and eales' disease. Retina. 2008;28(6):817-24.
45. Limb GA, Hickman-Casey J, Hollifield RD, Chignell AH. Vascular adhesion molecules in vitreous from eyes with proliferative diabetic retinopathy. Investigative ophthalmology & visual science. 1999;40(10):2453-7.
46. Shamri R, Grabovsky V, Feigelson SW, Dwir O, Van Kooyk Y, Alon R. Chemokine stimulation of lymphocyte alpha 4 integrin avidity but not of leukocyte function-associated antigen-1 avidity to endothelial ligands under shear flow requires cholesterol membrane rafts. The Journal of biological chemistry. 2002;277(42):40027-35.
47. Miyamoto K, Khosrof S, Bursell SE, Rohan R, Murata T, Clermont AC, et al. Prevention of leukostasis and vascular leakage in streptozotocin-induced diabetic retinopathy via intercellular adhesion molecule-1 inhibition. Proceedings of the National Academy of Sciences of the United States of America. 1999;96(19):10836-41.
48. McLeod DS, Lefer DJ, Merges C, Lutty GA. Enhanced expression of intracellular adhesion molecule-1 and P-selectin in the diabetic human retina and choroid. The American journal of pathology. 1995;147(3):642-53.
49. Joussen AM, Poulaki V, Le ML, Koizumi K, Esser C, Janicki H, et al. A central role for inflammation in the pathogenesis of diabetic retinopathy. FASEB journal : official publication of the Federation of American Societies for Experimental Biology. 2004;18(12):1450-2.
50. Bolton SJ, Anthony DC, Perry VH. Loss of the tight junction proteins occludin and zonula occludens-1 from cerebral vascular endothelium during neutrophil-induced blood-brain barrier breakdown in vivo. Neuroscience. 1998;86(4):1245-57.
51. Del Maschio A, Zanetti A, Corada M, Rival Y, Ruco L, Lampugnani MG, et al. Polymorphonuclear leukocyte adhesion triggers the disorganization of endothelial cell-to-cell adherens junctions. The Journal of cell biology. 1996;135(2):497-510.
52. Joussen AM, Murata T, Tsujikawa A, Kirchhof B, Bursell SE, Adamis AP. Leukocyte-mediated endothelial cell injury and death in the diabetic retina. The American journal of pathology. 2001;158(1):147-52.
53. Talahalli R, Zarini S, Tang J, Li G, Murphy R, Kern TS, et al. Leukocytes regulate retinal capillary degeneration in the diabetic mouse via generation of leukotrienes. Journal of leukocyte biology. 2013;93(1):135-43.
54. Lutty GA, Cao J, McLeod DS. Relationship of polymorphonuclear leukocytes to capillary dropout in the human diabetic choroid. The American journal of pathology. 1997;151(3):707-14.
55. Joussen AM, Poulaki V, Mitsiades N, Cai WY, Suzuma I, Pak J, et al. Suppression of Fas-FasL-induced endothelial cell apoptosis prevents diabetic blood-retinal barrier breakdown in a model of streptozotocin-induced diabetes. FASEB journal : official publication of the Federation of American Societies for Experimental Biology. 2003;17(1):76-8.

56. Ishida S, Yamashiro K, Usui T, Kaji Y, Ogura Y, Hida T, et al. Leukocytes mediate retinal vascular remodeling during development and vaso-obliteration in disease. Nature medicine. 2003;9(6):781-8.
57. Freedman SF, Hatchell DL. Enhanced superoxide radical production by stimulated polymorphonuclear leukocytes in a cat model of diabetes. Experimental eye research. 1992;55(5):767-73.
58. Karima M, Kantarci A, Ohira T, Hasturk H, Jones VL, Nam BH, et al. Enhanced superoxide release and elevated protein kinase C activity in neutrophils from diabetic patients: association with periodontitis. Journal of leukocyte biology. 2005;78(4):862-70.
59. Rashid G, Luzon AA, Korzets Z, Klein O, Zeltzer E, Bernheim J. The effect of advanced glycation end-products and aminoguanidine on TNFalpha production by rat peritoneal macrophages. Peritoneal dialysis international : journal of the International Society for Peritoneal Dialysis. 2001;21(2):122-9.
60. Lafaille JJ, Keere FV, Hsu AL, Baron JL, Haas W, Raine CS, et al. Myelin basic protein-specific T helper 2 (Th2) cells cause experimental autoimmune encephalomyelitis in immunodeficient hosts rather than protect them from the disease. J Exp Med. 1997;186(2):307-12.
61. Joussen AM, Poulaki V, Mitsiades N, Kirchhof B, Koizumi K, Dohmen S, et al. Nonsteroidal anti-inflammatory drugs prevent early diabetic retinopathy via TNF-alpha suppression. FASEB journal : official publication of the Federation of American Societies for Experimental Biology. 2002;16(3):438-40.
62. Zheng L, Howell SJ, Hatala DA, Huang K, Kern TS. Salicylate-based anti-inflammatory drugs inhibit the early lesion of diabetic retinopathy. Diabetes. 2007;56(2):337-45.
63. Kern TS, Engerman RL. Pharmacological inhibition of diabetic retinopathy: aminoguanidine and aspirin. Diabetes. 2001;50(7):1636-42.
64. Effect of aspirin alone and aspirin plus dipyridamole in early diabetic retinopathy. A multicenter randomized controlled clinical trial. The DAMAD Study Group. Diabetes. 1989;38(4):491-8.
65. Effects of aspirin treatment on diabetic retinopathy. ETDRS report number 8. Early Treatment Diabetic Retinopathy Study Research Group. Ophthalmology. 1991;98(5 Suppl):757-65.
66. Abraldes MJ, Fernandez M, Gomez-Ulla F. Intravitreal triamcinolone in diabetic retinopathy. Current diabetes reviews. 2009;5(1):18-25.
67. Jonas JB, Kreissig I, Degenring R. Intraocular pressure after intravitreal injection of triamcinolone acetonide. The British journal of ophthalmology. 2003;87(1):24-7.
68. Xu HE, Lambert MH, Montana VG, Plunket KD, Moore LB, Collins JL, et al. Structural determinants of ligand binding selectivity between the peroxisome proliferator-activated receptors. Proceedings of the National Academy of Sciences of the United States of America. 2001;98(24):13919-24.
69. Kliewer SA, Forman BM, Blumberg B, Ong ES, Borgmeyer U, Mangelsdorf DJ, et al. Differential expression and activation of a family of murine peroxisome proliferator-activated receptors. Proceedings of the National Academy of Sciences of the United States of America. 1994;91(15):7355-9.
70. Schmidt A, Endo N, Rutledge SJ, Vogel R, Shinar D, Rodan GA. Identification of a new member of the steroid hormone receptor superfamily that is activated by a peroxisome proliferator and fatty acids. Molecular endocrinology. 1992;6(10):1634-41.
71. Dreyer C, Krey G, Keller H, Givel F, Helftenbein G, Wahli W. Control of the peroxisomal beta-oxidation pathway by a novel family of nuclear hormone receptors. Cell. 1992;68(5):879-87.
72. Forman BM, Chen J, Evans RM. Hypolipidemic drugs, polyunsaturated fatty acids, and eicosanoids are ligands for peroxisome proliferator-activated receptors alpha and delta. Proceedings of the National Academy of Sciences of the United States of America. 1997;94(9):4312-7.
73. Lee CH, Kang K, Mehl IR, Nofsinger R, Alaynick WA, Chong LW, et al. Peroxisome proliferator-activated receptor delta promotes very low-density lipoprotein-derived fatty acid catabolism in the macrophage. Proceedings of the National Academy of Sciences of the United States of America. 2006;103(7):2434-9.
74. Shaw N, Elholm M, Noy N. Retinoic acid is a high affinity selective ligand for the peroxisome proliferator-activated receptor beta/delta. The Journal of biological chemistry. 2003;278(43):41589-92.

75. Hatae T, Wada M, Yokoyama C, Shimonishi M, Tanabe T. Prostacyclin-dependent apoptosis mediated by PPAR delta. The Journal of biological chemistry. 2001;276(49):46260-7.
76. Shearer BG, Steger DJ, Way JM, Stanley TB, Lobe DC, Grillot DA, et al. Identification and characterization of a selective peroxisome proliferator-activated receptor beta/delta (NR1C2) antagonist. Molecular endocrinology. 2008;22(2):523-9.
77. Oliver WR, Jr., Shenk JL, Snaith MR, Russell CS, Plunket KD, Bodkin NL, et al. A selective peroxisome proliferator-activated receptor delta agonist promotes reverse cholesterol transport. Proceedings of the National Academy of Sciences of the United States of America. 2001;98(9):5306-11.
78. Sznaidman ML, Haffner CD, Maloney PR, Fivush A, Chao E, Goreham D, et al. Novel selective small molecule agonists for peroxisome proliferator-activated receptor delta (PPARdelta)--synthesis and biological activity. Bioorganic & medicinal chemistry letters. 2003;13(9):1517-21.
79. Gilde AJ, van der Lee KA, Willemsen PH, Chinetti G, van der Leij FR, van der Vusse GJ, et al. Peroxisome proliferator-activated receptor (PPAR) alpha and PPARbeta/delta, but not PPARgamma, modulate the expression of genes involved in cardiac lipid metabolism. Circulation research. 2003;92(5):518-24.
80. Muoio DM, MacLean PS, Lang DB, Li S, Houmard JA, Way JM, et al. Fatty acid homeostasis and induction of lipid regulatory genes in skeletal muscles of peroxisome proliferator-activated receptor (PPAR) alpha knock-out mice. Evidence for compensatory regulation by PPAR delta. The Journal of biological chemistry. 2002;277(29):26089-97.
81. Riserus U, Sprecher D, Johnson T, Olson E, Hirschberg S, Liu A, et al. Activation of peroxisome proliferator-activated receptor (PPAR)delta promotes reversal of multiple metabolic abnormalities, reduces oxidative stress, and increases fatty acid oxidation in moderately obese men. Diabetes. 2008;57(2):332-9.
82. Saluja I, Granneman JG, Skoff RP. PPAR delta agonists stimulate oligodendrocyte differentiation in tissue culture. Glia. 2001;33(3):191-204.
83. Nadra K, Anghel SI, Joye E, Tan NS, Basu-Modak S, Trono D, et al. Differentiation of trophoblast giant cells and their metabolic functions are dependent on peroxisome proliferator-activated receptor beta/delta. Molecular and cellular biology. 2006;26(8):3266-81.
84. Kim DJ, Bility MT, Billin AN, Willson TM, Gonzalez FJ, Peters JM. PPARbeta/delta selectively induces differentiation and inhibits cell proliferation. Cell death and differentiation. 2006;13(1):53-60.
85. Wang YX, Lee CH, Tiep S, Yu RT, Ham J, Kang H, et al. Peroxisome-proliferator-activated receptor delta activates fat metabolism to prevent obesity. Cell. 2003;113(2):159-70.
86. Lim HJ, Moon I, Han K. Transcriptional cofactors exhibit differential preference toward peroxisome proliferator-activated receptors alpha and delta in uterine cells. Endocrinology. 2004;145(6):2886-95.
87. Shi Y, Hon M, Evans RM. The peroxisome proliferator-activated receptor delta, an integrator of transcriptional repression and nuclear receptor signaling. Proceedings of the National Academy of Sciences of the United States of America. 2002;99(5):2613-8.
88. Lee CH, Chawla A, Urbiztondo N, Liao D, Boisvert WA, Evans RM, et al. Transcriptional repression of atherogenic inflammation: modulation by PPARdelta. Science. 2003;302(5644):453-7.
89. Zingarelli B, Piraino G, Hake PW, O'Connor M, Denenberg A, Fan H, et al. Peroxisome proliferator-activated receptor {delta} regulates inflammation via NF-{kappa}B signaling in polymicrobial sepsis. The American journal of pathology. 2010;177(4):1834-47.
90. Matsusue K, Miyoshi A, Yamano S, Gonzalez FJ. Ligand-activated PPARbeta efficiently represses the induction of LXR-dependent promoter activity through competition with RXR. Molecular and cellular endocrinology. 2006;256(1-2):23-33.
91. Daynes RA, Jones DC. Emerging roles of PPARs in inflammation and immunity. Nature reviews Immunology. 2002;2(10):748-59.

92. Tan NS, Michalik L, Desvergne B, Wahli W. Multiple expression control mechanisms of peroxisome proliferator-activated receptors and their target genes. The Journal of steroid biochemistry and molecular biology. 2005;93(2-5):99-105.
93. Keech AC, Mitchell P, Summanen PA, O'Day J, Davis TM, Moffitt MS, et al. Effect of fenofibrate on the need for laser treatment for diabetic retinopathy (FIELD study): a randomised controlled trial. Lancet. 2007;370(9600):1687-97.
94. Group AS, Group AES, Chew EY, Ambrosius WT, Davis MD, Danis RP, et al. Effects of medical therapies on retinopathy progression in type 2 diabetes. The New England journal of medicine. 2010;363(3):233-44.
95. Ambrosius WT, Danis RP, Goff DC, Greven CM, Gerstein HC, Cohen RM, et al. Lack of Association Between Thiazolidinediones and Macular Edema in Type 2 Diabetes The ACCORD Eye Substudy. Archives of ophthalmology. 2010;128(3):312-8.
96. Idris I, Warren G, Donnelly R. Association Between Thiazolidinedione Treatment and Risk of Macular Edema Among Patients With Type 2 Diabetes. Arch Intern Med. 2012;172(13):1005-11.
97. Ravnskjaer K, Frigerio F, Boergesen M, Nielsen T, Maechler P, Mandrup S. PPAR delta is a fatty acid sensor that enhances mitochondrial oxidation in insulin-secreting cells and protects against fatty acid-induced dysfunction. J Lipid Res. 2010;51(6):1370-9.
98. Roberts LD, Hassall DG, Winegar DA, Haselden JN, Nicholls AW, Griffin JL. Increased hepatic oxidative metabolism distinguishes the action of Peroxisome proliferator-activated receptor d from Peroxisome proliferator-activated receptor g in the ob/ob mouse. Genome Med. 2009;1.
99. Chen W, Wang LL, Liu HY, Long L, Li S. Peroxisome proliferator-activated receptor delta-agonist, GW501516, ameliorates insulin resistance, improves dyslipidaemia in monosodium L-glutamate metabolic syndrome mice. Basic Clin Pharmacol. 2008;103(3):240-6.
100. Thamer C, Machann J, Stefan N, Schafer SA, Machicao F, Staiger H, et al. Variations in PPARD determine the change in body composition during lifestyle intervention: A whole-body magnetic resonance study. J Clin Endocr Metab. 2008;93(4):1497-500.
101. Burch LR, Donnelly LA, Doney ASF, Brady J, Tommasi AM, Whitley AL, et al. Peroxisome Proliferator-Activated Receptor-delta Genotype Influences Metabolic Phenotype and May Influence Lipid Response to Statin Therapy in Humans: A Genetics of Diabetes Audit and Research Tayside Study. J Clin Endocr Metab. 2010;95(4):1830-7.
102. Sprecher DL, Massien C, Pearce G, Billin AN, Perlstein I, Willson TM, et al. Triglyceride: High-density lipoprotein cholesterol effects in healthy subjects administered a peroxisome proliferator activated receptor delta agonist. Arterioscl Throm Vas. 2007;27(2):359-65.
103. Di Paola R, Esposito E, Mazzon E, Paterniti I, Galuppo M, Cuzzocrea S. GW0742, a selective PPAR-beta/delta agonist, contributes to the resolution of inflammation after gut ischemia/reperfusion injury. Journal of leukocyte biology. 2010;88(2):291-301.
104. Collino M, Benetti E, Miglio G, Castiglia S, Rosa AC, Aragno M, et al. Peroxisome proliferator-activated receptor beta/delta agonism protects the kidney against ischemia/reperfusion injury in diabetic rats. Free Radical Bio Med. 2011;50(2):345-53.
105. Yue TL, Nerurkar SS, Bao W, Jucker BM, Sarov-Blat L, Steplewski K, et al. In vivo activation of peroxisome proliferator-activated receptor-delta protects the heart from Ischemia/Reperfusion injury in Zucker fatty rats. J Pharmacol Exp Ther. 2008;325(2):466-74.
106. Galuppo M, Di Paola R, Mazzon E, Genovese T, Crisafulli C, Paterniti I, et al. Role of PPAR-delta in the development of zymosan-induced multiple organ failure: an experiment mice study. Journal of inflammation. 2010;7:12.
107. Kapoor A, Shintani Y, Collino M, Osuchowski MF, Busch D, Patel NS, et al. Protective role of peroxisome proliferator-activated receptor-beta/delta in septic shock. American journal of respiratory and critical care medicine. 2010;182(12):1506-15.

108. Shan W, Palkar PS, Murray IA, McDevitt EI, Kennett MJ, Kang BH, et al. Ligand activation of peroxisome proliferator-activated receptor beta/delta (PPARbeta/delta) attenuates carbon tetrachloride hepatotoxicity by downregulating proinflammatory gene expression. Toxicological sciences : an official journal of the Society of Toxicology. 2008;105(2):418-28.
109. Liang YJ, Jian JH, Liu YC, Juang SJ, Shyu KG, Lai LP, et al. Advanced glycation end products-induced apoptosis attenuated by PPARdelta activation and epigallocatechin gallate through NF-kappaB pathway in human embryonic kidney cells and human mesangial cells. Diabetes/metabolism research and reviews. 2010;26(5):406-16.
110. Ding G, Cheng L, Qin Q, Frontin S, Yang Q. PPARdelta modulates lipopolysaccharide-induced TNFalpha inflammation signaling in cultured cardiomyocytes. Journal of molecular and cellular cardiology. 2006;40(6):821-8.
111. Fan Y, Wang Y, Tang Z, Zhang H, Qin X, Zhu Y, et al. Suppression of pro-inflammatory adhesion molecules by PPAR-delta in human vascular endothelial cells. Arteriosclerosis, thrombosis, and vascular biology. 2008;28(2):315-21.
112. Alvarez-Guardia D, Palomer X, Coll T, Serrano L, Rodriguez-Calvo R, Davidson MM, et al. PPARbeta/delta activation blocks lipid-induced inflammatory pathways in mouse heart and human cardiac cells. Biochimica et biophysica acta. 2011;1811(2):59-67.
113. Schnegg CI, Kooshki M, Hsu FC, Sui GC, Robbins ME. PPAR delta prevents radiation-induced proinflammatory responses in microglia via transrepression of NF-kappa B and inhibition of the PK alpha/MEK1/2/ERK1/2/AP-1 pathway. Free Radical Bio Med. 2012;52(9):1734-43.
114. Bouhlel MA, Brozek J, Derudas B, Zawadzki C, Jude B, Staels B, et al. Unlike PPARgamma, PPARalpha or PPARbeta/delta activation does not promote human monocyte differentiation toward alternative macrophages. Biochemical and biophysical research communications. 2009;386(3):459-62.
115. Kang K, Reilly SM, Karabacak V, Gangl MR, Fitzgerald K, Hatano B, et al. Adipocyte-derived Th2 cytokines and myeloid PPARdelta regulate macrophage polarization and insulin sensitivity. Cell metabolism. 2008;7(6):485-95.
116. Kharroubi I, Lee CH, Hekerman P, Darville MI, Evans RM, Eizirik DL, et al. BCL-6: a possible missing link for anti-inflammatory PPAR-delta signalling in pancreatic beta cells. Diabetologia. 2006;49(10):2350-8.
117. Pollock CB, Rodriguez O, Martin PL, Albanese C, Li X, Kopelovich L, et al. Induction of metastatic gastric cancer by peroxisome proliferator-activated receptordelta activation. PPAR research. 2010;2010:571783.
118. Romanowska M, Reilly L, Palmer CN, Gustafsson MC, Foerster J. Activation of PPARbeta/delta causes a psoriasis-like skin disease in vivo. PloS one. 2010;5(3):e9701.
119. Abdollahi A, Schwager C, Kleeff J, Esposito I, Domhan S, Peschke P, et al. Transcriptional network governing the angiogenic, switch in human pancreatic cancer. Proceedings of the National Academy of Sciences of the United States of America. 2007;104(31):12890-5.
120. Jiang BM, Liang PF, Zhang B, Huang XY, Xiao XZ. Enhancement of PPAR-beta activity by repetitive low-grade H2O2 stress protects human umbilical vein endothelial cells from subsequent oxidative stress-induced apoptosis. Free Radical Bio Med. 2009;46(5):555-63.
121. Han JK, Lee HS, Yang HM, Hur J, Jun SI, Kim JY, et al. Peroxisome proliferator-activated receptor-delta agonist enhances vasculogenesis by regulating endothelial progenitor cells through genomic and nongenomic activations of the phosphatidylinositol 3-kinase/Akt pathway. Circulation. 2008;118(10):1021-33.
122. Stephen RL, Gustafsson MC, Jarvis M, Tatoud R, Marshall BR, Knight D, et al. Activation of peroxisome proliferator-activated receptor delta stimulates the proliferation of human breast and prostate cancer cell lines. Cancer Res. 2004;64(9):3162-70.

123. Gaudel C, Schwartz C, Giordano C, Abumrad NA, Grimaldi PA. Pharmacological activation of PPARbeta promotes rapid and calcineurin-dependent fiber remodeling and angiogenesis in mouse skeletal muscle. American journal of physiology Endocrinology and metabolism. 2008;295(2):E297-304.
124. Muller R, Komhoff M, Peters JM, Muller-Brusselbach S. A Role for PPARbeta/delta in Tumor Stroma and Tumorigenesis. PPAR research. 2008;2008:534294.
125. Savage SR, McCollum GW, Yang R, Penn JS. RNA-seq identifies a role for the PPARbeta/delta inverse agonist GSK0660 in the regulation of TNFalpha-induced cytokine signaling in retinal endothelial cells. Molecular vision. 2015;21:568-76.
126. Joussen AM, Doehmen S, Le ML, Koizumi K, Radetzky S, Krohne TU, et al. TNF-alpha mediated apoptosis plays an important role in the development of early diabetic retinopathy and long-term histopathological alterations. Molecular vision. 2009;15:1418-28.
127. Theodossiadis PG, Liarakos VS, Sfikakis PP, Vergados IA, Theodossiadis GP. Intravitreal administration of the anti-tumor necrosis factor agent infliximab for neovascular age-related macular degeneration. American journal of ophthalmology. 2009;147(5):825-30, 30 e1.
128. Wu L, Hernandez-Bogantes E, Roca JA, Arevalo JF, Barraza K, Lasave AF. intravitreal tumor necrosis factor inhibitors in the treatment of refractory diabetic macular edema: a pilot study from the Pan-American Collaborative Retina Study Group. Retina. 2011;31(2):298-303.
129. Tsilimbaris MK, Panagiotoglou TD, Charisis SK, Anastasakis A, Krikonis TS, Christodoulakis E. The use of intravitreal etanercept in diabetic macular oedema. Seminars in ophthalmology. 2007;22(2):75-9.
130. Crane IJ, Wallace CA, Mckillop-Smith S, Forrester JV. Control of chemokine production at the blood-retina barrier. Immunology. 2000;101(3):426-33.
131. Mackay F, Loetscher H, Stueber D, Gehr G, Lesslauer W. Tumor-Necrosis-Factor-Alpha (Tnf-Alpha)-Induced Cell-Adhesion to Human Endothelial-Cells Is under Dominant Control of One Tnf Receptor Type, Tnf-R55. J Exp Med. 1993;177(5):1277-86.
132. Zhang QH, Jiang YD, Toutounchian JJ, Soderland C, Yates CR, Steinle JJ. Insulin-like growth factor binding protein-3 inhibits monocyte adhesion to retinal endothelial cells in high glucose conditions. Molecular vision. 2013;19:796-803.
133. Huang H, Gandhi JK, Zhong XF, Wei YH, Gong JS, Duh EJ, et al. TNF alpha Is Required for Late BRB Breakdown in Diabetic Retinopathy, and Its Inhibition Prevents Leukostasis and Protects Vessels and Neurons from Apoptosis. Investigative ophthalmology & visual science. 2011;52(3):1336-44.
134. Piqueras L, Sanz MJ, Perretti M, Morcillo E, Norling L, Mitchell JA, et al. Activation of PPARbeta/delta inhibits leukocyte recruitment, cell adhesion molecule expression, and chemokine release. Journal of leukocyte biology. 2009;86(1):115-22.
135. Zhao S, Fung-Leung WP, Bittner A, Ngo K, Liu X. Comparison of RNA-Seq and microarray in transcriptome profiling of activated T cells. PloS one. 2014;9(1):e78644.
136. Kim D, Pertea G, Trapnell C, Pimentel H, Kelley R, Salzberg SL. TopHat2: accurate alignment of transcriptomes in the presence of insertions, deletions and gene fusions. Genome biology. 2013;14(4):R36.
137. Guo Y, Zhao S, Ye F, Sheng Q, Shyr Y. MultiRankSeq: multiperspective approach for RNAseq differential expression analysis and quality control. BioMed research international. 2014;2014:248090.
138. Anders S, Pyl PT, Huber W. HTSeq--a Python framework to work with high-throughput sequencing data. Bioinformatics. 2015;31(2):166-9.
139. Chen H, Boutros PC. VennDiagram: a package for the generation of highly-customizable Venn and Euler diagrams in R. BMC bioinformatics. 2011;12:35.
140. Huang da W, Sherman BT, Lempicki RA. Systematic and integrative analysis of large gene lists using DAVID bioinformatics resources. Nature protocols. 2009;4(1):44-57.
141. Huang da W, Sherman BT, Lempicki RA. Bioinformatics enrichment tools: paths toward the comprehensive functional analysis of large gene lists. Nucleic acids research. 2009;37(1):1-13.

142. Shannon P, Markiel A, Ozier O, Baliga NS, Wang JT, Ramage D, et al. Cytoscape: A software environment for integrated models of biomolecular interaction networks. Genome Res. 2003;13(11):2498-504.
143. Wu JM, Vallenius T, Ovaska K, Westermarck J, Makela TP, Hautaniemi S. Integrated network analysis platform for protein-protein interactions. Nat Methods. 2009;6(1):75-7.
144. Miscia S, Marchisio M, Grilli A, Di Valerio V, Centurione L, Sabatino G, et al. Tumor necrosis factor alpha (TNF-alpha) activates Jak1/Stat3-Stat5B signaling through TNFR-1 in human B cells. Cell growth & differentiation : the molecular biology journal of the American Association for Cancer Research. 2002;13(1):13-8.
145. Syed MM, Phulwani NK, Kielian T. Tumor necrosis factor-alpha (TNF-alpha) regulates Toll-like receptor 2 (TLR2) expression in microglia. Journal of neurochemistry. 2007;103(4):1461-71.
146. Sheerin NS, Zhou W, Adler S, Sacks SH. TNF-alpha regulation of C3 gene expression and protein biosynthesis in rat glomerular endothelial cells. Kidney international. 1997;51(3):703-10.
147. Miyamoto K, Ogura Y, Kenmochi S, Honda Y. Role of leukocytes in diabetic microcirculatory disturbances. Microvasc Res. 1997;54(1):43-8.
148. Downey GP, Doherty DE, Schwab B, 3rd, Elson EL, Henson PM, Worthen GS. Retention of leukocytes in capillaries: role of cell size and deformability. Journal of applied physiology. 1990;69(5):1767-78.
149. Cipolletta C, Ryan KE, Hanna EV, Trimble ER. Activation of peripheral blood CD14+ monocytes occurs in diabetes. Diabetes. 2005;54(9):2779-86.
150. de Vries MA, Alipour A, Klop B, van de Geijn GJ, Janssen HW, Njo TL, et al. Glucose-dependent leukocyte activation in patients with type 2 diabetes mellitus, familial combined hyperlipidemia and healthy controls. Metabolism: clinical and experimental. 2015;64(2):213-7.
151. Schroder S, Palinski W, Schmid-Schonbein GW. Activated monocytes and granulocytes, capillary nonperfusion, and neovascularization in diabetic retinopathy. The American journal of pathology. 1991;139(1):81-100.
152. Pettersson US, Christoffersson G, Massena S, Ahl D, Jansson L, Henriksnas J, et al. Increased recruitment but impaired function of leukocytes during inflammation in mouse models of type 1 and type 2 diabetes. PloS one. 2011;6(7):e22480.
153. Abu El-Asrar AM, Struyf S, Kangave D, Geboes K, Van Damme J. Chemokines in proliferative diabetic retinopathy and proliferative vitreoretinopathy. Eur Cytokine Netw. 2006;17(3):155-65.
154. Rasmussen LM, Schmitz O, Ledet T. Increased expression of vascular cell adhesion molecule-1 (VCAM-1) in cultured endothelial cells exposed to serum from type 1 diabetic patients: no effects of high glucose concentrations. Scand J Clin Lab Inv. 2002;62(7):485-93.
155. Sheng WS, Hu S, Ni HT, Rowen TN, Lokensgard JR, Peterson PK. TNF-alpha-induced chemokine production and apoptosis in human neural precursor cells. Journal of leukocyte biology. 2005;78(6):1233-41.
156. Andoh A, Takaya H, Saotome T, Shimada M, Hata K, Araki Y, et al. Cytokine regulation of chemokine (IL-8, MCP-1, and RANTES) gene expression in human pancreatic periacinar myofibroblasts. Gastroenterology. 2000;119(1):211-9.
157. Bojic LA, Sawyez CG, Telford DE, Edwards JY, Hegele RA, Huff MW. Activation of peroxisome proliferator-activated receptor delta inhibits human macrophage foam cell formation and the inflammatory response induced by very low-density lipoprotein. Arteriosclerosis, thrombosis, and vascular biology. 2012;32(12):2919-28.
158. Hwang JS, Kim HJ, Kim G, Kang ES, Ham SA, Yoo T, et al. PPARdelta reduces abdominal aortic aneurysm formation in angiotensin II-infused apolipoprotein E-deficient mice by regulating extracellular matrix homeostasis and inflammatory responses. International journal of cardiology. 2014;174(1):43-50.

159. Matsushita Y, Ogawa D, Wada J, Yamamoto N, Shikata K, Sato C, et al. Activation of peroxisome proliferator-activated receptor delta inhibits streptozotocin-induced diabetic nephropathy through anti-inflammatory mechanisms in mice. Diabetes. 2011;60(3):960-8.
160. Dumé B. Silicon nanowires could improve drug delivery 2009. Available from: http://nanotechweb.org/cws/article/tech/37650.
161. Baeuerle PA, Henkel T. Function and activation of NF-kappa B in the immune system. Annual review of immunology. 1994;12:141-79.
162. Hu J, Nakano H, Sakurai H, Colburn NH. Insufficient p65 phosphorylation at S536 specifically contributes to the lack of NF-kappaB activation and transformation in resistant JB6 cells. Carcinogenesis. 2004;25(10):1991-2003.
163. Serrano-Marco L, Chacon MR, Maymo-Masip E, Barroso E, Salvado L, Wabitsch M, et al. TNF-alpha inhibits PPARbeta/delta activity and SIRT1 expression through NF-kappaB in human adipocytes. Biochimica et biophysica acta. 2012;1821(9):1177-85.
164. Yang X, Kume S, Tanaka Y, Isshiki K, Araki S, Chin-Kanasaki M, et al. GW501516, a PPARdelta agonist, ameliorates tubulointerstitial inflammation in proteinuric kidney disease via inhibition of TAK1-NFkappaB pathway in mice. PloS one. 2011;6(9):e25271.
165. Bao XC, Fang YQ, You P, Zhang S, Ma J. Protective role of peroxisome proliferator-activated receptor beta/delta in acute lung injury induced by prolonged hyperbaric hyperoxia in rats. Respiratory physiology & neurobiology. 2014;199:9-18.
166. Paterniti I, Esposito E, Mazzon E, Galuppo M, Di Paola R, Bramanti P, et al. Evidence for the role of peroxisome proliferator-activated receptor-beta/delta in the development of spinal cord injury. The Journal of pharmacology and experimental therapeutics. 2010;333(2):465-77.
167. Hall JM, McDonnell DP. The molecular mechanisms underlying the proinflammatory actions of thiazolidinediones in human macrophages. Molecular endocrinology. 2007;21(8):1756-68.
168. Hack K, Reilly L, Palmer C, Read KD, Norval S, Kime R, et al. Skin-targeted inhibition of PPAR beta/delta by selective antagonists to treat PPAR beta/delta-mediated psoriasis-like skin disease in vivo. PloS one. 2012;7(5):e37097.
169. Marusiak AA, Edwards ZC, Hugo W, Trotter EW, Girotti MR, Stephenson NL, et al. Mixed lineage kinases activate MEK independently of RAF to mediate resistance to RAF inhibitors. Nature communications. 2014;5:3901.
170. Lin Z, Natesan V, Shi H, Hamik A, Kawanami D, Hao C, et al. A novel role of CCN3 in regulating endothelial inflammation. Journal of cell communication and signaling. 2010;4(3):141-53.
171. Capozzi ME, McCollum GW, Savage SR, Penn JS. Peroxisome proliferator-activated receptor-beta/delta regulates angiogenic cell behaviors and oxygen-induced retinopathy. Investigative ophthalmology & visual science. 2013;54(6):4197-207.
172. Watkins WM, McCollum GW, Savage SR, Capozzi ME, Penn JS, Morrison DG. Hypoxia-induced expression of VEGF splice variants and protein in four retinal cell types. Experimental eye research. 2013;116:240-6.
173. Xu L, Han C, Lim K, Wu T. Cross-talk between peroxisome proliferator-activated receptor delta and cytosolic phospholipase A(2)alpha/cyclooxygenase-2/prostaglandin E(2) signaling pathways in human hepatocellular carcinoma cells. Cancer Res. 2006;66(24):11859-68.
174. Hollingshead HE, Killins RL, Borland MG, Girroir EE, Billin AN, Willson TM, et al. Peroxisome proliferator-activated receptor-beta/delta (PPARbeta/delta) ligands do not potentiate growth of human cancer cell lines. Carcinogenesis. 2007;28(12):2641-9.
175. Yao PL, Morales JL, Zhu B, Kang BH, Gonzalez FJ, Peters JM. Activation of peroxisome proliferator-activated receptor-beta/delta (PPAR-beta/delta) inhibits human breast cancer cell line tumorigenicity. Molecular cancer therapeutics. 2014;13(4):1008-17.

176. Hicks D, Courtois Y. The growth and behaviour of rat retinal Muller cells in vitro. 1. An improved method for isolation and culture. Experimental eye research. 1990;51(2):119-29.
177. Browning AC, Gray T, Amoaku WM. Isolation, culture, and characterisation of human macular inner choroidal microvascular endothelial cells. The British journal of ophthalmology. 2005;89(10):1343-7.
178. Penn JS, Henry MM, Tolman BL. Exposure to alternating hypoxia and hyperoxia causes severe proliferative retinopathy in the newborn rat. Pediatric research. 1994;36(6):724-31.
179. Smith LE, Wesolowski E, McLellan A, Kostyk SK, D'Amato R, Sullivan R, et al. Oxygen-induced retinopathy in the mouse. Investigative ophthalmology & visual science. 1994;35(1):101-11.
180. Babapoor-Farrokhran S, Jee K, Puchner B, Hassan SJ, Xin X, Rodrigues M, et al. Angiopoietin-like 4 is a potent angiogenic factor and a novel therapeutic target for patients with proliferative diabetic retinopathy. Proceedings of the National Academy of Sciences of the United States of America. 2015;112(23):E3030-9.
181. Inoue T, Kohro T, Tanaka T, Kanki Y, Li G, Poh HM, et al. Cross-enhancement of ANGPTL4 transcription by HIF1 alpha and PPAR beta/delta is the result of the conformational proximity of two response elements. Genome biology. 2014;15(4):R63.
182. Perdiguero EG, Galaup A, Durand M, Teillon J, Philippe J, Valenzuela DM, et al. Alteration of developmental and pathological retinal angiogenesis in angptl4-deficient mice. The Journal of biological chemistry. 2011;286(42):36841-51.
183. Kaddatz K, Adhikary T, Finkernagel F, Meissner W, Muller-Brusselbach S, Muller R. Transcriptional profiling identifies functional interactions of TGF beta and PPAR beta/delta signaling: synergistic induction of ANGPTL4 transcription. The Journal of biological chemistry. 2010;285(38):29469-79.
184. Naruhn S, Toth PM, Adhikary T, Kaddatz K, Pape V, Dorr S, et al. High-affinity peroxisome proliferator-activated receptor beta/delta-specific ligands with pure antagonistic or inverse agonistic properties. Molecular pharmacology. 2011;80(5):828-38.
185. Suarez S, McCollum GW, Bretz CA, Yang R, Capozzi ME, Penn JS. Modulation of VEGF-induced retinal vascular permeability by peroxisome proliferator-activated receptor-beta/delta. Investigative ophthalmology & visual science. 2014;55(12):8232-40.
186. Bullard LE, Qi X, Penn JS. Role for extracellular signal-responsive kinase-1 and -2 in retinal angiogenesis. Investigative ophthalmology & visual science. 2003;44(4):1722-31.
187. Viemann D, Goebeler M, Schmid S, Nordhues U, Klimmek K, Sorg C, et al. TNF induces distinct gene expression programs in microvascular and macrovascular human endothelial cells. Journal of leukocyte biology. 2006;80(1):174-85.
188. Zorena K, Mysliwska J, Mysliwiec M, Balcerska A, Hak L, Lipowski P, et al. Serum TNF-alpha level predicts nonproliferative diabetic retinopathy in children. Mediators of inflammation. 2007;2007:92196.
189. Gustavsson C, Agardh E, Bengtsson B, Agardh CD. TNF-alpha is an independent serum marker for proliferative retinopathy in type 1 diabetic patients. Journal of diabetes and its complications. 2008;22(5):309-16.
190. Polunovsky VA, Wendt CH, Ingbar DH, Peterson MS, Bitterman PB. Induction of endothelial cell apoptosis by TNF alpha: modulation by inhibitors of protein synthesis. Experimental cell research. 1994;214(2):584-94.
191. Delton-Vandenbroucke I, Grammas P, Anderson RE. Polyunsaturated fatty acid metabolism in retinal and cerebral microvascular endothelial cells. J Lipid Res. 1997;38(1):147-59.
192. Yu K, Bayona W, Kallen CB, Harding HP, Ravera CP, McMahon G, et al. Differential activation of peroxisome proliferator-activated receptors by eicosanoids. The Journal of biological chemistry. 1995;270(41):23975-83.

193. Van der Poll T, Romijn JA, Endert E, Borm JJ, Buller HR, Sauerwein HP. Tumor necrosis factor mimics the metabolic response to acute infection in healthy humans. The American journal of physiology. 1991;261(4 Pt 1):E457-65.
194. Fulkerson PC, Zimmermann N, Hassman LM, Finkelman FD, Rothenberg ME. Pulmonary chemokine expression is coordinately regulated by STAT1, STAT6, and IFN-gamma. Journal of immunology. 2004;173(12):7565-74.
195. Kerfoot SM, Lord SE, Bell RB, Gill V, Robbins SM, Kubes P. Human fractalkine mediates leukocyte adhesion but not capture under physiological shear conditions; a mechanism for selective monocyte recruitment. European journal of immunology. 2003;33(3):729-39.
196. Gerszten RE, Garcia-Zepeda EA, Lim YC, Yoshida M, Ding HA, Gimbrone MA, Jr., et al. MCP-1 and IL-8 trigger firm adhesion of monocytes to vascular endothelium under flow conditions. Nature. 1999;398(6729):718-23.
197. Porter JC, Falzon M, Hall A. Polarized localization of epithelial CXCL11 in chronic obstructive pulmonary disease and mechanisms of T cell egression. Journal of immunology. 2008;180(3):1866-77.
198. Milior G, Lecours C, Samson L, Bisht K, Poggini S, Pagani F, et al. Fractalkine receptor deficiency impairs microglial and neuronal responsiveness to chronic stress. Brain, behavior, and immunity. 2015.
199. Barroso E, Eyre E, Palomer X, Vazquez-Carrera M. The peroxisome proliferator-activated receptor beta/delta (PPARbeta/delta) agonist GW501516 prevents TNF-alpha-induced NF-kappaB activation in human HaCaT cells by reducing p65 acetylation through AMPK and SIRT1. Biochemical pharmacology. 2011;81(4):534-43.
200. Piqueras L, Reynolds AR, Hodivala-Dilke KM, Alfranca A, Redondo JM, Hatae T, et al. Activation of PPARbeta/delta induces endothelial cell proliferation and angiogenesis. Arteriosclerosis, thrombosis, and vascular biology. 2007;27(1):63-9.
201. Yang L, Zhou J, Ma Q, Wang C, Chen K, Meng W, et al. Knockdown of PPAR delta gene promotes the growth of colon cancer and reduces the sensitivity to bevacizumab in nude mice model. PloS one. 2013;8(4):e60715.
202. Guo L, Li SY, Ji FY, Zhao YF, Zhong Y, Lv XJ, et al. Role of Angptl4 in vascular permeability and inflammation. Inflammation research : official journal of the European Histamine Research Society [et al]. 2014;63(1):13-22.
203. Zeng L, Geng Y, Tretiakova M, Yu X, Sicinski P, Kroll TG. Peroxisome proliferator-activated receptor-delta induces cell proliferation by a cyclin E1-dependent mechanism and is up-regulated in thyroid tumors. Cancer Res. 2008;68(16):6578-86.